

Technical Report Documentation Page

1. Report No.	2. Government Accession No.	3. Recipient's Catalog No.	
4. Title and Subtitle Investigation of Dual Roller-Integrated MDP/CMV Compaction Monitoring Technologies and Measurement Influence Depth		5. Report Date	
		6. Performing Organization Code	
7. Author(s) David J. White, Pavana K. Vennapusa, Heath Gieselman		8. Performing Organization Report No.	
9. Performing Organization Name and Address Center for Transportation Research and Education Iowa State University 2711 South Loop Drive, Suite 4700 Ames, IA 50010-8664		10. Work Unit No. (TRAIS)	
		11. Contract or Grant No.	
12. Sponsoring Organization Name and Address Caterpillar Inc. 100 NE Adams Street Peoria, IL 61629		13. Type of Report and Period Covered	
		14. Sponsoring Agency Code	
15. Supplementary Notes			
16. Abstract <p>CS-563 and CS-683 smooth drum vibratory machines and a CP-563 padfoot machine were used to constructed controlled soil test beds to evaluate the repeatability of CMV and MDP roller-integrated measurements, compare integrated CMV and MDP measurements, and evaluate and document CMV and MDP for a given machine as it relates to measurement influence depth.</p> <p>The repeatability study involved conducting about 15 passes of each machine over relatively uniform and hard ground at two speeds and two amplitudes. A statistically sound approach to evaluating and presenting the raw data to the end user (e.g. compute average values for selected interval, etc.) was developed as part of this study. Results show that there is a machine specific and unique relationship between CMV and RMV and that speed, amplitude, travel direction, and drum-ground behavior mode can be statistically significant parameters in repeatability analysis.</p> <p>Test beds constructed to evaluate two different subsurface conditions – hard and soft – demonstrated that roller and in-situ compaction measurements are influenced by the stiffness and heterogeneity of the supporting layer conditions. Further, although the compaction layer properties are relatively uniform, the roller measurements tend to capture the variability of the underlying layers, which is important for properly results during field calibration. Post-construction tests of the multi-lift test beds clearly demonstrated that compaction layers stiffness increases due to deep densification of underlying layers during compaction.</p>			
17. Key Words Intelligent compaction, subgrade, roller, light weight deflectometer		18. Distribution Statement	
19. Security Classification (of this report)	20. Security Classification (of this page)	21. No. of Pages	22. Price

INVESTIGATION OF DUAL ROLLER- INTEGRATED MDP/CMV COMPACTION MONITORING TECHNOLOGIES AND MEASUREMENT INFLUENCE DEPTH

Principal Investigator

David J. White, Associate Professor
Iowa State University

Research Assistants

Pavana Vennapusa, Graduate Research Assistant
Heath Gieselman, Research Scientist

Department of Civil, Construction and Environmental Engineering
Iowa State University

Authors

David White, Pavana Vennapusa, Heath Gieselman

Preparation of this report was financed in part
through funds provided by the Iowa Department of Transportation
through its research management agreement with the
Center for Transportation Research and Education.

Center for Transportation Research and Education

Iowa State University

2901 South Loop Drive, Suite 3100

Ames, IA 50010-8632

Phone: 515-294-8103

Fax: 515-294-0467

www.ctre.iastate.edu

Final Report • August 2008

TABLE OF CONTENTS

ACKNOWLEDGMENTS	VIII
EXECUTIVE SUMMARY	IX
Research Summary	ix
Research Conclusions	ix
Recommendations for Implementation.....	ix
INTRODUCTION	1
Phase I Summary	2
Phase II Summary	2
Phase III Summary.....	4
BACKGROUND	7
Overview of Compaction Monitoring Technologies	7
Machine Drive Power (MDP).....	7
Compaction Meter Value (CMV) and Resonant Meter Value (RMV).....	8
LABORATORY AND FIELD TESTING METHODS	14
Laboratory Testing Methods.....	14
Soil Index Properties.....	14
Proctor Compaction	14
In-Situ Testing Methods	14
Zorn Light Weight Deflectometer	14
Dynamic Cone Penetrometer	15
Clegg Hammer	15
Nuclear Gauge	15
Earth Pressure Cells (EPCs).....	16
Description of the EPC Calibration Chamber.....	18
Calibration Procedure	18
Field Installation of EPCs.....	21
Compaction Machines	23
REPEATABILITY AND REPRODUCIBILITY OF CMV, RMV, AND MDP	26
Experimental Plan.....	26
CS-563 Smooth Drum Roller Measurements	28
CS 683 Smooth Drum Roller Measurements.....	34
CP 563 Padfoot Roller Measurements.....	35
Statistical Evaluation of Results	39
Discussion on CS-563 and 683 Smooth Drum Roller Results	42
Discussion on CP-563 Padfoot Roller Results.....	42

Summary and Key Conclusions.....	50
TEST BED STUDIES ON CS 563, CS 683, AND CP 563 ROLLERS WITH DIFFERENT SUBSURFACE CONDITIONS	52
Description of Test Bed 1	54
Roller-Integrated Compaction Measurements and EPC Measurements.....	59
CMV Comparison to In-Situ Soil Properties	73
Description of Test Bed 2	78
Description of Test Bed 3	97
Roller-Integrated Compaction Measurements	101
MDP Comparison to In-Situ Soil Properties	108
Statistical Analysis on Influence of Support Conditions	114
Summary and Key Conclusions.....	115
RESEARCH CONCLUSIONS.....	117
Repeatability and Reproducibility Study	117
Test Bed Studies	118
REFERENCES	120

LIST OF FIGURES

Figure 1. Machine calibration procedure (White et al. 2006).....	8
Figure 2. Illustration of relationship between subsurface conditions and CMV	9
Figure 3. Variation in CMV with change in elastic modulus of the soil and relative vertical amplitude at excitation frequency $f = 28$ Hz (modified from Adam and Kopf 2004)	10
Figure 4. Variation of CMV with frequency and amplitude of the roller for constant soil conditions (Shear Modulus, $G = 80$ MPa, and plastic deformation, $p = 0.5$ mm) (modified from Sandström (1994)).....	11
Figure 5. CMV and RMV change with drum behavior and soil stiffness based on numerical simulations (reproduced from Adam 1996).....	12
Figure 6. Influence of amplitude on CMV in relationship to soil stiffness based on numerical simulations (reproduced from Sandström 1994).....	12
Figure 7. CMV, RMV, amplitude data for 2.7 km test section (White et al. 2008)	13
Figure 8. (a) 300-mm Zorn LWD, (b) DCP, (c), 20-kg Clegg hammer, (d) Nuclear moisture- density gauge	16
Figure 9. Schematic cross-section of the EPC calibration chamber	18
Figure 10. Calibration setup with placement of sand layer above and below the sensor	20
Figure 11. Complete setup of the EPC calibration chamber.....	20
Figure 12. EPC calibration test results (sensor 8993).....	21
Figure 13. Excavation to install EPC's (left) and installation of EPC's in orthogonal directions.....	22
Figure 14. Leveling of EPC's and placement of thin layer of silica sand below EPC's	22
Figure 15. GPS readings on EPC's	23
Figure 16. Placement of sand (~ 2 in) around the EPCs	23
Figure 17. Caterpillar CS563 smooth drum vibratory roller.....	25
Figure 18. Caterpillar CS683 smooth drum vibratory roller.....	25
Figure 19. Caterpillar CS563 padfoot vibratory roller.....	25
Figure 20. (a) Strip 1 – CS-563 and CS-683 smooth drum rollers (CMV, RMV) – hard unsurfaced aggregate road, (b) Strip 2 – CP-563 padfoot roller (MDP, CMV, and RMV) – compacted glacial till subgrade.....	27
Figure 21. Summary of average CMV and speed of operation on test strip 1	29
Figure 22. CMV and RMV data plots for pass 1 to 17 using CS 563 roller at $a = 0.85$ mm	30
Figure 23. CMV and RMV data plots for pass 18 to 31 using CS 563 roller at $a = 0.85$ mm	31
Figure 24. CMV and RMV data plots for pass 32 to 43 using CS 563 roller at $a = 1.70$ mm	31
Figure 25. CMV and RMV data plots for pass 43 to 45 using CS 563 roller at $a = 1.70$ mm	32
Figure 26. CMV and RMV data plots for pass 46 to 57 using CS 563 roller at $a = 1.70$ mm	32
Figure 27. CMV and RMV comparison plots to define double jump and partial uplift zones for CS-563 and CS-683 rollers	33
Figure 28. Comparison of CMV / RMV to E_{LWD} and CIV measurement values	33
Figure 29. Comparison of CMV / RMV to DCP measurement values	34
Figure 30. CMV and RMV data plots for passes 58 to 69 using CS 683 roller at $a = 0.85$ mm.....	35
Figure 31. Summary of average MDP, CMV, and speed of operation for several passes on repeatability test strip 2	36
Figure 32. MDP raw data plots for pass 13 to 24 using CP 563 (padfoot) roller at $a = 0.31$ mm.....	37
Figure 33. MDP and CMV raw data plots for pass 25 to 36 using CP 563 (padfoot) roller at $a =$ 1.87 mm	38

Figure 34. Comparison between MDP and in-situ compaction test measurement values.....	39
Figure 35. Comparison of actual CMV data output and 0.305 m (1 ft.) averaged data.....	40
Figure 36. Repeatability analysis for CS 563 CMV/RMV measurement values at $a = 0.85$ mm and $v = 3.2$ km/h (nominal).....	46
Figure 37. Repeatability analysis for CS 563 CMV/RMV measurement values at $a = 0.85$ mm and $v = 4.8$ km/h (nominal).....	46
Figure 38. Repeatability analysis for CS 563 CMV/RMV measurement values at $a = 1.70$ mm and $v = 3.2$ km/h (nominal).....	47
Figure 39. Repeatability analysis for CS 563 CMV/RMV measurement values at $a = 1.70$ mm and $v = 4.8$ km/h (nominal).....	47
Figure 40. Repeatability analysis for CS 683 CMV/RMV measurement values at $a = 0.85$ mm and $v = 3.2$ km/h (nominal).....	48
Figure 41. Repeatability analysis for CP 563 MDP measurement values at $a = 0.31$ mm and $v =$ 3.2 km/h (nominal).....	49
Figure 42. Repeatability analysis for CP 563 MDP measurement values at $a = 0.31$ mm and $v =$ 4.8 km/h (nominal).....	49
Figure 43. Repeatability analysis for CP 563 MDP measurement values at $a = 1.87$ mm and $v =$ 3.2 km/h (nominal).....	50
Figure 44. TB 1 plan view and profile with location of in-ground EPCs.....	54
Figure 45. Concrete base and lifts 1 to 3 of CA6-G material in TB 1.....	55
Figure 46. Lifts 4 to 7 of CA6-G material placed in TB 1.....	56
Figure 47. Placement of biaxial Geogrid in TB 1.....	57
Figure 48. Process of excavation to the top of each underlying lift to perform LWD and NG testing.....	59
Figure 49. CMV and in-ground stress measurements for CS 563 roller passes – lift 1.....	61
Figure 50. CMV and in-ground stress measurements for CS 563 roller passes – lift 2.....	62
Figure 51. CMV and in-ground stress measurements for CS 563 roller passes – lift 3.....	63
Figure 52. CMV and in-ground stress measurements for CS 563 roller passes – lift 4.....	64
Figure 53. CMV and in-ground stress measurements for CS 563 roller passes – lift 5.....	65
Figure 54. CMV and in-ground stress measurements for CS 563 roller passes – lift 6.....	66
Figure 55. CMV and in-ground stress measurements for CS 683 roller passes – lift 6.....	67
Figure 56. CMV and in-ground stress measurements for CS 563 roller passes – lift 7.....	68
Figure 57. CMV and in-ground stress measurements for CS 683 roller passes – lift 7.....	69
Figure 58. Stress distribution under the roller at $a = 0.85$ mm – TB 1.....	70
Figure 59. Stress distribution under the roller at $a = 1.70$ mm – TB 1.....	71
Figure 60. Stress distribution under the roller in static mode – TB 1.....	72
Figure 61. CMV and E_{LWD} measurement values after final pass on each lift – TB 1.....	74
Figure 62. CMV and CBR measurement values after final pass on each lift – TB 1.....	75
Figure 63. CMV, E_{LWD} , and CBR comparison – TB 1.....	76
Figure 64. DCP-CBR profiles on each lift at seven points along the test bed with comparison to CMV measurements on each lift.....	77
Figure 64. TB 2 plan view and profile with in-ground EPC's.....	78
Figure 65. Preparation of wet subgrade portion of TB 2.....	79
Figure 66. Wet/dry subgrade and lifts 1 to 3 of CA6-G material placed in TB 2.....	80
Figure 67. Lifts 4 to 7 of CA6-G material placed in TB 2.....	81
Figure 68. Placement of geogrid layer on soft subgrade.....	82

Figure 69. CMV and in-ground stress measurements for CE 563 roller passes – lift 1	84
Figure 70. CMV and in-ground stress measurements for CS 563 roller passes – lift 2.....	85
Figure 71. CMV and in-ground stress measurements for CS 563 roller passes – lift 3.....	86
Figure 72. CMV and in-ground stress measurements for CS 563 roller passes – lift 4.....	87
Figure 73. CMV and in-ground stress measurements for CS 563 roller passes – lift 5.....	88
Figure 74. CMV and in-ground stress measurements for CS 563 roller passes – lift 6.....	89
Figure 75. CMV and in-ground stress measurements for CS 563 roller passes – lift 7.....	90
Figure 76. CMV and E_{LWD} measurement values after final pass on each lift – TB 2	91
Figure 77. CMV and CBR measurement values after final pass on each lift – TB 2	92
Figure 78. CMV, E_{LWD} , and CBR comparison – TB 2	93
Figure 79. Stress distribution under the roller at $a = 0.85$ mm – TB 2	94
Figure 80. Stress distribution under the roller at $a = 1.70$ mm – TB 2	95
Figure 81. Stress distribution under the roller in static mode – TB 2	96
Figure 82. TB 3 plan view and profile with location of in-ground EPCs.....	97
Figure 83. Concrete and soft/wet subgrade base and lifts 1 to 3 of CA6-G material placed in TB 3.....	98
Figure 84. Lifts 4 to 7 of CA6-G material placed in TB 3.....	99
Figure 85. Process of excavation to the top of each underlying lift to perform LWD testing.....	101
Figure 86. Raw data plots of MDP, CMV, and RMV measurements on lift 1 (picture showing the rutting observed on lift 1 after pass 9)	102
Figure 87. Raw data plots of MDP, CMV, and RMV measurements on lifts 2 and 3	103
Figure 88. Raw data plots of MDP, CMV, and RMV measurements on lifts 4 and 5	104
Figure 89. Raw data plots of MDP, CMV, and RMV measurements on lifts 6 and 7	105
Figure 90. Caterpillar viewer program screen shots of MDP final static pass on each lift – TB 3 (color).....	106
Figure 91. Pass 9 MDP measurements on lifts 1 to 7 – TB 3 (color).....	107
Figure 92. MDP compaction growth curves – TB 3	107
Figure 93. GPS position of roller drum during compaction passes on each lift – TB 3 (color) ..	108
Figure 94. MDP and E_{LWD} comparison plot after final pass on each lift – TB 3	110
Figure 95. MDP and CBR comparison plot after final pass on each lift – TB 3	111
Figure 96. Relationships between CBR, E_{LWD} , and MDP from TB 3	112
Figure 97. Average MDP, E_{LWD} , and CBR measurement values on all compaction lifts – TB3	113

LIST OF TABLES

Table 1. Observed modes of vibratory roller drum (Adam 1997)	10
Table 2. Factors affecting EPC measurements and measures taken to minimize the errors	17
Table 3. Specifications of the machines used in this study (from Caterpillar, Inc. Manuals)	24
Table 4. Summary of repeated roller passes	27
Table 5. Difference in roller and in-situ compaction measurements	34
Table 6. Summary of repeatability analysis results	43
Table 7. Summary of R&R analysis results	44
Table 7. Summary of R&R analysis results (contd.)	45
Table 8. Summary of test strips	52
Table 9. Summary of soil index properties	53
Table 10. Summary of experimental testing on TB 1 – concrete base	58
Table 11. Summary of experimental testing on TB 2 – wet/dry subgrade	83
Table 12. Summary of experimental testing on TB 3 – concrete/soft subgrade	100
Table 13. Effect of underlying layer measurements on surface layer measurements	116

ACKNOWLEDGMENTS

This study was funded by Caterpillar Inc. (CAT). This support is greatly appreciated. E. Tom Cackler of the Center for Transportation Research and Education helped organized this research effort. Allen DeClerk, Bill Evans, Liqun Chi, Donald Hutchen, and Ron Faber of CAT provided assistance with field testing. The authors would also like to acknowledge the assistance of Mike Kruse, Dan Enz and Alexandra Buchanan for providing assistance with field testing.

EXECUTIVE SUMMARY

Research Summary

Research Conclusions

Recommendations for Implementation

INTRODUCTION

The Phase IV intelligent compaction research study set out to evaluate dual roller-integrated MDP/CMV compaction monitoring technologies and measurement influence depth. This phase of the research followed three previous research phases that are summarized later for reference. For the phase IV study, CS-563 and CS-683 smooth drum vibratory machines and CP-563 padfoot machine were evaluated. The primary objectives of the test program were to (1) evaluate the repeatability of CMV and MDP measurements for different machines, (2) compare CMV and MDP measurements for the different machines, (3) compare CMV and MDP for a given machine as it relates to measurement influence depth, and (4) document the measurement influence depths of the two machines. To achieve these objectives, a detailed experimental plan was developed. Key elements of the proposed experimental plan include:

1. Operating the machines repeatedly (~15 passes each) over relatively uniform and hard ground at two speeds and two amplitudes.
2. Constructing a single 12 inch thick layer of CA6-G material over an area of 10 ft x 80 ft to evaluate both machines in terms of compaction performance.
3. Constructing two test beds each of plan dimensions of about 10 ft x 80 ft at the base with a height of about 8 ft for two different subsurface layer conditions;
4. Installing soil-specific, calibrated earth pressure cells within the test beds at three elevations to obtain triaxial applied stresses during roller compaction thus verifying the measurement influence depth;
5. Performing density and LWD measurements as a function of roller pass to develop compaction curves for comparison to CMV and MDP measurements for both rollers.

For the repeatability study, the machines were operated at different speeds and amplitude settings, and the CMV and MDP measurements were compared and evaluated for repeatability. The outcome of this study was development of a statistically sound approach to evaluating and presenting the raw data to the end user (e.g. compute average values for selected interval, etc.). Test beds were constructed for two different subsurface conditions — hard and soft.

Test beds were constructed by excavating a 4 to 5 feet trench below existing grade. One test bed consisted of a 1 foot thick concrete pad at the base, while the other test bed consisted of a 1 foot thick soft/wet soil subgrade, underlain by native glacial till. Each test bed has plan area of about 10 ft x 80 ft at the base of the excavation. Seven to eight lifts of CA6-G material (loose lift thickness ~ 12 inches) were placed and compacted in each test bed. The fill material will be moisture conditioned before compacting to within -2 to 0% of optimum moisture content (8 - 10%). After machine passes, spot test measurements were conducted to determine dry unit weight, moisture content, DCP index, LWD modulus, and static plate load modulus. Specially fabricated and calibrated semi-conductor earth pressure cells (EPC's) were installed in several layers of test bed materials. To obtain stress measurements in three directions (triaxial: vertical, longitudinal, and transverse) during roller compaction, the EPC's were installed in three orthogonal directions.

Phase I Summary

Phase I was initiated in 2003 to begin evaluating the compaction monitoring technology developed by Caterpillar Inc. The technology consists of an instrumented prototype padfoot roller that monitors changes in machine drive power (MDP) resulting from soil compaction and the corresponding changes in machine-soil interaction. The roller is additionally fitted with a global positioning system (GPS) so that coverage (i.e., history of the roller location) and MDP are mapped and viewed in real-time during compaction operations. The specific objectives of Phase I included (1) a literature review of current compaction monitoring technologies, (2) data collection using the compaction monitoring system and in situ testing devices for comparing MDP to physical soil properties (e.g., density, strength, stiffness), (3) identification of modifications to be made to the technological and communication systems, and (4) identification of the benefits to contractors and owners who may use the technology.

The Phase I report summarized preliminary analyses of data collected during pilot studies at Caterpillar Inc. facilities in Peoria, Illinois, and on an actual earthwork project in West Des Moines, Iowa. In these pilot studies, in situ tests were conducted using currently accepted practices to evaluate the technology. The field measurements of soil density, moisture content, strength, and stiffness showed a high level of promise for MDP to indicate soil compaction.

The significant research findings from Phase I (White et al. 2004) are summarized as follows:

- Multiple linear regression analyses were performed using machine power and various field measurements (nuclear moisture and density, dynamic cone penetrometer index, Clegg impact value). The R^2 values of the models indicated that compaction energy accounts for more variation in dry unit weight than dynamic cone penetrometer (DCP) index or Clegg impact values (CIV).
- Incorporating moisture content in the regression analyses improved model R^2 values for DCP index and CIV, indicating the influence of moisture content on soil strength and stiffness parameters.
- The compaction monitoring technology showed a high level of promise for use as a quality control/quality assurance (QC/QA) tool, but was demonstrated for a relatively narrow range of field conditions.

The results of this proof-of-concept study provided evidence that machine power may reliably indicate soil compaction with the advantages of 100% coverage and real-time results. Additional field trials were recommended, however, to expand the range of correlations to other soil types, roller configurations, lift thicknesses, and moisture contents. The observed promise for using such compaction monitoring technology in earthwork QC/QA practices also required developing guidelines for its use, considering a statistical framework for analyzing the near-continuous data.

Phase II Summary

Primary research tasks for the Phase II study involved (1) performing experimental testing and statistical analyses to relate MDP to soil engineering properties (e.g., density, strength, stiffness) and (2) developing recommendations for using the compaction monitoring technology in

practice. For this study, data were collected at three test sites. The first two projects (February and May 2005) were conducted at Caterpillar Inc. facilities near Peoria, Illinois, and included constructing and testing relatively uniform test strips using different soil types, moisture contents, and lift thicknesses. The data collected facilitated linear and multiple linear regression analyses with moisture content, lift thickness, and soil type as regression parameters. The third test site (June 2005) was conducted at an earthwork construction project for the TH 14 bypass near Janesville, Minnesota. For this final project, the ability of the compaction monitoring technology to identify localized areas of weak or poorly-compacted soil was demonstrated by mapping select locations of the project and comparing to the test rolling.

For all test projects, in situ testing of soil density (nuclear moisture-density gauge), strength (DCP, Clegg impact hammer), and stiffness (GeoGauge, light weight deflectometer, plate load test) provided data to characterize the soil at various stages of compaction (i.e., roller passes). For each test strip (i.e., uniform soil type and moisture content) or test area (variable conditions), in situ soil properties were compared directly to MDP measurement values to establish statistical relationships. Using a physical model developed from laboratory compaction energy-dry unit weight moisture content measurements as a basis, statistical models were developed to predict soil density, strength, and stiffness from the machine power values. Field data for multiple test strips (i.e., multiple moisture contents, lift thicknesses, and/or soil types) were evaluated. The R^2 correlation coefficient value was generally used to assess the quality of the regressions.

The established research objectives were achieved because the testing methods and operations generated usable data for relating MDP to soil engineering properties. MDP and in-situ test measurements were collected at various levels of compaction, including at selected locations soft, intermediate, and hard materials. Also, using a variety of in situ testing devices to characterize soil density, strength, and stiffness facilitated multiple interpretations about MDP response, not just the conventional approach of determining relative compaction. Future research to investigate compaction monitoring technology may use similar testing procedures, but will isolate other variables affecting machine-soil response (e.g., speed, slope, accelerations, turning radius, etc.).

The major findings from the Phase II study of the MDP system (White et al. 2006) include the following:

- Using averaged machine power and field measurement data, strong correlations ($R^2 \geq 0.9$) were developed to characterize the machine-soil interaction. These correlations (i.e., models) were initially derived from laboratory compaction data relating compaction energy, moisture content, and dry unit weight. The final models for each combination of soil type, lift thickness, and test device show that machine power is statistically significant in predicting various soil properties. Since the initial physical model was derived from moisture-density relationships, predictions of dry unit weight were often more accurate than predictions of soil strength or stiffness. The complexity of soil strength and stiffness requires that a more complicated physical model be used. Nevertheless, by incorporating moisture content and moisture-energy (i.e., machine power) interaction terms into the regressions, high correlations were achieved and indicate the promise of using such compaction monitoring technology as a tool for

earthwork quality control.

- The compaction monitoring technology identified “wet” and “soft” spots incorporated into a test strip, evidenced by relatively high net power values observed at these locations and displayed on the compaction monitor. The difference in net power observed between these locations and the rest of the test strip was considerable; this observation reflects the extreme conditions (i.e., high lift thickness and moisture content) built into the strip design. Future testing may be required to determine and quantify the roller sensitivity to these changes in moisture content and soil lift thickness resulting from variation in construction operations (e.g., fill placement, moisture conditioning, existing site conditions) for a wider range of soil types and for larger test areas.
- The compaction monitoring technology may identify areas of weak or poorly compacted soil with real-time readings and 100% coverage. Two-dimensional spatial mapping trials conducted at the TH 14 bypass earthwork pilot project showed that in situ test measurements and proof rolling verified the compaction monitoring output for cohesive subgrade soils, but showed less certainly in some areas for fine sandy soils.
- The research program revealed that a single in situ test point does not provide a high level of confidence for being representative of the average soil engineering property value over a given area. Rather, variation always exists, and several samples must be tested to determine the soil properties with any confidence. In the case of comparing compaction monitoring output to field measurements, soil property variation and measurement influence area must be considered.
- Investigating the influence of lift thickness on the machine power output data provided important insight into the factors affecting machine-soil response. The summary of R^2 values for multiple linear regression analyses per soil showed that correlation coefficients for thicker lifts were consistently higher than for the thin lifts. The relative change in R^2 values between thin and thick lifts suggests that the depth influencing machine power response exceeds representative lift thicknesses encountered in field conditions. While the depth to a stabilized base (e.g., any soil layer with differing stiffness properties) affects the field measurements to some degree, the measurement influence depth affects the roller response (higher weight and contact area than in situ test devices) to a greater extent than the in situ tests.

Phase III Summary

A field study comprised of experimental testing and statistical analyses was conducted to evaluate the machine drive power (MDP) and Geodynamik compaction meter value (CMV) compaction monitoring technologies applied to Caterpillar rollers. The study consisted of three projects, all of which were conducted at the Caterpillar Edwards Demonstration facility near Peoria, Illinois.

The first project investigated the feasibility of using MDP applied to a Caterpillar self-propelled non-vibratory 825G roller. A test strip was constructed, compacted using the prototype 825G roller, and tested with in situ test devices. The second project also consisted of experimental testing on one-dimensional test strips. This project, however, used five aggregate base materials, which were compacted using a CS-533E vibratory smooth drum roller equipped with both MDP and CMV measurement capabilities. The independent roller measurements were compared and

described in terms of soil engineering properties. The final project was conducted with only one cohesionless material. Four test strips (three uniform strips at different moisture contents and one with variable lift thickness) were constructed and tested to develop relationships between roller measurement values and soil engineering properties. Using the material from these test strips, two-dimensional test areas with variable lift thickness and moisture content were then tested. Spatial analyses of the in situ measurements were performed to identify the spatial distribution of soil properties. The interpretation of the ground condition was then compared to machine output for evaluating the roller measurement systems and the proposed calibration procedure.

Some of the significant conclusions drawn from the Phase III study (White et al. 2007) are as follows:

- Testing a single test point does not provide a high level of confidence for being representative of the average material characteristics, particularly when dealing with variable compaction monitoring data and variable soil conditions. In the case of comparing machine parameters to field measurements, soil property variation and measurement influence area must be considered. For performing statistical analyses, data were averaged over the test strip area at each stage of compaction.
- The effect of soil compaction on roller machine-ground interaction is to decrease MDP (rolling resistance) and increase CMV (soil stiffness response). The change in compaction monitoring data with each roller pass can be described in terms of compaction measurements through logarithmic or linear relationships. Correlation coefficients (i.e., R^2 values) for the regressions often exceed 0.90.
- The local variation in MDP is generally greater than that of CMV for soils tested during this field study. Coefficients of variation and standard deviations for CMV and MDP, respectively, vary between test strips (soil types), despite being within a relatively narrow range for an individual test strip.
- MDP was shown to be locally variable, but repeatable for multiple passes. The measurement was noted to be significantly affected by the soil characteristics of the compaction layer. For a two-dimensional test area, MDP provided some indication of differential lift thickness.
- CMV accurately identified the regions of thick lift on a two-dimensional test area with variable lift thickness and moisture content.
- Several challenges in generating a precise and reliable map of a compaction measurement based on compaction monitoring data and a calibration equation were identified, including (1) measurement influence depth, (2) variable compaction monitoring measurements, and (3) influences of underlying soil layers on machine response.

MDP technology was evaluated on a Caterpillar 825G roller to indicate compaction of Edwards till material. Additional field investigations were recommended to evaluate the feasibility of using the MDP compaction monitoring technology for alternative roller configurations as such an effort would have broader implications for earthwork construction. Specifically, it is suggested that the mechanical performance of various machines be investigated with the goal of identifying machine internal loss coefficients for correcting gross power output for net power.

BACKGROUND

Overview of Compaction Monitoring Technologies

Machine Drive Power (MDP)

The use of MDP as a measure of soil compaction is a concept originating from study of vehicle-terrain interaction. MDP, which relates to the soil properties controlling drum sinkage, uses the concepts of rolling resistance and sinkage to determine the stresses acting on the drum and the energy necessary to overcome the resistance to motion. Using MDP to describe soil compaction, where higher power indicates soft or weak material and lower power indicates compact or stiff material, is documented by White et al. (2004, 2005, 2006, and 2007b). The net MDP required to propel the machine over a layer of soil can be represented as

$$MDP = P_g - WV \left(\sin \theta + \frac{a}{g} \right) - (mV + b) \quad (1)$$

where P_g is the gross power needed to move the machine, W is the roller weight, V is the roller velocity, θ is a slope angle, a is acceleration of the machine, g is acceleration of gravity, and m and b are machine internal loss coefficients specific to a particular machine (White et al. 2006). The second and third terms of Equation 1 account for the machine power associated with sloping grade and internal machine loss, respectively.

The procedure for calibrating machine power consists of three steps (Figure 1). Machine power calibration is begun by identifying the orientation of the pitch sensor on the machine (step 1). The roller is parked on a sloping surface with a known inclination (facing uphill), and the pitch reading is noted (positive slope). The roller is then rotated to face downhill, and the new pitch sensor is noted (negative slope). The average pitch reading for these cases is the offset applied to all sensor readings. The internal loss coefficients (m and b in Equation 1) are then determined by operating the roller on a relatively uniform reference surface (i.e., net power is a relative value referencing the physical properties of this surface, with positive values indicating a less compact state). Gross power and slope compensation are then monitored while operating the roller at 3.2, 4.8, and 6.4 km/h in both forward and reverse directions (step 2). At each roller speed, the difference between the gross power output and slope compensation is the internal loss (i.e., propel power). Plotting the slope-compensated machine power against roller speed then provides a linear relationship from which the internal loss coefficients are calculated (Step 3). Application of the pitch offset and internal loss coefficients to Equation 1 thus gives net power readings of about zero for roller operation on the calibration surface.

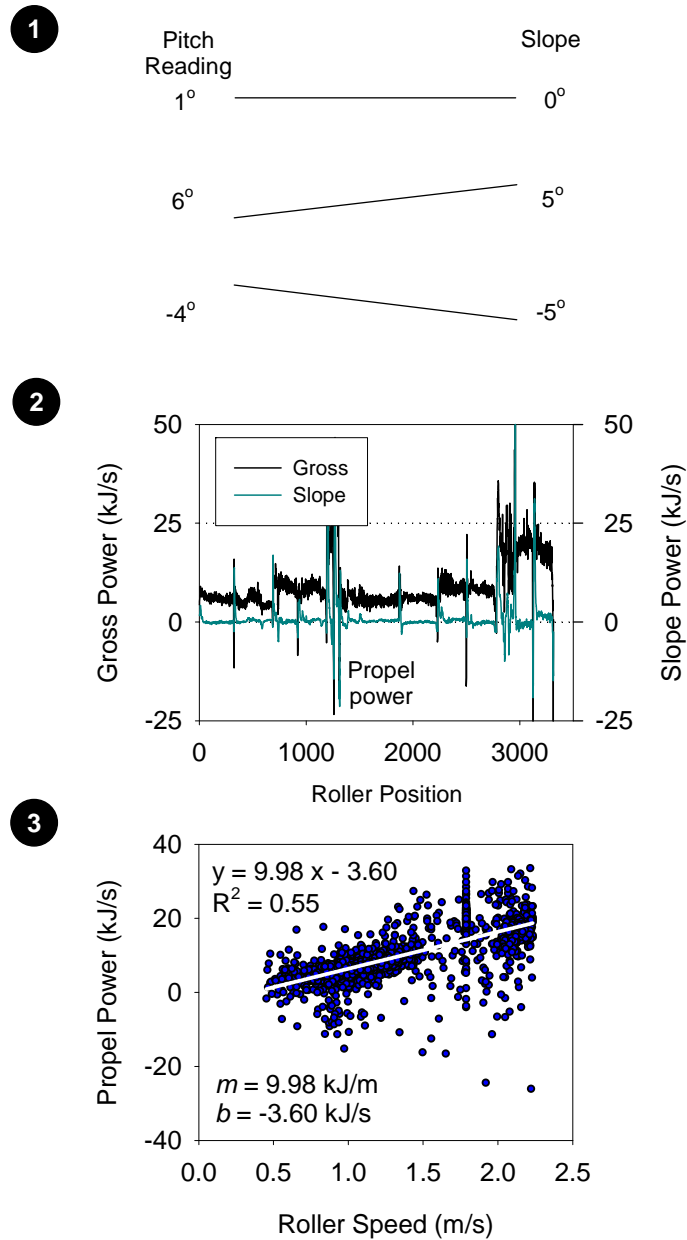


Figure 1. Machine calibration procedure (White et al. 2006)

Compaction Meter Value (CMV) and Resonant Meter Value (RMV)

Compaction meter value (CMV) was developed in the late 1970's by *Geodynamik* in Sweden (Thurner and Sandström 1980, Frossblad 1980). This technology uses accelerometers installed on the drum of a vibratory roller to measure drum accelerations in response to soil behavior during compaction operations. The ratio of the amplitude of the first harmonic and the amplitude of the fundamental frequency is found to provide a good indication of soil compaction level and to correlate well with soil stiffness (Thurner and Sandström 1980). Accordingly, CMV is calculated as shown in Equation 2.

$$CMV = C \cdot \frac{A_{2\Omega}}{A_{\Omega}} \quad (2)$$

where $C = \text{constant (300)}$, $A_{2\Omega} = \text{acceleration of the first harmonic component of the vibration}$, and $A_{\Omega} = \text{acceleration of the fundamental component of the vibration}$ (Sandström and Pettersson, 2004). The concept of CMV for a simplified condition is illustrated by Thurner and Sandström (1980) as shown in Figure 2. When roller drum interacts with a compaction layer consisting of “soft” rubber material, there would be no first harmonic motion and the CMV is theoretically zero. If the compaction layer consists of uncompacted sand material the vibration amplitude of the first harmonic increases with increasing compaction effort (number of passes) and consequently, this results in a higher CMV. CMV at a given point indicates an average value over an area whose width equals the width of the drum and length equal to the distance the roller travels in 0.5 seconds (Geodynamik ALFA-030).

The relationship between CMV and soil density, soil stiffness and soil modulus is empirical and is influenced by roller dimensions (e.g. drum diameter, weight), roller operation parameters (e.g., frequency, amplitude, speed), and soil conditions (soil type and underlying soil stratigraphy) (Sandström and Pettersson 2004). Forssblad (1980) pointed out that the roller direction of travel (forward or reverse) can affect the CMV measurement values.

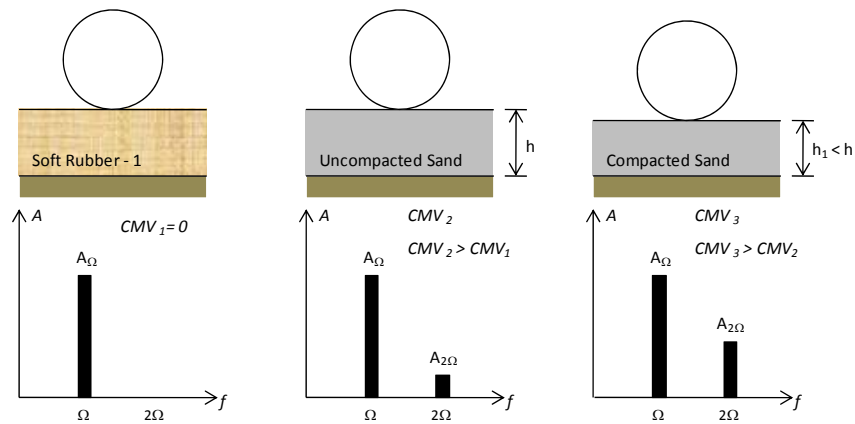


Figure 2. Illustration of relationship between subsurface conditions and CMV

Based on numerical investigations Adam (1996) identified five significant vibratory drum operation modes of motion (see Table 1) that are related to soil stiffness and roller operation parameters (i.e., vibration frequency and amplitude). These different operation modes influence the roller compaction measurements significantly and have to be considered in evaluating the data. The difference between the operation modes is the number of excitation cycles where the motion behavior of the drum repeats itself (Adam 1997). Continuous contact occurs only when the soil stiffness is very low (relatively uncompacted soils). Partial uplift and double jump are the most frequent drum operation modes. When the compacting soil stiffness is high and if the roller is being operated at higher amplitudes roller drum enters into a rocking or chaotic motion.

The roller compaction measurements are considered unreliable when the drum is in rocking or chaotic motion (Adam 1997). Adam and Kopf (2004) presented numerical simulation results of change in CMV with increasing soil stiffness and amplitude at constant frequency, identifying the different zones of drum operating modes (Figure 3). Similarly, Sandström (1994) presented numerical analysis results of change in CMV with frequency and amplitude for a particular soil condition (Figure 4). The roller configuration in that study consisted of 2,400 kg frame mass, 3,200 kg drum mass, 1.5 m diameter by 2.10 m wide drum, and eccentric mass of 50 kg.

Table 1. Observed modes of vibratory roller drum (Adam 1997)

Drum Motion	Drum-Soil Interaction	Operation Mode	Validity of compaction values	Soil Stiffness
Periodic	Continuous Contact	Continuous Contact	Yes	Low ↓ High
	Periodic loss of contact	Partial Uplift	Yes	
		Double Jump	Yes	
		Rocking Motion	No	
Chaotic	Non-periodic loss of contact	Chaotic Motion	No	

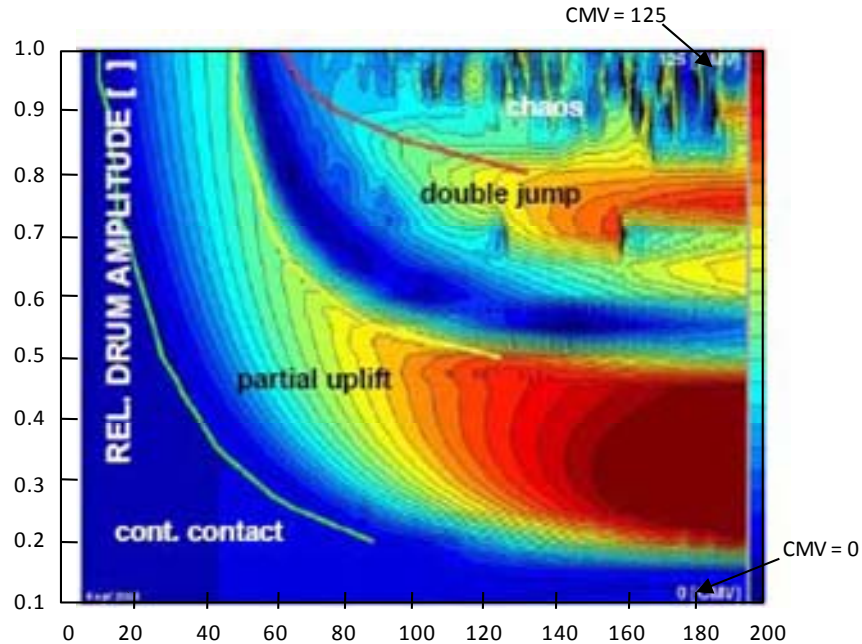


Figure 3. Variation in CMV with change in elastic modulus of the soil and relative vertical amplitude at excitation frequency $f = 28$ Hz (modified from Adam and Kopf 2004)

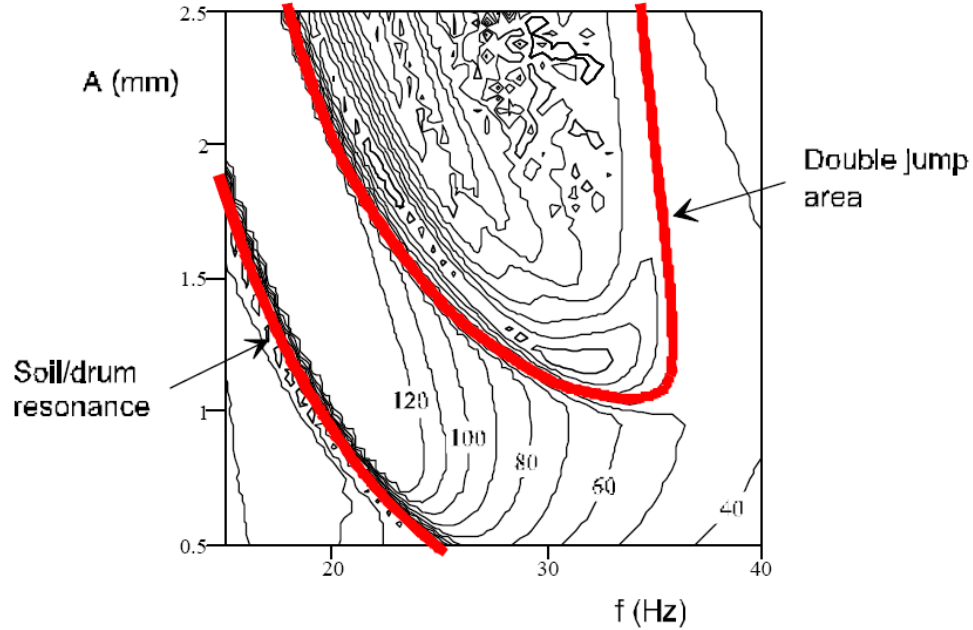


Figure 4. Variation of CMV with frequency and amplitude of the roller for constant soil conditions (Shear Modulus, $G = 80$ MPa, and plastic deformation, $p = 0.5$ mm) (modified from Sandström (1994))

The drum operation mode can also be differentiated using the *Geodynamik* resonant meter value (RMV) which is calculated using Equation 3, where $A_{0.5\Omega}$ = subharmonic acceleration amplitude caused by jumping (the drum skips every other cycle).

$$RMV = C \cdot \frac{A_{0.5\Omega}}{A_{\Omega}} \quad (3)$$

According to Brandl and Adam (2004), $RMV > 0$ indicates that the drum is a double jump, rocking or chaotic mode. Based on numerical studies Adam (1996) presented the relative change in CMV and RMV with increasing soil stiffness as shown in Figure 5. This figure shows that as the soil stiffness increases the CMV increases almost linearly with roller drum in a partial uplift mode, and when the drum starts double jumping, CMV decreases while RMV increases. After CMV decreases to a minimum, it starts increasing again with increasing soil stiffness. This is noted as a distinctive feature of CMV (Adam 1997). Sandström (1994) also found similar trends in CMV at high amplitude ($a = 1.6$ mm) while the CMV increased monotonously with increasing soil stiffness at low amplitude ($a = 0.8$ mm).

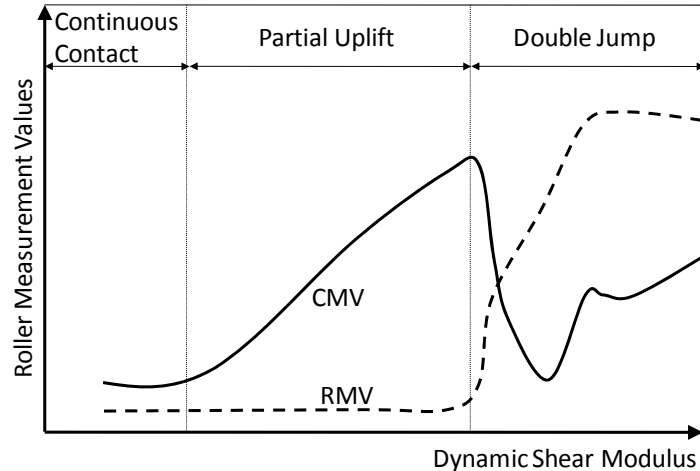


Figure 5. CMV and RMV change with drum behavior and soil stiffness based on numerical simulations (reproduced from Adam 1996)

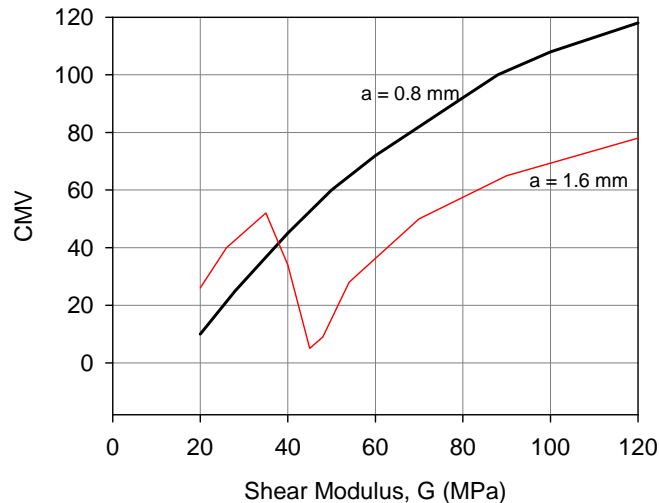


Figure 6. Influence of amplitude on CMV in relationship to soil stiffness based on numerical simulations (reproduced from Sandström 1994)

The RMV system was used as a means for variable feedback control in the CS-563 machine used on the TH 64 reconstruction project in Ackeley, MN (White et al. 2008). As a means of preventing double jump, the machine on that project was programmed to decrease the vibration amplitude when the roller RMV measurements approached 17. Figure 7 shows the CMV, RMV, and amplitude data obtained on the project for a stretch of about 2.7 km. The roller was operated in manual mode at $a = 0.7$ mm heading north from Sta. 160 to 250. Then travelling in the same path in the opposite direction, the roller was operated in manual mode at $a = 1.4$ mm from Sta. 250 to 240, and $a = 1.1$ mm from Sta. 240 to 160. The variable feedback control mode was used on several sections across the stretch as noted on Figure 6. In variable feedback control mode the machine was always attempting to operate at high amplitude and was lowering the amplitude if the RMV approached 17. Inspection of the results shows that these settings did not control amplitude to the extent needed to prevent double jump mode.

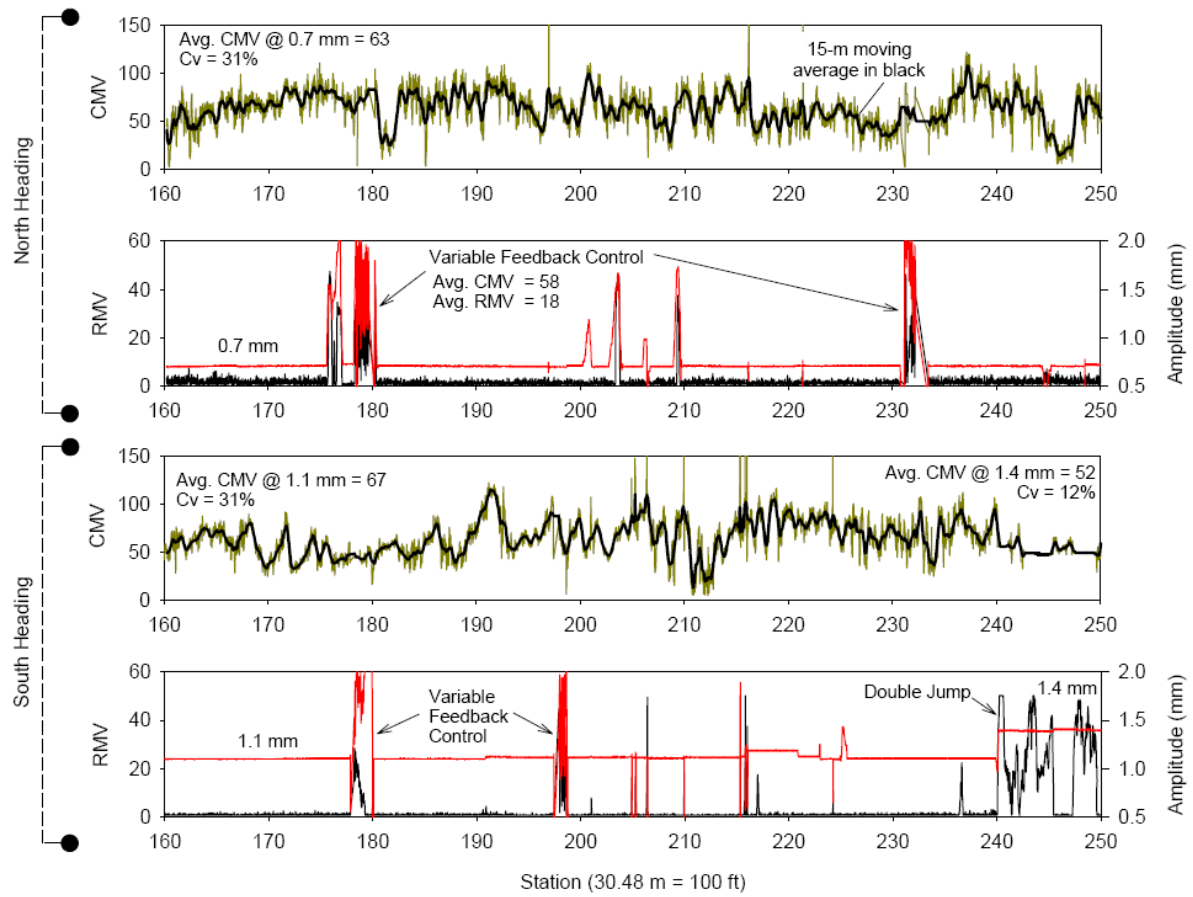


Figure 7. CMV, RMV, amplitude data for 2.7 km test section (White et al. 2008)

LABORATORY AND FIELD TESTING METHODS

Laboratory Testing Methods

Soil Index Properties

Particle-size analysis was conducted in accordance with ASTM D422-63(2002) “*Standard Test Method for Particle-Size Analysis of Soils*.” The coarse grained analysis was performed on samples of approximately 2000 g of air dried soil. Material retained on the No. 10 sieve was washed and oven dried prior to sieving. Fine-grained analysis was conducted using the hydrometer method on approximately 60 g air dried soil, passed through the No. 10 sieve. Following the completion of the hydrometer test, the material was washed through a No. 200 sieve and oven dried prior to sieving.

Atterberg limits were determined in accordance with ASTM D4318-05, “*Liquid Limit, Plastic Limit, and Plasticity Index of Soils*.” Liquid limit tests were performed according to Method A (multi-point liquid limit method). Based on the Atterberg limits and particle size analysis test results, the soils were classified according to AASHTO and Unified Soil Classification System (USCS).

Specific gravity was determined in accordance with ASTM D 854-06, “*Standard Test Methods for Specific Gravity of Soil Solids by Water Pycnometer*”. Representative samples for the test were prepared and tested according to Method A – Procedure for oven-dried specimens.

Proctor Compaction

Laboratory Proctor compaction tests were performed in accordance with the ASTM D 698–00 “*Standard Test Methods for Laboratory Compaction Characteristics of Soil Using Standard Effort*”, and the ASTM D 1557–02 “*Standard Test Methods for Laboratory Compaction Characteristics of Soil Using Modified Effort*” standard test procedures. An automated, calibrated mechanical rammer was used to perform these tests.

In-Situ Testing Methods

Zorn Light Weight Deflectometer

Zorn light weight deflectometer (LWD) setup with a 10-kg drop weight at drop height of 71-cm and 300-mm plate diameter is used for this project (see Figure 8(a)). The device uses a constant plate contact force of 7.07 kN in the modulus calculation procedure, which is based on calibration measurements made on a concrete pad. Deflections are obtained from an in-built accelerometer mounted in the loading plate. Using the contact stress and deflection values, the elastic modulus is then calculated as:

$$E_{LWD-23(71)} = \frac{(1 - \nu^2) \sigma_0 a}{d_0} \times f \quad (4)$$

Where, E_{LWD} = elastic modulus determined using 300-mm Zorn LWD setup with 71-cm drop height (MPa), d_0 = measured settlement (mm), ν = Poisson's Ratio (assumed as 0.4), σ_0 = applied stress (MPa), a = radius of the plate (mm), f = shape factor assumed as $8/3$ (Note that the Zorn LWD outputs the E_{LWD} value using manufacturer settings as $\nu = 0.5$ and $f = 2$, and these values are corrected using the values stated above for theoretical reasons (for details see Vennapusa and White 2008).

Dynamic Cone Penetrometer

The dynamic cone penetrometer (DCP) is shown in (Figure 8b) is used to measure of strength characteristics of compacted fill materials in accordance with ASTM D6951 “*Standard Test Method for Use of Dynamic Cone Penetrometer for Shallow Pavement Applications*”. The test procedure involves dropping an 8-kg hammer from a drop height of 575 mm and measuring the penetration rate of a 20-mm-diameter cone. Dynamic penetration index (DPI) with units of mm/blow is determined from the test. The DPI values are inversely related to penetration resistance (i.e. soil strength). An average DCP index value (DPI_{300}) for the upper 300-mm depth of the compaction layer is calculated as a ratio of penetration depth and cumulative blows required to reach the penetration depth. DPI values are empirically correlated to California Bearing Ratio (CBR) using Equation 5 provided by ASTM D6951.

$$CBR_{300} = \frac{292}{(DPI_{300})^{1.12}}, \text{ all soils except for CH and CL soils with } CBR < 10 \quad (5)$$

Clegg Hammer

Clegg impact hammers were developed by Clegg during late 1970's and later standardized as ASTM D5874 for evaluating compacted fill and pavement foundation layers (see Figure 8(c)). A 20-kg weight Clegg hammer was used on the project. The Clegg impact value ($CIV_{20\text{-kg}}$) is derived from the peak deceleration of a 20-kg hammer free falling 450 mm in a guide sleeve for four consecutive drops.

Nuclear Gauge

A calibrated nuclear gauge (NG) device (see Figure 8(d)) was used on this project to provide rapid measurement of soil unit weight and moisture content. Tests were performed following ASTM WK218 “*New Test Method for In-Place Density and Water (Moisture) Content of Soil*”. Two measurements of moisture and dry unit weight were obtained at a particular location and an average value is reported. Probe penetration depths varying from 200 mm (8 in.) to 250 mm (10 in.) were used in performing the tests.

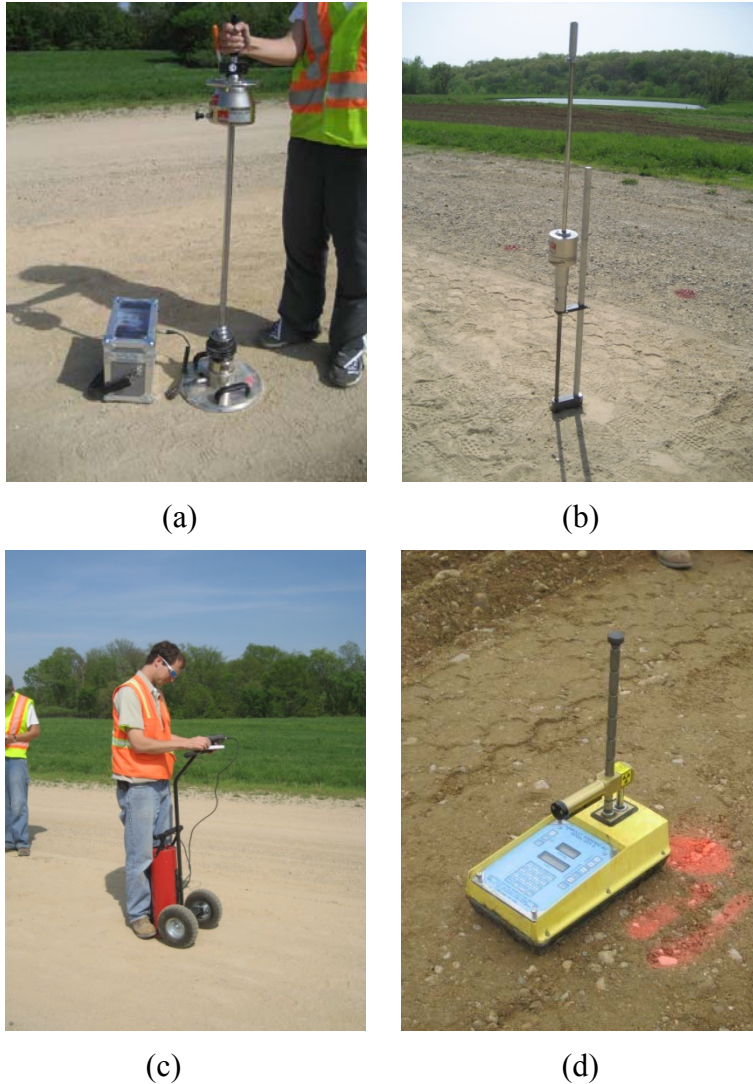


Figure 8. (a) 300-mm Zorn LWD, (b) DCP, (c), 20-kg Clegg hammer, (d) Nuclear moisture-density gauge

Earth Pressure Cells (EPCs)

EPCs of three measurement ranges (0 – 600 kPa, 0 – 1000 kPa, and 0 – 2500 kPa) were used in this study to measure the in-ground triaxial stresses developed under the roller during soil compaction operations. The EPCs used are semiconductor type sensors manufactured by Geokon[®] (3500 series). They are made of two stainless steel plates welded together around their periphery and separated by a narrow gap filled with deaired hydraulic fluid. Weiler and Kulhawy (1982) stated several possible factors that can affect the stress cell measurements of which many can be minimized by selecting appropriate stress cell type and controlling its geometry, and others by performing careful laboratory calibration (Labuz and Theroux 2005). A summary of several factors that affect these measurements along with appropriate measures taken to minimize the associated errors in the current study are provided in Table 12.

Table 2. Factors affecting EPC measurements and measures taken to minimize the errors

No	Factor	Wieler and Kulhawy (1982) recommended correction method	Procedure followed to minimize the errors
1	Cell thickness (T) to diameter (D) aspect ratio	Use relatively thin cells ($T/D < 1.5$)	$T = 10$ mm, $D = 100$ mm $T/D = 0.1 < 1.5$
2	Ratio of soil to cell stiffness, S	Design cell for high stiffness ($S < 0.5$) and use correction factors	Stainless steel gauges designed to minimize these effects
3	Diaphragm deflection (arching)	Design cell such that diaphragm diameter to diameter deflection ratio (d/Δ) $> 2,000 - 5000$	
4	Eccentric, non-uniform and point loads	Increase stress cell active diameter ($d/D_{50} \geq 50$)	
5	Stress concentrations at cell corners	Use inactive outer rims to reduce sensitive area ($d^2/D^2 < 0.25 - 0.45$). Perform laboratory calibration of EPC measurements using same soil used around the EPCs in field (Labuz and Theroux 2005).	Laboratory calibration of EPCs in Ottawa sand layer compacted to its maximum density and maintaining similar conditions in field
6	Lateral stress rotation	Use theoretical correction factors	
7	Stress-strain soil behavior of soil	Calibrate cell under near-usage conditions	
8	Placement effects	Random error; use duplicate measurements	
9	Proximity of structures and other stress cells	Minimum distance between EPCs is recommended as follows: 1. clear horizontal spacing $> 1.5 D$ 2. clear vertical spacing $> 4D$	Used minimum horizontal spacing of 250 mm ($> 1.5 \times 100$ mm), and minimum vertical spacing of 450 mm ($> 4 \times 100$ mm)
10	Dynamic stress measurements	Use dynamic calibration or use cells that have high frequency response rate (e.g. semiconductor type gauges).	Semiconductor type EPCs with frequency response of 2000 Hz (roller vibration frequency ~ 30 Hz)
11	Applied stresses	Check cell design for yield strength (steel and titanium cells have high yield strength)	Stainless steel strain gauges
12	Temperature	Calibrate or use balance resistors	Thermistor inside the cell to monitor temperature variations

Description of the EPC Calibration Chamber

The EPC manufacturer provided a fluid calibration, however, this calibration does not account for the effects of stress-strain behavior of the soil surrounded by the sensor and errors associated with stress concentration at cell corners, lateral stress rotation, and placement effects as stated in Table 2. It is important that the soil type and density used in the calibration procedure be maintained in the field to obtain reliable stress measurements (Labuz and Theroux 2005). To account for these effects the EPCs were calibrated in a uniform graded dry Ottawa # 10 sand using a specially fabricated calibration chamber at Iowa State University. A schematic cross-section of the calibration chamber is shown in Figure 9.

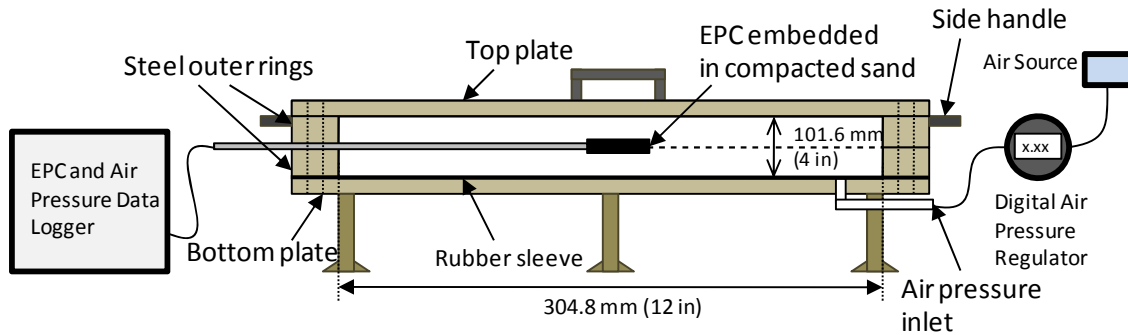


Figure 9. Schematic cross-section of the EPC calibration chamber

The calibration chamber setup consists of three main components namely: (a) a stainless steel chamber with 305 mm and 280 mm internal and external diameters, respectively, (b) a digital air pressure regulator (0 to 200 psi range), and (c) a data logger to record the EPC and air pressure readings. The steel chamber is composed of five parts: (a) bottom plate, (b) rubber sleeve placed on the bottom plate, (c) bottom outer ring, (d) top outer ring, and (e) top plate. The bottom portion of the chamber consists of a steel plate connected to an outer ring with 12 bolts by sandwiching the rubber sleeve as shown in Figure 9 and Figure 10(a). The rubber sleeve is used for uniform air pressure distribution in the sand. The upper portion of the chamber consists of another outer ring and a solid steel plate on the top together connecting to the bottom portion using 12 additional bolts (see Figure 10(d)). The EPC is embedded in the compacted sand layer of the chamber (see Figure 9 and Figure 10(c)) and is connected to a data logging system as illustrated in Figure 9. The digital air pressure regulator is used to regulate the applied air pressure in the chamber through a pressure inlet as shown in Figure 9. The pressure regulator is connected to the data logger to record the air pressure measurements simultaneously with EPC readings. A picture of complete setup of the EPC calibration chamber is shown in Figure 11.

Calibration Procedure

A total of 15 stress sensors were calibrated for this study. Calibration was conducted by placing the sensors in a clean Ottawa sand compacted to an average dry density of 101.3 pcf (1623.6 kg/m³) with a standard deviation of 1.01 pcf (16.3 kg/m³).

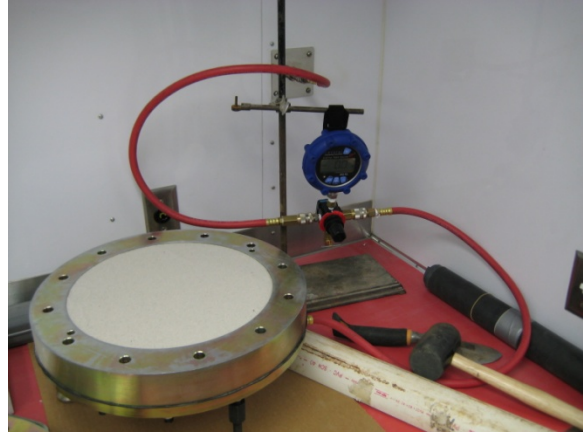
Steps followed in performing each calibration test are as follows:

1. The bottom portion of the chamber is first setup as shown in Figure 10(a).
2. Sand material is poured into the chamber to form a cone shape, leveled, and then compacted by tamping on the chamber using a rubber hammer. Extra sand was placed as the sand gets compacted until a level surface is obtained with the top of the outer ring as shown in Figure 10(b).
3. An EPC is placed in the chamber such that the sensing portion of the cell is at the center of the chamber.
4. The upper outer ring is placed on top of the bottom ring (Figure 10(c)).
5. Sand material is poured on top of the cell to fill the outer ring and the process in step 2 is repeated until a level surface is reached (see Figure 10(d)).
6. The top plate is placed on the outer ring and bolts are tightened to ensure an air tight seal around the edges.
7. Air pressure in increments of 10 psi (69 kPa) starting from 0 psi (0 kPa) is applied (loading) to the pressure chamber. EPC readings (mV output) are recorded from each pressure increment. Maximum air pressures of 80 psi (550 kPa), 100 psi (690 kPa), and 120 psi (827 kPa) were applied to the 0-600 kPa, 0-1000 kPa, and 0-2500 kPa range stress sensors, respectively.
8. After reaching the maximum pressures, the air pressure is reduced (unloading) in increments of 10 psi (69 kPa).
9. The loading and unloading procedure is repeated for at least two cycles to evaluate repeatability of the measurements.
10. The results obtained are presented in a graphical format as shown in Figure 12 (for a 0-1000 kPa stress sensor), to obtain the calibration factors for converting mV output to applied stresses in kPa.

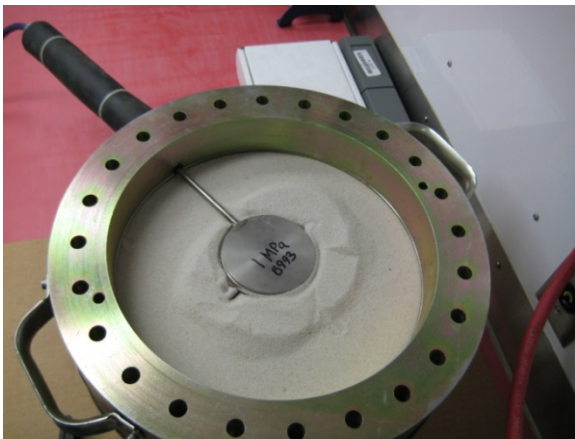
Figure 12 also presents results of air pressure and corresponding stress sensor readings obtained from a test where the air pressure was gradually increased to a maximum of about 690 kPa. The stress sensor readings were plotted using the calibration factors obtained from the test. These results demonstrate that the calibration factors obtained are appropriate. Example results from a stress cell calibration test are shown on Figure 12.



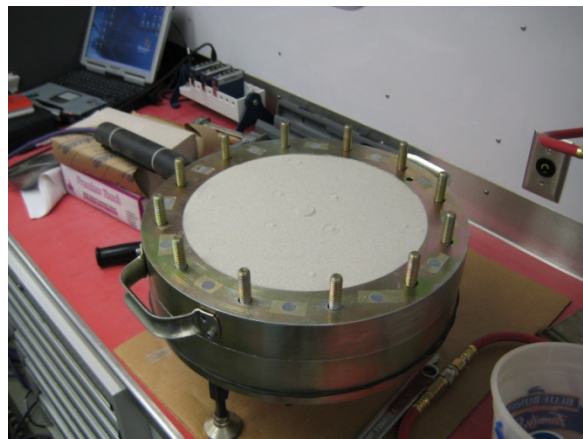
(a)



(b)



(c)



(d)

Figure 10. Calibration setup with placement of sand layer above and below the sensor

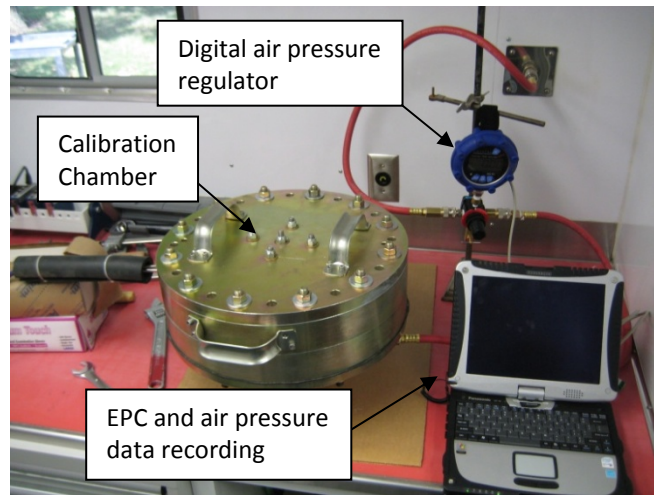


Figure 11. Complete setup of the EPC calibration chamber

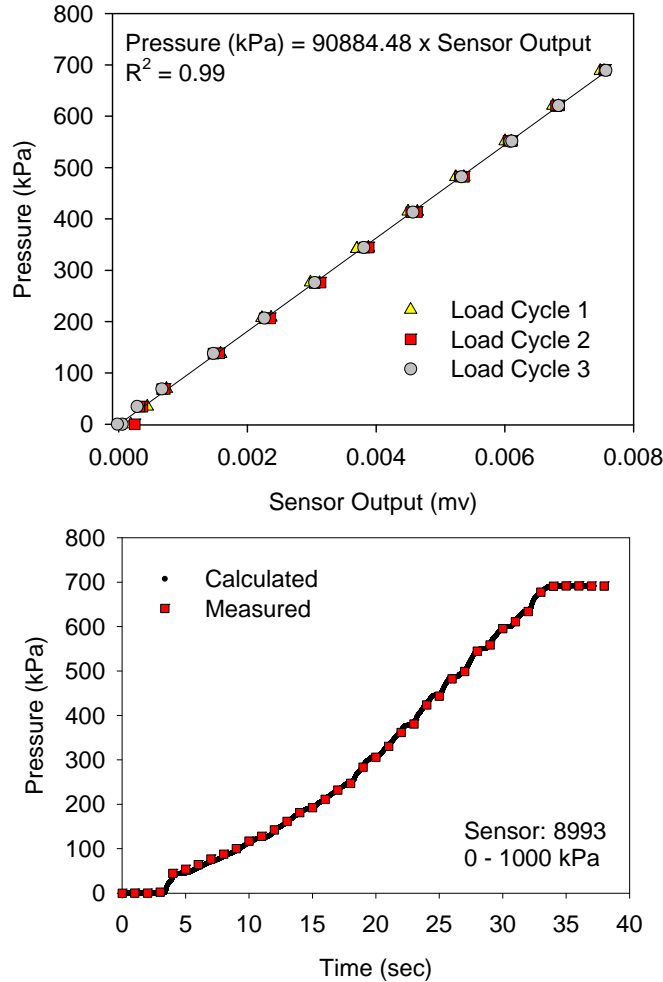


Figure 12. EPC calibration test results (sensor 8993)

Field Installation of EPCs

To simulate conditions consistent with the laboratory calibration procedure, the sensors were embedded in the test beds within a layer of the dry Ottawa sand. The loads applied onto the stress sensors would thus be transferred through the sand similar to the calibration testing. The sand was compacted by hand, and it is anticipated that the sand would reach its density similar to calibration conditions as roller compaction occurs. The following steps were followed in installing the EPCs in the test beds:

1. A trench was excavated to the desired elevation,
2. Locations and spacings for EPCs to place in orthogonal directions (following recommendations outlined in Table 2) were selected,
3. EPCs were placed on a thin layer of sand and sensors were leveled using a bubble level,
4. GPS readings were obtained (for spatial co-ordinates) on top of the sensors,
5. A thin layer of sand was placed around the sensors with the aid of thin cardboard forms,
6. Fill material was placed around the cardboard form, and the material was compacted by

- hand tamping,
7. After compacting the material around the sensors, the cardboard forms were slowly removed from the ground while concurrently compacting soil outside the forms.

Pictures following these steps during the field installation procedure are shown in Figure 13 to Figure 16. Sensors were installed in several intermediate layers of fill placed in the test beds. A minimum vertical spacing of 450 mm was maintained between sensors placed in different lifts of fill material.



Figure 13. Excavation to install EPC's (left) and installation of EPC's in orthogonal directions



Figure 14. Leveling of EPC's and placement of thin layer of silica sand below EPC's



Figure 15. GPS readings on EPC's



Figure 16. Placement of sand (~ 2 in) around the EPCs

Compaction Machines

The three machines (CS 563, CS 683, and CP 563) used in this study are shown in Figure 17, Figure 18, and Figure 19, respectively. Details for each machine including roller configuration, weight and dimensions, and operation parameters (frequency and amplitude) are provided in Table 2. The smooth drum CS 563 and 683 rollers were equipped with CMV and RMV, and the padfoot roller was equipped with CMV, RMV, and MDP compaction measurement technologies.

Table 3. Specifications of the machines used in this study (from Caterpillar, Inc. Manuals)

Parameter	CS 563 (smooth drum)	CS 683 (smooth drum)	CP 563 (pad foot)
Compaction Measurement Values	CMV, RMV	CMV, RMV	MDP, CMV, RMV
Drum width	2.13 m (7 ft)	2.13 m (7 ft)	2.134 m (7 ft)
Drum Diameter	1.52 m (5 ft)	1.52 m (5 ft)	1.30 m (4.25 ft) 1.55 m (5.08 ft)*
Machine Operating Weight	11,120 kg (24,520 lb)	18,500 kg (40,785 lb)	11,555 kg (25,479 lb)
Weight at Drum [§]	5780 kg (12,745 lb)	13,200 kg (29,100 lb)	6020 kg (13,274 lb)
<i>Centrifugal force at standard operating frequency</i>			
High Amplitude	266 kN (60,000 lb-f)	332 kN (74,600 lb)	266 kN (60,000 lb-f)
Low Amplitude	133 kN (30,000 lb-f)	166 kN (37,300 lb)	133 kN (30,000 lb-f)
Standard Frequency	31.9 Hz (1914 vpm)	30 Hz (1800 vpm)	31.9 Hz (1914 vpm)
Nominal High Amplitude	1.70 mm	1.70 mm	1.87 mm
Nominal Low Amplitude	0.85 mm	0.85 mm	0.85 mm
<i>Pads</i>			
Number of pads	—	—	140
Pad height	—	—	127 mm (5 in)
Pad face area	—	—	8940 mm ² (13.9 in ²)

* Diameter over pads

[§] Includes the canopy weight



Figure 17. Caterpillar CS563 smooth drum vibratory roller



Figure 18. Caterpillar CS683 smooth drum vibratory roller



Figure 19. Caterpillar CS563 padfoot vibratory roller

REPEATABILITY AND REPRODUCIBILITY OF CMV, RMV, AND MDP

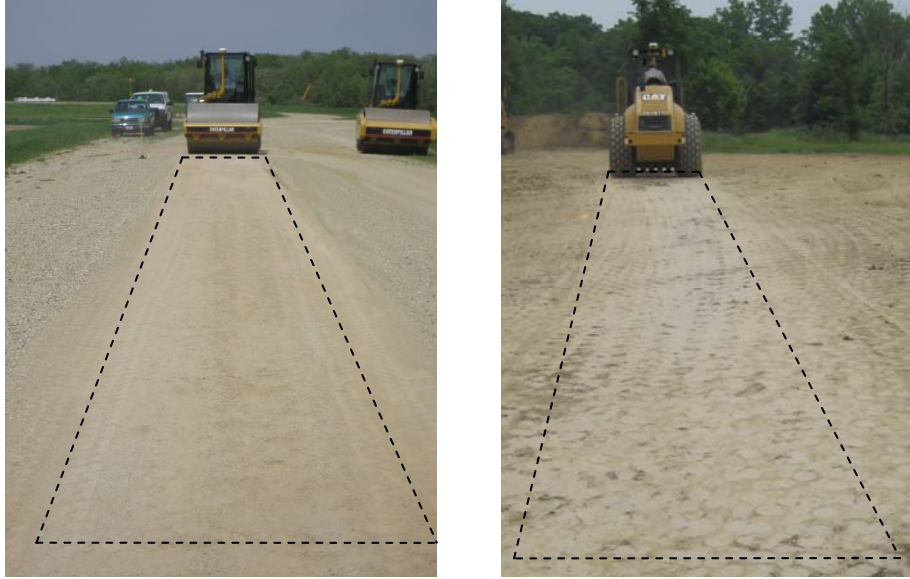
The precision of roller-integrated compaction measurement values CMV, RMV, and MDP in a repeatability and reproducibility context for three different machines is described herein. As with any in-situ device, assessment of the precision of its measurements plays a major role in interpreting the reliability of the data and establishing credible specifications. The error associated with roller-integrated measurements is one of the contributors to scatter in relationships with in-situ compaction test measurements (White et al. 2008). Repeatability and reproducibility variations associated with the roller measurement values from CS-563 smooth drum, CS-683 smooth drum, and CP 563 padfoot rollers are quantified in this study. The smooth drum rollers were equipped with CMV and RMV, and the padfoot roller was equipped with CMV, RMV, and MDP monitoring technologies. New insights are also reported herein with respect to relationships between CMV and RMV that have implications on how RMV differs between two different sized machines and how RMV could be used in a variable feedback control mode to control drum operation mode..

Repeatability refers to the variation in repeat measurements made on the same subject under identical conditions (Taylor and Kuyatt 1994). This explains the variations observed in measurements made using the same machine, operator, and method over which the measuring property can be considered to be “constant” (or negligible change). Reproducibility refers to the variation in repeat measurements on the same subject under changing conditions (Taylor and Kuyatt 1994). The changing conditions may be due to different measurement methods, or machines used, or measurements made by different operators over which change in the measuring property could be non-negligible.

In this study, the repeatability variation was quantified from measurements collected by making repeated passes using a single operator that maintained constant amplitude and speed during roller operations. The reproducibility variation was determined from measurements collected by making repeated passes using a single operator that changed the vibration amplitude and roller speed and direction (forward or reverse) during roller operations.

Experimental Plan

Repeated passes using CS-563 and CS-683 rollers were performed on a compacted crushed aggregate surface road (test strip 1, Figure 20(a)), and repeated passes using the CP-563 roller were performed on a compacted glacial till subgrade surface (test strip 2, Figure 20(b)). This work was performed at the Caterpillar, Inc., Edwards, IL research facility on May 07, 2007. A summary of roller passes made for the two test strips is provided in Table 4. At least 10 repeated passes were made on each test strip by each machine under similar operating conditions to evaluate the measurement repeatability. Rollers were also operated under changing conditions to evaluate measurement reproducibility which included: (a) forward and reverse directions, (b) high and low amplitude (0.85 mm and 1.70 mm), and (c) high and low speed (3.2 km/h and 4.8 km/h nominal).



(a)

(b)

Figure 20. (a) Strip 1 – CS-563 and CS-683 smooth drum rollers (CMV, RMV) – hard unsurfaced aggregate road, (b) Strip 2 – CP-563 padfoot roller (MDP, CMV, and RMV) – hard compacted glacial till subgrade

Table 4. Summary of repeated roller passes

Roller	Drum	Material	Pass	Machine Gear/Direction	a (mm)	Nominal Speed, v (km/h)
CS-563 (strip 1)	Smooth	Compacted Crushed Aggregate Road	1	Forward	0.85	5.9
			2	Reverse	0.85	4.8
			3	Forward	0.85	4.8
			4	Reverse	0.85	4.8
			5 – 17	Forward	0.85	3.2
			18 – 30	Forward	0.85	4.8
			31	Reverse	0.85	4.8
			32 – 43	Forward	1.70	4.8
			44 – 45	Forward (Opposite)	1.70	4.8
CS-683 (strip 1)	Smooth	Compacted Crushed Aggregate Road	46 – 57*	Forward	1.70	3.2
			58 – 63	Forward	0.85	3.2
			64 – 69	Forward	0.85	4.8
CS-563 (strip 2)	Padfoot	Compacted Glacial Till Subgrade	1 – 12	Forward	0.31	3.2
			13 – 24*	Forward	0.31	4.8
			25 – 36	Forward	1.87	4.8

* followed by 300 mm Zorn LWD, 20-kg Clegg Hammer, and DCP tests

CS-563 Smooth Drum Roller Measurements

Average values of CMV, RMV, operating speed, and amplitude at different passes for the CS-563 roller are presented in Figure 21. Raw data plots from pass 1 to pass 57 are presented in Figure 22 to Figure 26. Visual interpretation of these figures indicates the following and these aspects are further addressed using statistical analysis later in this chapter.

- a. The CMV and RMV data visually appears repeatable i.e., the data from each pass parallels the consecutive pass data when identical operation parameters are used (i.e., similar amplitude, speed, and direction of travel). However, some differences can be noted between each pass. These differences can partially be due to the inherent measurement error (repeatability variation) and unavoidable systematic change in soil properties with increasing passes (i.e., compaction or de-compaction of the material).
- b. Differences are observed in CMV with change in nominal speed from 3.2 km/h to 4.8 km/h, roller gear direction (forward or reverse), and amplitude from 0.85 to 1.70 mm, which are related to inherent variation within each operating speed (repeatability) and variation between the two speeds of operation (reproducibility).

Figure 24 shows CMV and RMV data for passes 32 to 37 operated at $a = 1.70$ mm and $v = 3.2$ km/h (nominal). The data shows that as the RMV increased (above about 4) the CMV decreased. This response is consistent with results from Adam (1996). Figure 26 shows CMV and RMV data for passes 46 to 57 where the roller was operated at $a = 1.70$ mm and $v = 4.8$ km/h. The figure shows that the RMV gradually decreased and CMV increased for each pass in the zone where $RMV > 4$ was measured for passes 32 to 37. While the reasons for this gradual decrease are not clear at this point, it can likely be related to possible changing ground conditions (e.g. surficial material de-compaction).

Based on numerical simulations, Adam (1996) showed that the CMV tends to decrease rapidly with increasing RMV, i.e., when roller is in double jump mode. Double jumping has been theoretically defined as $RMV > 0$ (Adam and Kopf 2004). The data obtained from the current study also showed a decrease in CMV with increasing RMV (as discussed above), however, the effect is most predominant when $RVM > 4$ (see Figure 27). Therefore, $RMV > 4$ for this machine could be a suitable target for feedback control.

Results in Figure 27 show that double jumping was not occurring at low amplitude setting ($a = 0.85$ mm). Figure 27 also shows CMV-RMV relationship for the 683 machine (at $a = 0.85$ mm only). In this case CMV increased almost linearly with increasing RMV. Further investigation is warranted on this machine to check the CMV-RMV behavior at low and high amplitude settings.

The CS-563E machine used on a recently completed project on TH 64 in Ackeley, MN, used an RMV of 17 for controlling the amplitude in a variable feedback control mode of operation. Based on results presented in Figure 27, RMV of 17 may be too high for automatic feedback reduction of amplitude. Operation of the machine on-site supports this finding (see Figure 7). Further studies are warranted to check the efficiency of the variable feedback control system by reducing the controlling RMV-value to about 4.

To verify the ground stiffness conditions, 20-kg Clegg Hammer, 300-mm Zorn LWD, and DCP tests were conducted at 6 to 15 test locations across the strip 1. The in-situ spot test results along with CMV/RMV data from pass 16 ($a = 0.85$ mm) and pass 34 ($a = 1.70$ mm) are presented in Figure 28. The $CIV_{20\text{-kg}}$ and E_{LWD} values show variation similar to CMV measured at pass 16 where no double jump was observed. On average, the $CIV_{20\text{-kg}}$ and E_{LWD} values were about 1.2 times higher in the zone where RMV is > 4 when compared to where RMV is < 4 in pass 34 (see Table 5). Comparison to DCP in the top 300 mm test results did not show a clear distinction between the two zones. Table 5 presents a comparison summary between average CMV and RMV values for pass 16 and 34 along with in-situ spot test measurement values for the two zones. On average, the CMV measurements in pass 16 (no double jumping occurred in this pass) were about 2.1 times higher in the zone where RMV is > 4 when compared to where RMV is < 4 in pass 34 (see Table 5). A comparison to RMV of 17 is also presented in Table 5.

The relative change between CMV and RMV is important to document when evaluating roller measurement values in any earthwork construction project as it can affect the correlations and target values significantly, especially for hard ground conditions and high amplitude comaction operations.

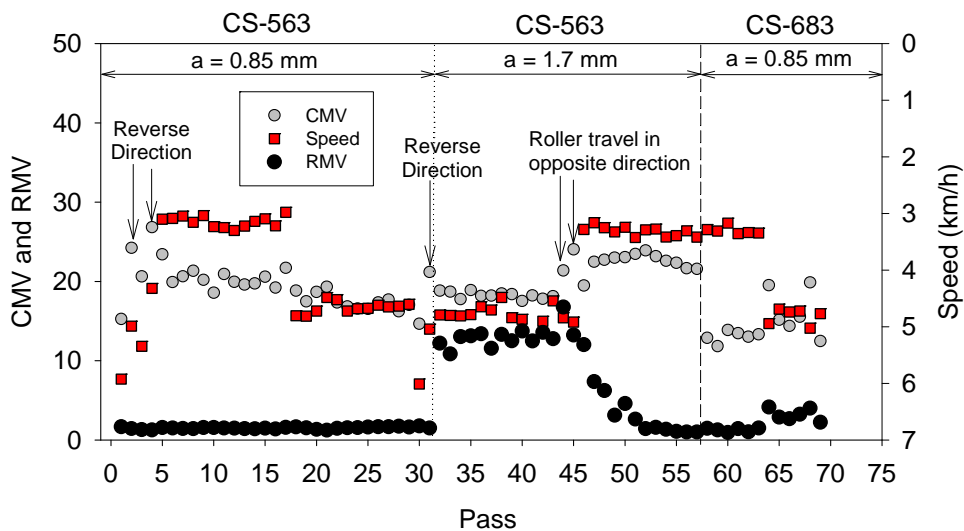


Figure 21. Summary of average CMV and speed of operation for test strip 1

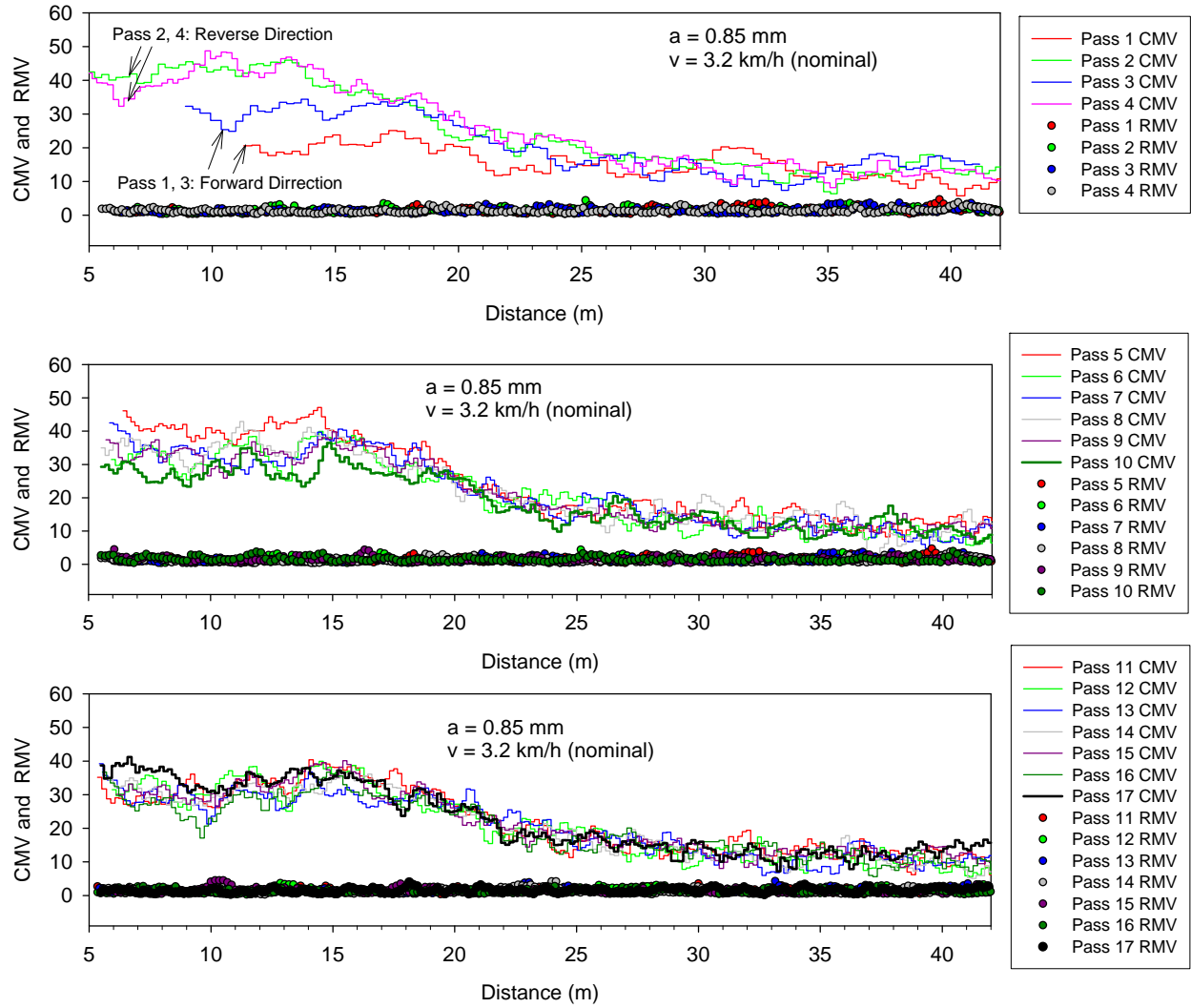


Figure 22. CMV and RMV data plots for pass 1 to 17 using CS 563 roller at $a = 0.85 \text{ mm}$

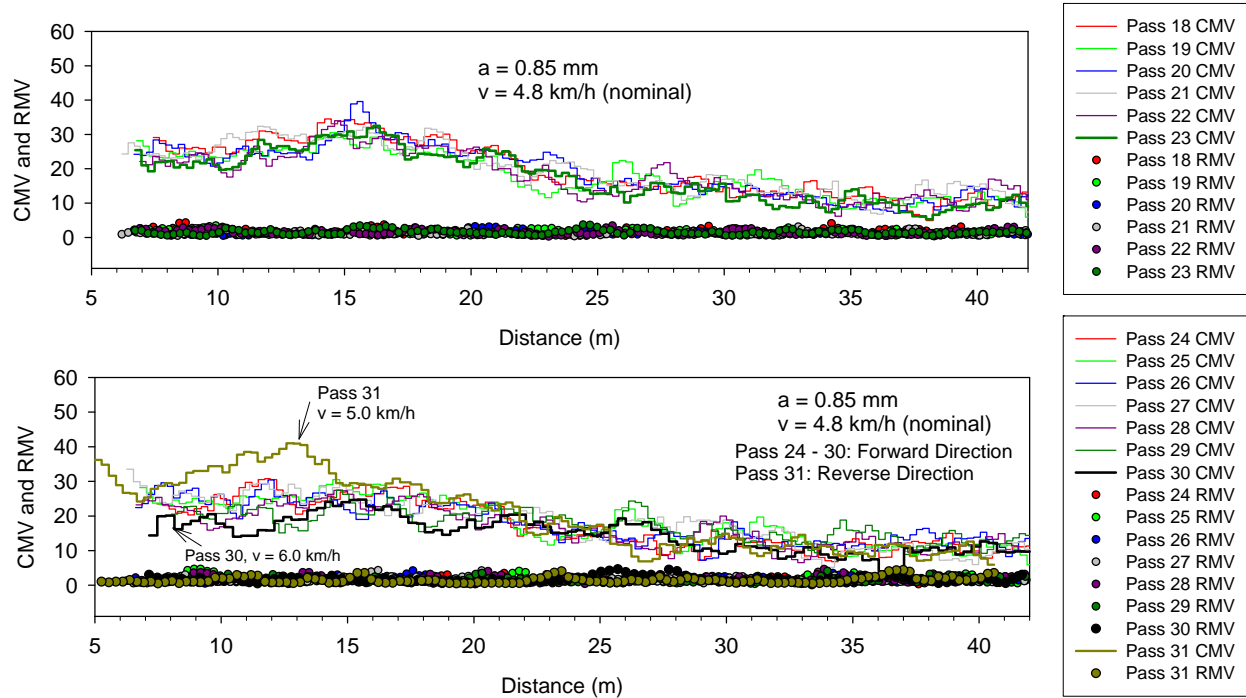


Figure 23. CMV and RMV data plots for pass 18 to 31 using CS 563 roller at $a = 0.85$ mm

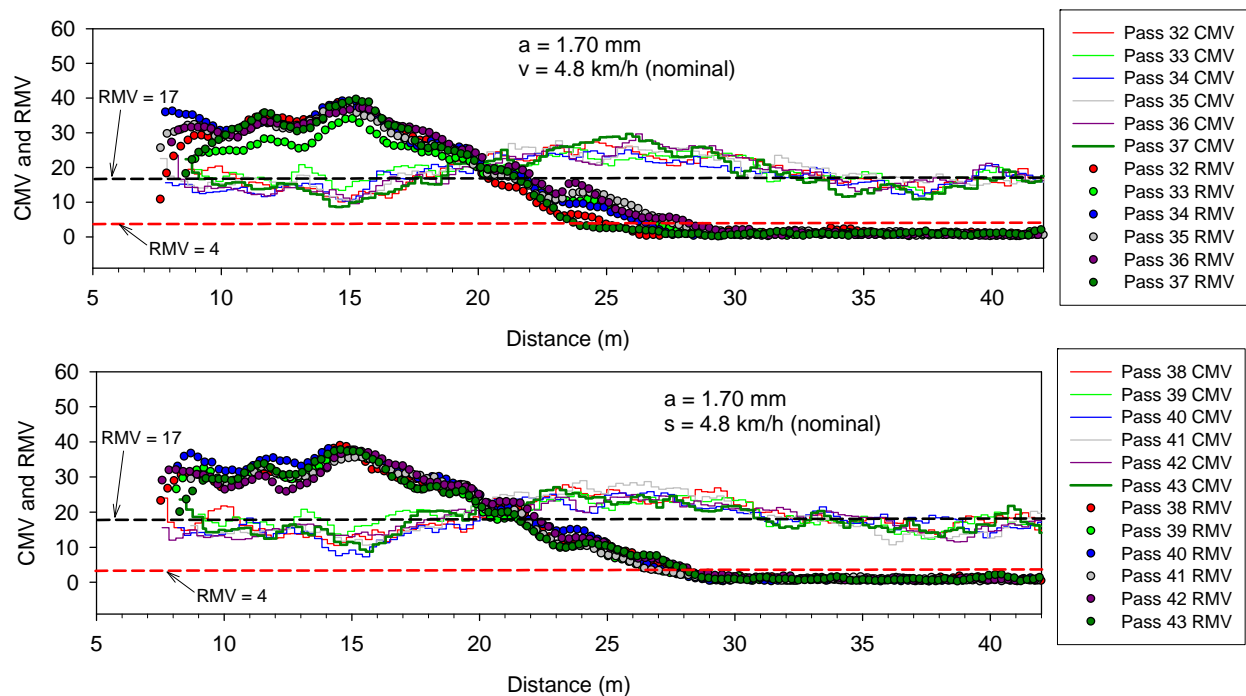


Figure 24. CMV and RMV data plots for pass 32 to 43 using CS 563 roller at $a = 1.70$ mm

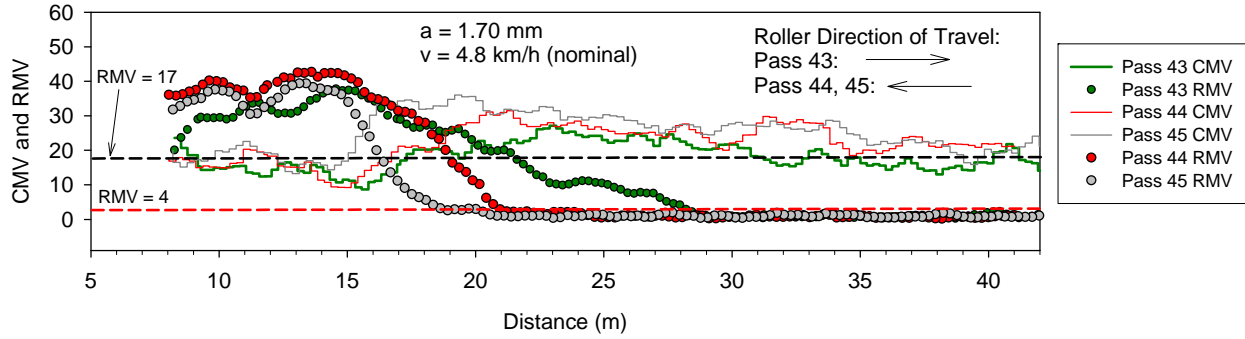


Figure 25. CMV and RMV data plots for pass 43 to 45 using CS 563 roller at $a = 1.70 \text{ mm}$

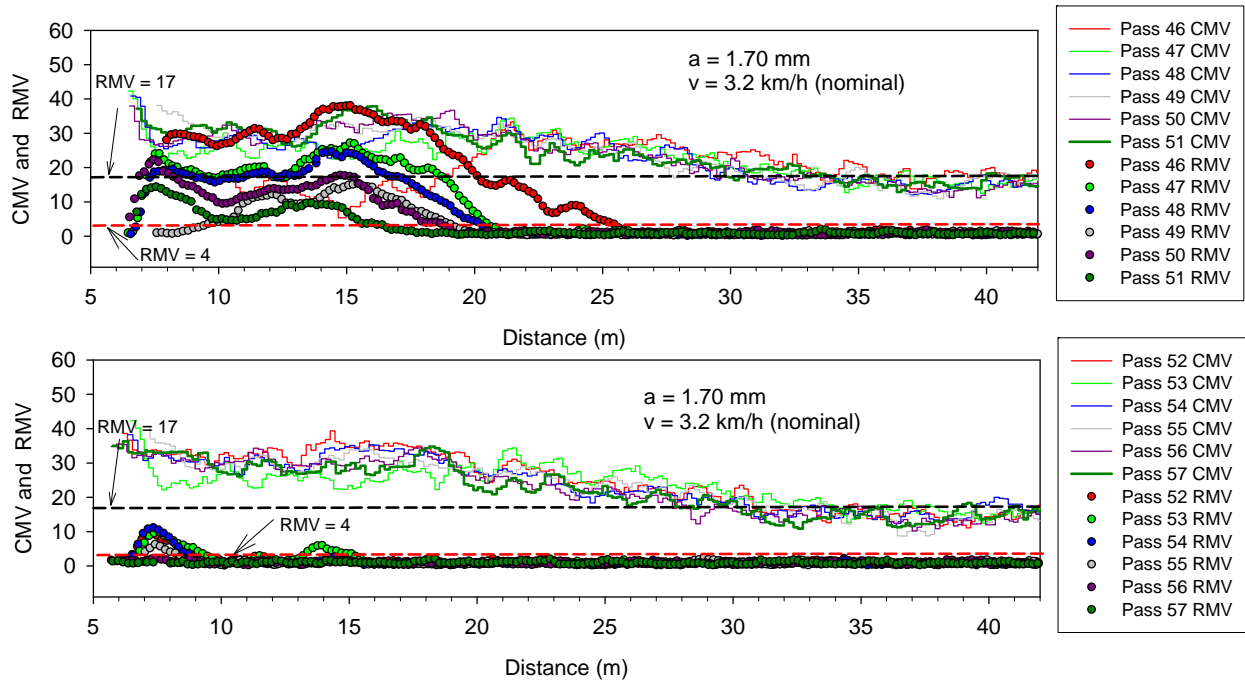


Figure 26. CMV and RMV data plots for pass 46 to 57 using CS 563 roller at $a = 1.70 \text{ mm}$

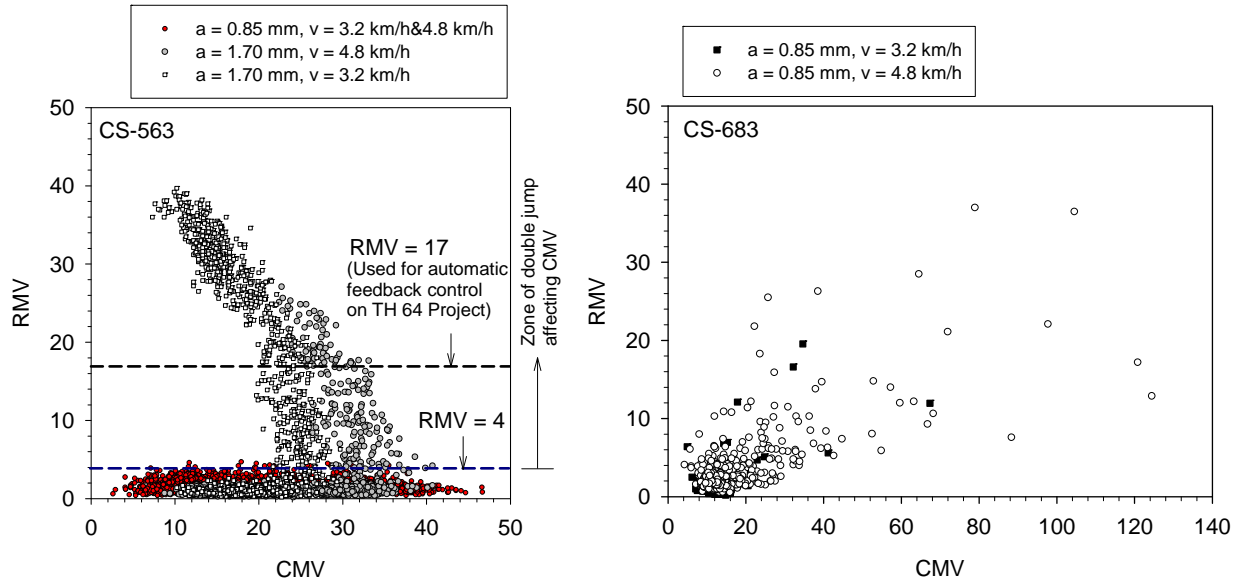


Figure 27. CMV and RMV comparison plots to define double jump and partial uplift zones for CS-563 and CS-683 rollers

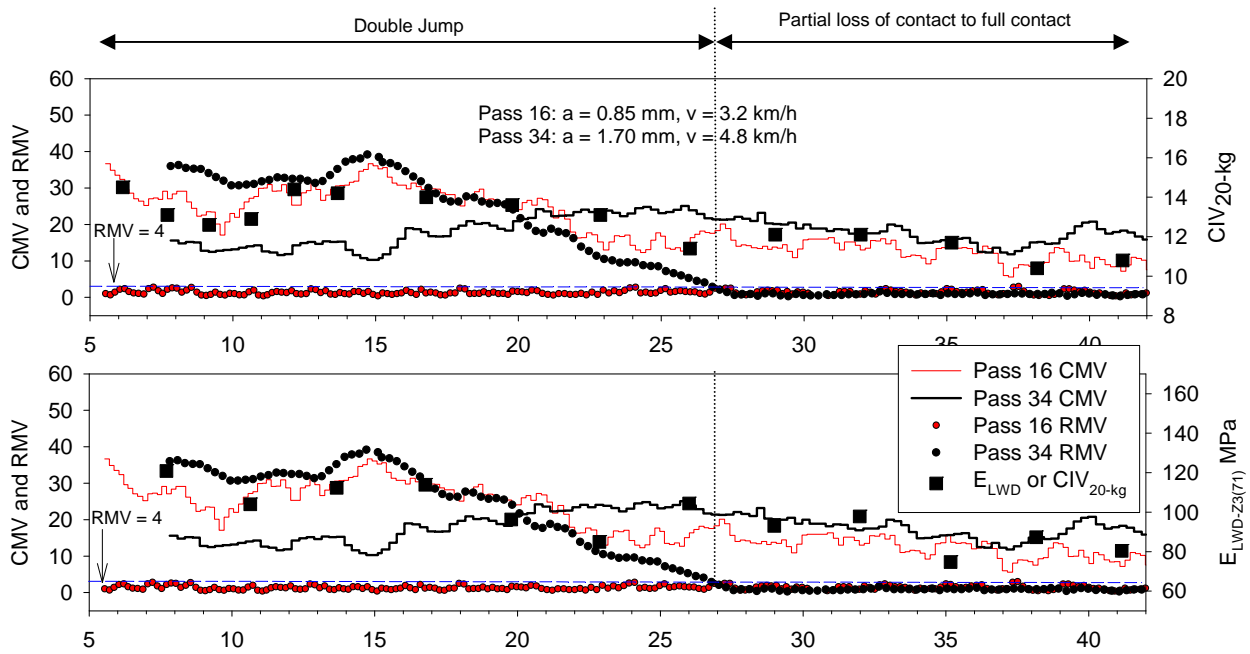


Figure 28. Comparison of CMV / RMV to E_{LWD} and CIV measurement values

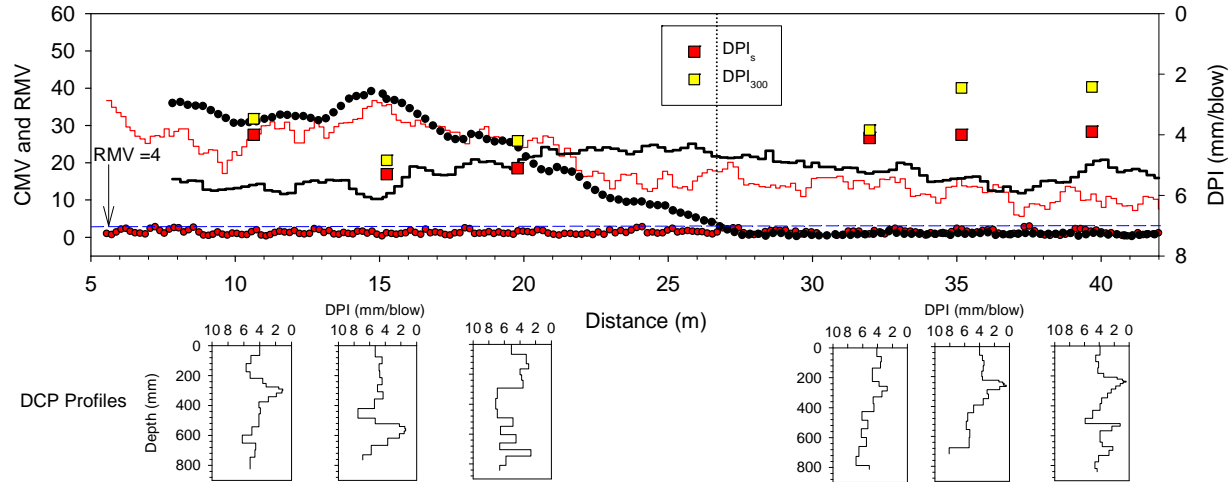


Figure 29. Comparison of CMV / RMV to DCP measurement values

Table 5. Difference in roller and in-situ compaction measurements

Parameter	Pass	v (km/h)	a (mm)	Average values over zone of RMV (given condition) for pass 34			
				< 17	> 17	< 4	> 4
CMV	16	3.2	0.85	13.4	28.1	11.5	24.7
	34	4.8	1.70	20.1	16.2	17.5	18.3
RMV	16	3.2	0.85	1.5	1.3	1.4	1.4
	34	4.8	1.70	4.1	30.4	0.9	24.3
$E_{LWD-Z3(71)}$ (MPa)	—	—	—	11.7	13.7	11.3	13.6
$CIV_{20\text{-kg}}$	—	—	—	91.1	109.4	87.2	105.3
DPI_{300} (mm/blow)	—	—	—	3.2	4.2	3.2	4.2

CS 683 Smooth Drum Roller Measurements

CMV and RMV data plots from CS 683 roller pass 58 to pass 69 are presented in Figure 30. The roller was operated at 3.2 and 4.8 km/h nominal speeds at $a = 0.85$ mm. It must be noted that this is a heavier roller (13,200 kg) and is expected to have differences in measurement influence depths when compared to the CS 563 roller (5780 kg). This consequently is expected to vary the CMV measurements. Average values shown on Figure 21 indicate that the CMV measurements from the 683 machine at $a = 0.85$ mm and $v = 3.2$ km/h are about 1.4 times lower than from the 563 machine at similar operating conditions. At higher speeds (4.8 km/h) the average CMV measurement values are more variable between each pass. Significantly higher CMV (> 30) measurement values were repeatedly recorded at several isolated locations especially when the machine was operated at higher speed (4.8 km/h). The RMV also generally increase at these

higher CMV locations. The reason is attributed to possible deep compaction, underlying hard layers or boulders, but will require detailed in-situ testing for further verification. The influence of underlying layer stiffnesses and possible change in compaction state of these underlying layers violates the assumption of material properties being “constant” for repeated passes. Therefore, the roller measurements at $v = 4.8$ km/h are not considered in the repeatability evaluation.

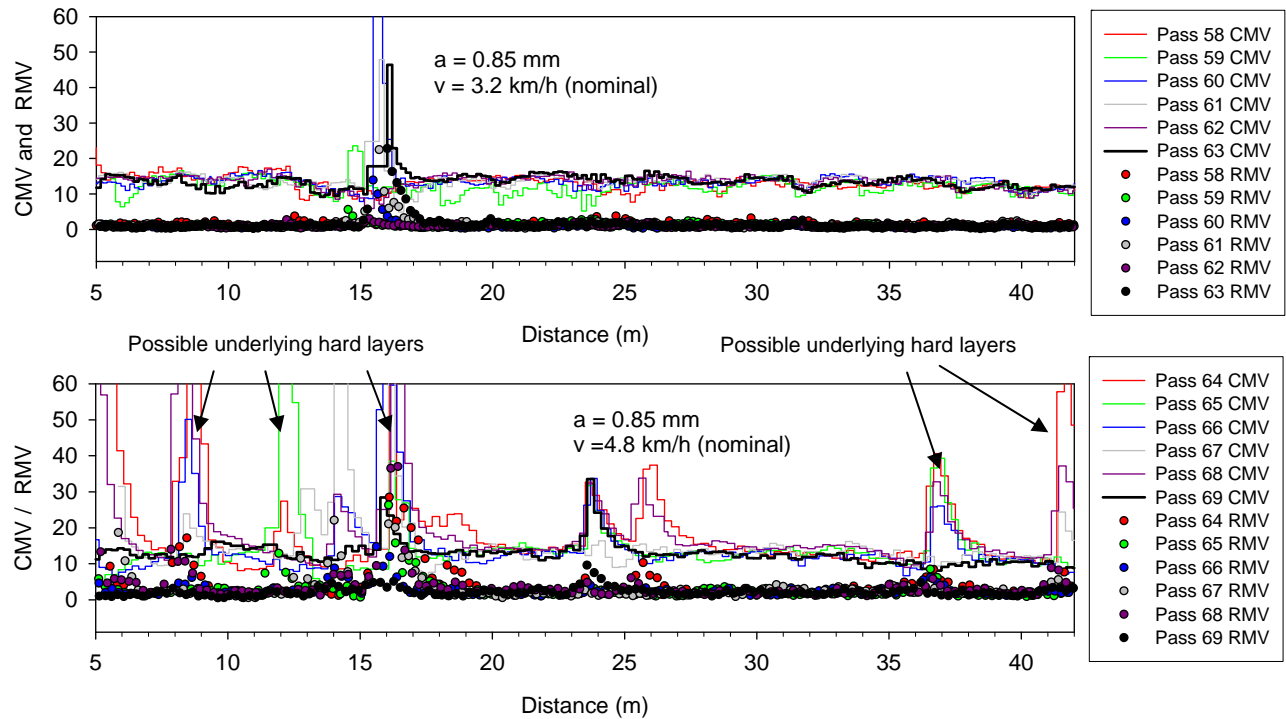


Figure 30. CMV and RMV data plots for passes 58 to 69 using CS 683 roller at $a = 0.85$ mm

CP 563 Padfoot Roller Measurements

Average values of MDP, CMV, operating speed, and amplitude at different passes from the CP-563 padfoot roller are presented in Figure 31. Raw data plots from pass 1 to pass 36 are presented in Figure 32 and Figure 33. Visual interpretation of these figures indicates the following and these aspects are further addressed from statistical analysis in the later sections of this chapter.

- a. The MDP data visually appears repeatable i.e., the data from each pass parallels the consecutive pass data under identical operating conditions (i.e., similar amplitude, speed, and direction of travel). On average, the MDP results appear to stay constant for each condition of operation. However, some differences can be noted in the raw data plots between each pass. These differences are partially due to the inherent measurement error (repeatability variation) and unavoidable systematic change in soil properties with increasing passes (i.e., compaction or de-compaction of the material).

- b. On average, the MDP values decreased from about -0.67 to -1.03 kJ/s with increase in nominal speed from 3.2 km/h to 4.8 km/h. However, some differences can be noted in the raw data plots and the reasons are attributed to inherent repeatability variation and reproducibility variation with change in operating conditions.
- c. On average, increase in amplitude from 0.85 mm to 1.87 mm increased the MDP values from about -0.67 to +0.69 kJ/s (for $v = 3.2$ km/h).
- d. The CMV raw data plots indicate that the CMV is not repeatable across the test strip between each pass. No additional repeatability analysis was performed on the CMV dataset.

Following roller pass 24, 300-mm Zorn LWD and DCP tests were conducted at 4 to 10 locations across the test strip. The test results in comparison to MDP measurement values at 0.85 and 1.87 mm amplitude is presented in Figure 34. The in-situ test measurements, especially, E_{LWD} measurement values generally followed the variation observed in MDP from pass 24 ($a = 0.85$ mm).

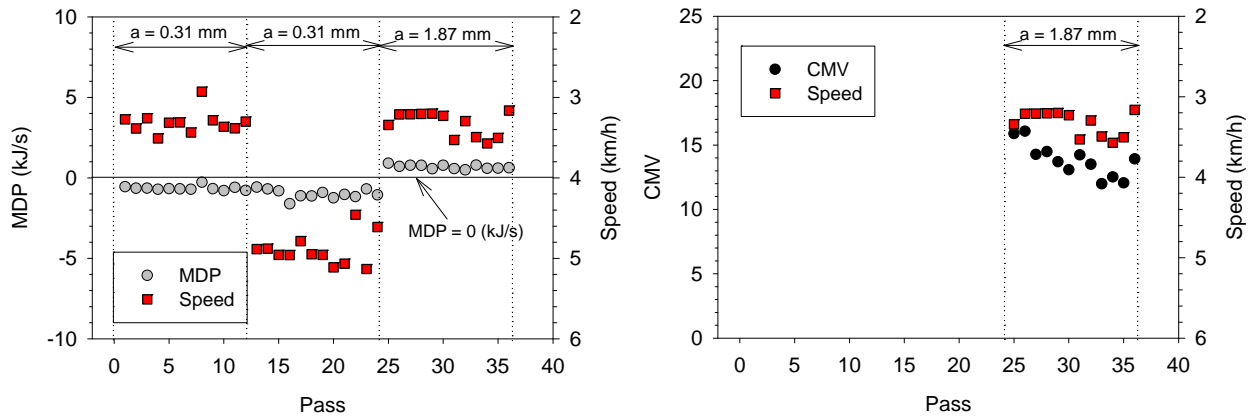


Figure 31. Summary of average MDP, CMV, and speed of operation for several passes on repeatability test strip 2

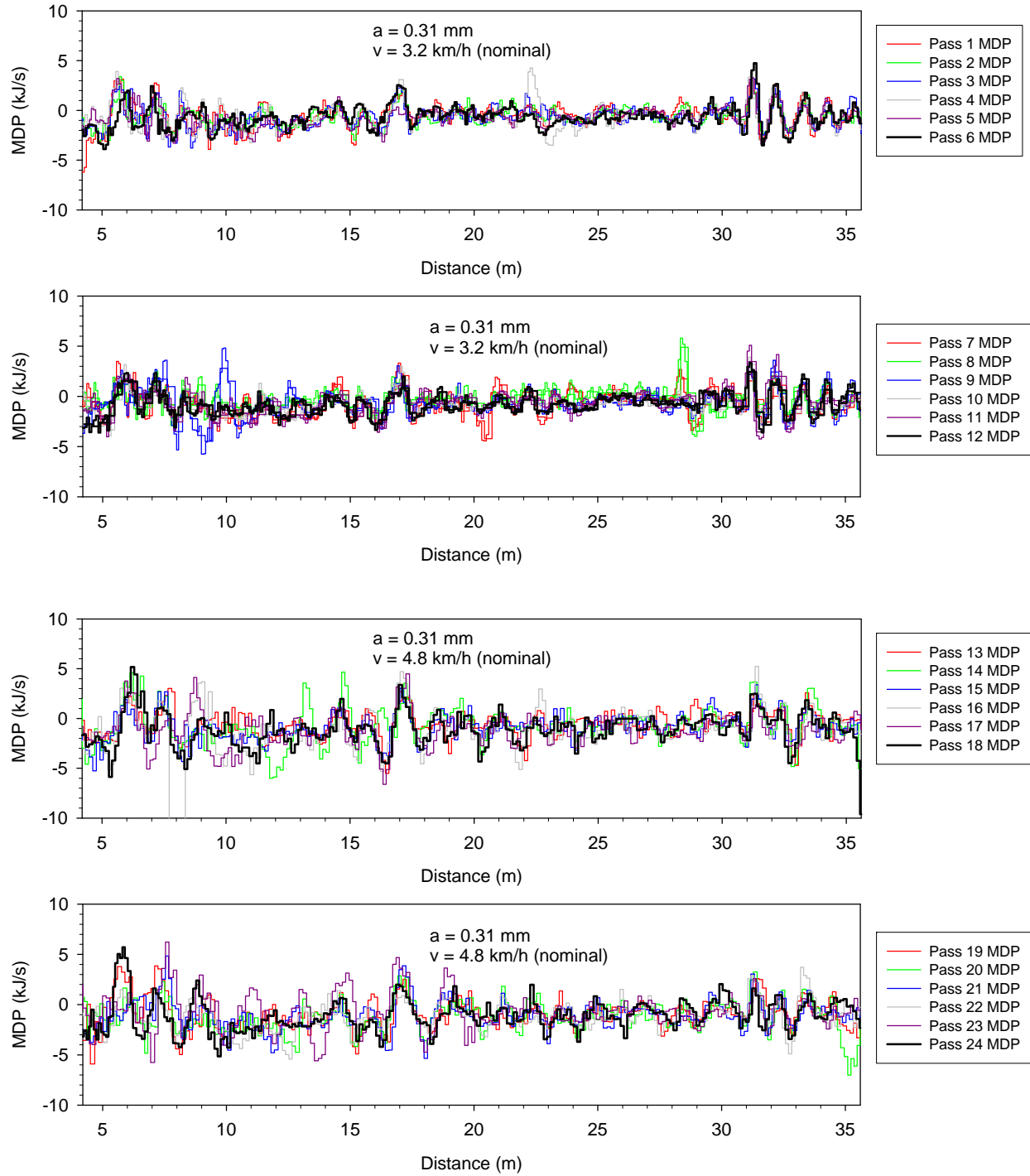


Figure 32. MDP raw data plots for pass 13 to 24 using CP 563 (padfoot) roller at $a = 0.31$ mm

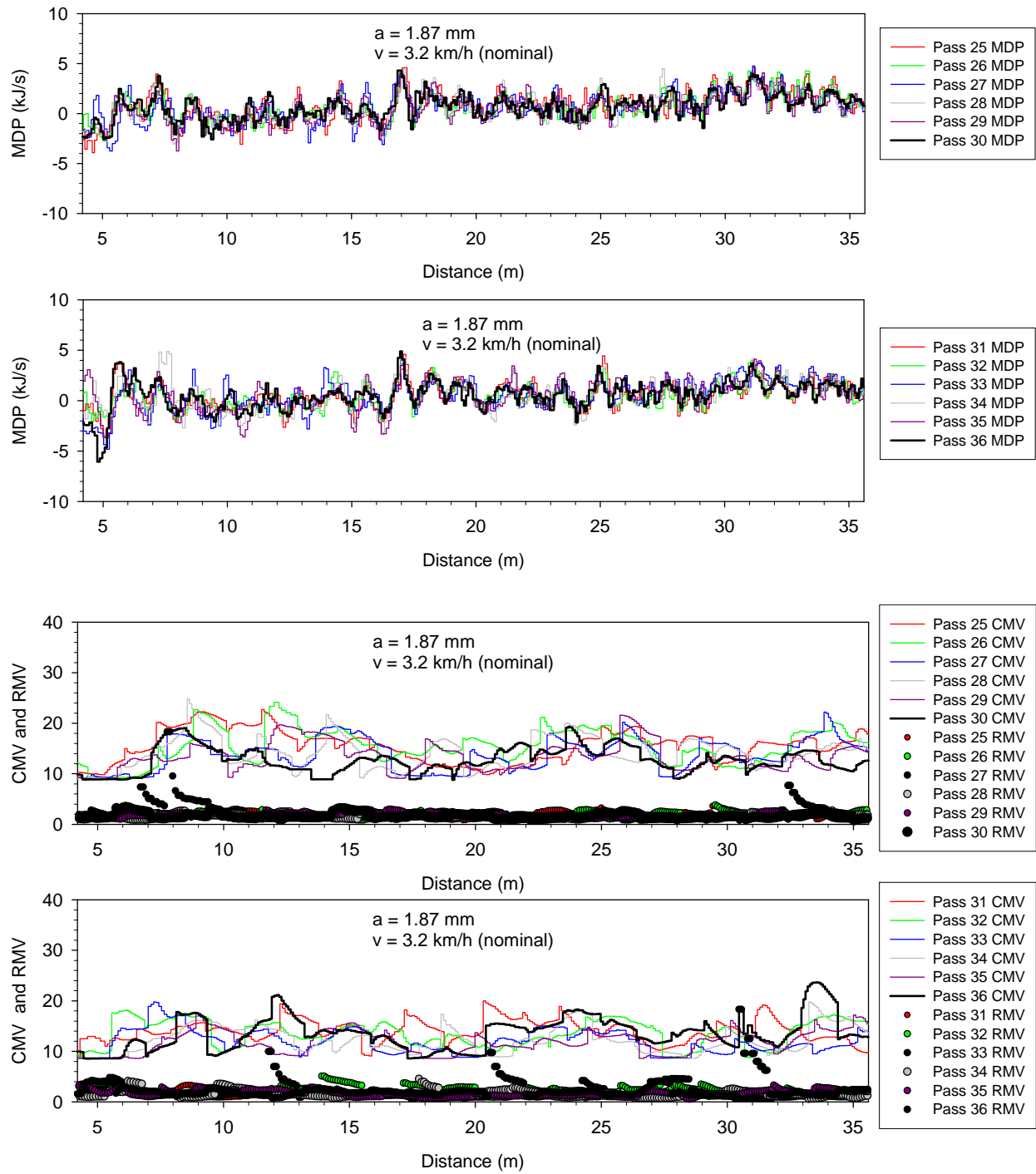


Figure 33. MDP and CMV raw data plots for pass 25 to 36 using CP 563 (padfoot) roller at $a = 1.87 \text{ mm}$

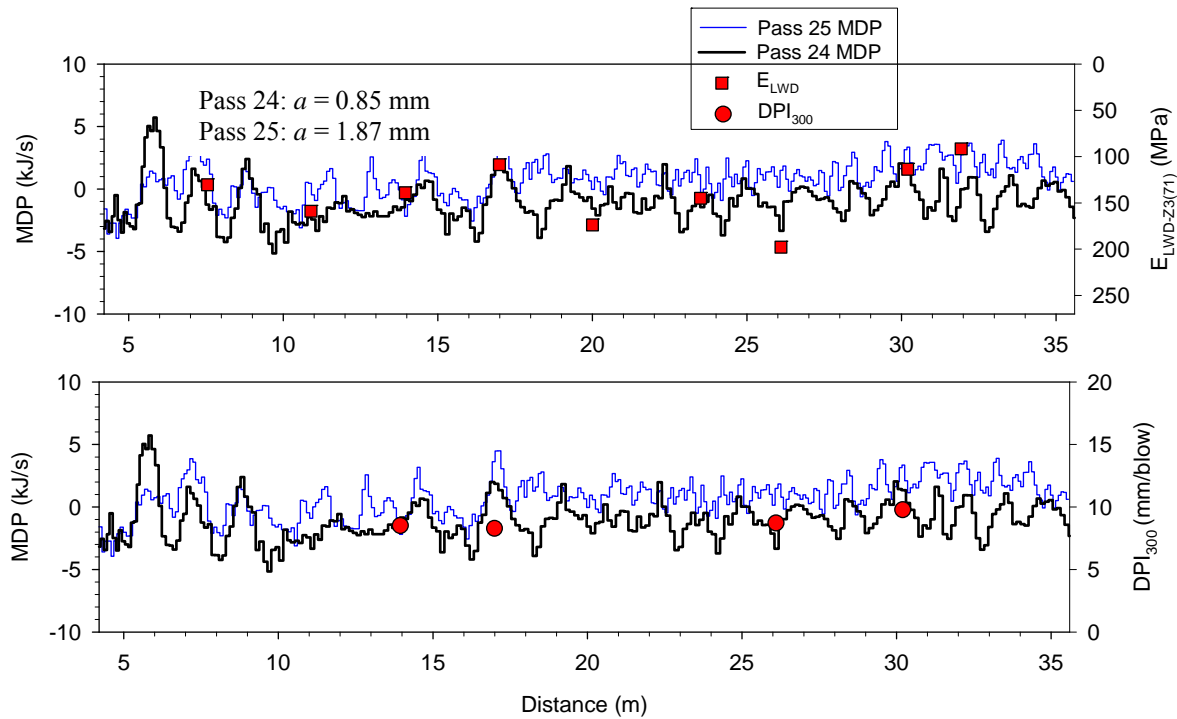


Figure 34. Comparison between MDP and in-situ compaction test measurement values

Statistical Evaluation of Results

The measurement precision can be evaluated only when repeated measurements are made at one particular location. However, the roller measurement values are not reported to exactly the same spatial location for each pass. To overcome this problem, the data output files were processed in such a way that an averaged data is assigned to a preset grid point along the roller path. Each grid point was spaced at 0.305 m (1 ft) along the roller path which represents an average of compaction measurement data that fall within a window of size 0.15 m (0.5 ft) in forward and backward directions. To validate this approach, an example dataset comparing the actual and averaged values is presented in Figure 35. The figure shows excellent agreement between the actual and averaged values. All output data files were filtered and organized in the same way using a customized VB program called as *IC-REPEAT* developed at Iowa State University.

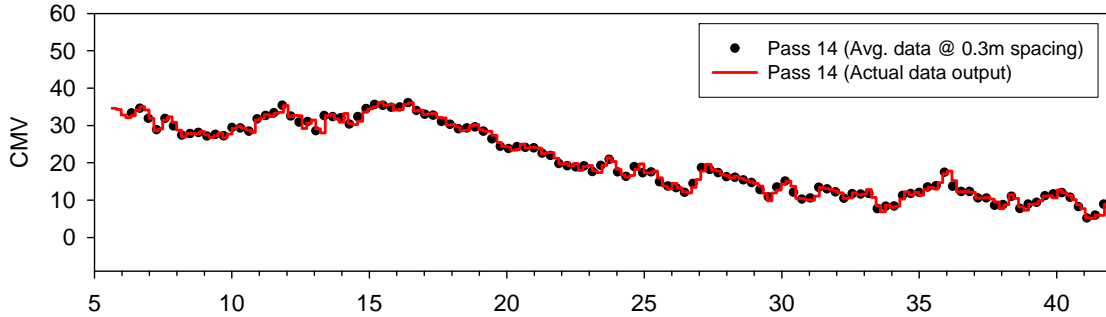


Figure 35. Comparison of actual CMV data output and 0.305 m (1 ft.) averaged data

Repeatability analysis to quantify measurement error or $\sigma_{\text{repeatability}}$ is performed on CMV, RMV, and MDP measurements made by several consecutive passes (2 to 12) under identical operating conditions (i.e., same amplitude, nominal speed, and direction). Although repeated passes were performed on “compacted” surfaces, some systematic change in soil properties with each pass is expected. Therefore, the effect of pass on roller measurement values is also considered in the analysis. This is accomplished by performing Two-Way Analysis of Variance (ANOVA), by taking both pass and measurement location as random effects (Vardeman and Jobe 1999). The parameter of interest from this analysis results is the root mean squared error (\sqrt{MSE}) which represents the measurement error or $\sigma_{\text{repeatability}}$. Detailed procedure for calculating $\sigma_{\text{repeatability}}$ is provided in Appendix B.

Reproducibility analysis is performed to quantify the variability in roller measurement values associated with change in operating conditions, $\sigma_{\text{reproducibility}}$ (i.e., change in amplitude, speed, and gear). This analysis is classified into five cases (described below). In each case, one change in operating condition is evaluated by using measurements made by three consecutive passes for each condition. Similar to described above, increasing pass would have some systematic effect on the measurement values. One way to approach this is to include pass effect into the ANOVA along with the measurement location and operating condition effects. This would involve performing a Three-Way ANOVA. An alternate approach is to check if the pass effect is significant on the repeated measurement values. This is performed by Two-Way ANOVA including location and pass effects on three repeated passes made under constant operating conditions. If the difference in \sqrt{MSE} calculated with and without pass effect is logically negligible (< 0.3 for CMV and < 0.1 for MDP) then it is justified to perform the ANOVA without including the pass effect. For all the cases described below, the three consecutive passes selected were based on the negligible pass effect criteria. Detailed procedures for calculating $\sigma_{\text{reproducibility}}$ from a Two-Way ANOVA results are provided in Appendix B. Further, $\sigma_{R\&R}$ which is a measure of overall variability (the two R’s represent repeatability and reproducibility) is calculated using Eq. 1, to determine the contribution of $\sigma_{\text{reproducibility}}$ to the overall observed variability (Vardeman and Jobe 1999).

$$\sigma_{R\&R} = \sqrt{\sigma^2_{repeatability} + \sigma^2_{reproducibility}} \quad (1)$$

Following output datasets were selected for repeatability analysis:

CS 563 roller

- Reverse Gear, $a = 0.85$ mm, $v = 3.2$ km/h (nominal): Pass 2 and 4
- $a = 0.85$ mm, $v = 3.2$ km/h (nominal): Pass 6 to 17
- $a = 0.85$ mm, $v = 4.8$ km/h (nominal): Pass 18 to 29
- $a = 1.70$ mm, $v = 3.2$ km/h (nominal): Pass 32 to 43
- $a = 1.70$ mm, $v = 4.8$ km/h (nominal): Pass 46 to 57

CS 683 roller

- $a = 0.85$ mm, $v = 3.2$ km/h (nominal): Pass 58 to 63

CP 563 roller

- $a = 0.31$ mm, $v = 3.2$ km/h (nominal): Pass 1 to 12
- $a = 0.31$ mm, $v = 4.8$ km/h (nominal): Pass 13 to 24
- $a = 1.87$ mm, $v = 3.2$ km/h (nominal): Pass 1 to 12

Following output data sets were selected for the R&R analysis on roller measurement values:

- CS 563 Case I: Effect of change in speed at $a = 0.85$ mm
 - Pass 14 to 16, $v = 3.2$ km/h (nominal)
 - Pass 18 to 20, $v = 4.8$ km/h (nominal)
- CS 563 Case II: Effect of change in speed at $a = 1.70$ mm
 - Pass 41 to 43, $v = 4.8$ km/h (nominal)
 - Pass 47 to 49, $v = 3.2$ km/h (nominal)
- CS 563 Case III: Effect of change in amplitude at $v = 3.2$ km/h (nominal)
 - Pass 14 to 16, $a = 0.85$ mm
 - Pass 47 to 49, $a = 1.70$ mm
- CS 563 Case IV: Effect of change in amplitude at $v = 4.8$ km/h (nominal)
 - Pass 18 to 20, $a = 0.85$ mm
 - Pass 47 to 49, $a = 1.70$ mm

- CS 563 Case V: Effect of change in gear (forward or reverse) at $a = 0.85$ mm and $v = 3.2$ km/h
 - Pass 2 and 4, reverse gear
 - Pass 6 and 7, forward gear
- CP 563 Case I: Effect of change in speed at $a = 0.85$ mm
 - Pass 10 to 12, $v = 3.2$ km/h (nominal)
 - Pass 13 to 15, $v = 4.8$ km/h (nominal)
- CP 563 Case II: Effect of change in speed at $a = 0.85$ mm
 - Pass 10 to 12, $v = 3.2$ km/h (nominal)
 - Pass 25 to 27, $v = 4.8$ km/h (nominal)

The results from the statistical analyses are summarized in Table 6 and Table 7. Figures 36 to 43 present the averaged roller data plots for different passes and operating conditions along with measured standard deviation of measurements (σ) at each location.

Discussion on CS-563 and 683 Smooth Drum Roller Results

The measurement error associated with CS 563 roller measured CMV is found to vary between 1.7 and 2.8. It is also found that the measurement error when the drum is double jumping is also within these limits (1.9 to 2.3), while it is lower when data from double jump mode is ignored (1.7 to 1.9). The CMV measurement error under high amplitude operation is lower compared to low amplitude operation for the two speeds tested especially when data from double jump is ignored. The measurement error associated with CS 683 roller measured CMV is found to be about 3.0.

The $\sigma_{\text{reproducibility}}$ observed for change in each operating condition (amplitude, speed, and direction of travel) and its contribution to the overall variability $\sigma_{\text{R\&R}}$ is summarized in Table 6. To quantitatively consider that there is no effect of change in the operating condition on the roller measurement values (CMV, RMV, and MDP), the contribution of $\sigma_{\text{reproducibility}}$ to the overall variability $\sigma_{\text{R\&R}}$ should be negligible (say <15%). Based on this criterion, the results presented in Table 6 indicate that only two of the cases evaluated appear to produce good reproducibility: (1) Case I: change in speed from 3.2 to 4.8 km/h at low amplitude operations, (2) Case II: change in speed from 3.2 to 4.8 km/h at high amplitude operations ignoring the data in double jump zone. The data obtained from these two changes in conditions can be considered to produce as precise measurements as under identical operating conditions.

Discussion on CP-563 Padfoot Roller Results

For the CP 563 padfoot roller, the MDP measurement error is found to vary between 0.6 and 1.07, and the error appears to increase when the machine is operated at higher speeds (see Table 6). R&R analysis show that the results are not reproducible when speed is changed from 3.2 to

4.8 km/h (see Table 7). The standard calibration procedure for MDP typically accounts for roller speeds between 3.2 km/h and 6.4 km/h. Increasing measurement error with increasing speed suggests that the MDP values do not have constant bias in the measurement range. A well-calibrated machine should exhibit constant bias over the calibrated measurement range. These errors are expected to be minimized with careful calibration procedures. Additional trials are warranted to further evaluate the repeatability and reproducibility of MDP measurement values. The MDP values are clearly not reproducible with change in amplitude from 0.31 mm to 1.90 mm for the conditions evaluated.

Table 6. Summary of repeatability analysis results

Roller	Drum Type	Gear	Amp (mm)	Nominal Speed (km/h)	Double jumping across the strip	$\sigma_{\text{repeatability}}$ or Measurement Error		
						CMV	RMV	MDP (kJ/s)
563	Smooth	Reverse	0.85	4.8	No	2.17	0.59	
563	Smooth	Forward	0.85	3.2	No	2.67	0.62	—
563	Smooth	Forward	0.85	4.8	No	2.76	0.67	—
563	Smooth	Forward	1.70	4.8	Yes	1.86	1.63	—
						1.79*	1.21*	—
						1.72 [§]	0.48 [§]	—
563	Smooth	Forward	1.70	3.2	Yes	2.29	3.64	—
						1.87*	2.41*	—
						1.81 [§]	0.45 [§]	—
683	Smooth	Forward	0.85	3.2	No	3.00	1.11	—
563	Padfoot	Forward	0.31	3.2	No	—	—	0.70
563	Padfoot	Forward	0.31	4.8	No	—	—	1.07
563	Padfoot	Forward	1.90	3.2	No	—	—	0.60

* Excluding data where RMV > 17

§ Excluding data where RMV > 4

Table 7. Summary of R&R analysis results

Description of change in conditions	Parameter	Range (Max-Min)	Measurement Variability			Percent contribution [¥] of $\sigma_{\text{reproducibility}}$	Impact of change in machine operating parameters (<i>a</i> , <i>v</i> , <i>direction</i>) on measurement values
			$\sigma_{\text{repeatability}}$	$\sigma_{\text{reproducibility}}$	$\sigma_{\text{R\&R}}$		
CS 563 Case I: Change in <i>v</i> = 3.2 to 4.8 km/h at <i>a</i> = 0.85 mm	CMV	35.5	2.51	0.93	2.67	12	Not significant
	RMV	4.1	0.66	0.07	0.66	1	
CS 563 Case II: Change in <i>v</i> = 3.2 to 4.8 km/h at <i>a</i> = 1.70 mm	CMV	25.8	2.16	5.47	5.88	87	Significant
	RMV	37.6	2.70	7.27	7.76	88	
	CMV*	20.7	1.93	0.62	2.03	9	Not significant for CMV if data ignored at locations where RMV > 17. Effect of RMV is significant.
	RMV*	15.8	0.63	3.22	3.28	96	
	CMV [§]	13.9	1.77	0.49	1.84	7	Not significant for CMV and RMV if data ignored at locations where RMV > 4.
	RMV [§]	2.5	0.37	0.22	0.43	26	
CS 563 Case III: Change in <i>a</i> = 0.85 to 1.70 mm at <i>v</i> = 3.2 km/h	CMV	35.5	2.39	4.05	4.70	74	Significant
	RMV	26.9	2.57	5.57	6.14	83	
	CMV*	35.5	2.15	3.40	4.03	72	Significant
	RMV*	16.7	1.42	3.83	4.08	88	
	CMV [§]	30.3	1.99	1.38	2.42	33	Significant
	RMV [§]	3.1	0.45	0.03	0.45	< 1	

* Excluding data where RMV > 17

§ Excluding data where RMV > 4

¥ $100 \times \sigma_{\text{repeatability}}^2 / \sigma_{\text{R\&R}}^2$

Table 7. Summary of R&R analysis results (contd.)

Description of change in conditions	Parameter	Range (Max-Min)	Measurement Variability			Percent contribution _σ of σ _{reproducibility}	Impact of change in machine operating parameters (<i>a</i> , <i>v</i> , <i>direction</i>) on CMV, RMV, and MDP measurement values
			σ _{repeatability}	σ _{reproducibility}	σ _{R&R}		
CS 563 Case IV: Change in <i>a</i> = 0.85 to 1.70 mm at <i>v</i> = 4.8 km/h	CMV	37.5	2.29	6.08	6.49	88	Significant
	RMV	34.7	1.07	12.31	12.36	99	
	CMV*	23.8	2.27	4.41	4.96	79	Significant
	RMV*	14.6	0.73	2.59	2.70	93	
	CMV [§]	19.7	2.02	3.91	4.40	79	Significant
	RMV [§]	3	0.51	0.25	0.57	20	
CS 563 Case V: Change in gear (forward or reverse) at <i>a</i> = 0.85 mm and <i>v</i> = 3.2 km/h	CMV	42.2	2.53	2.95	3.89	58	Significant for CMV and not significant for RMV
	RMV	3.3	0.59	0.16	0.61	7	
CP 563 Case I: Change in <i>v</i> = 3.2 to 4.8 km/h at <i>a</i> = 0.31 mm	MDP (kJ/s)	9.5	0.78	0.65	1.02	41	Significant (This effect can potentially be minimized with careful calibration procedures at different speeds)
CP 563 Case II: Change in <i>a</i> = 0.31 to 1.90 mm	MDP (KJ/s)	7.8	0.56	1.21	1.33	82	Significant (MDP is not calibrated for different amplitudes)

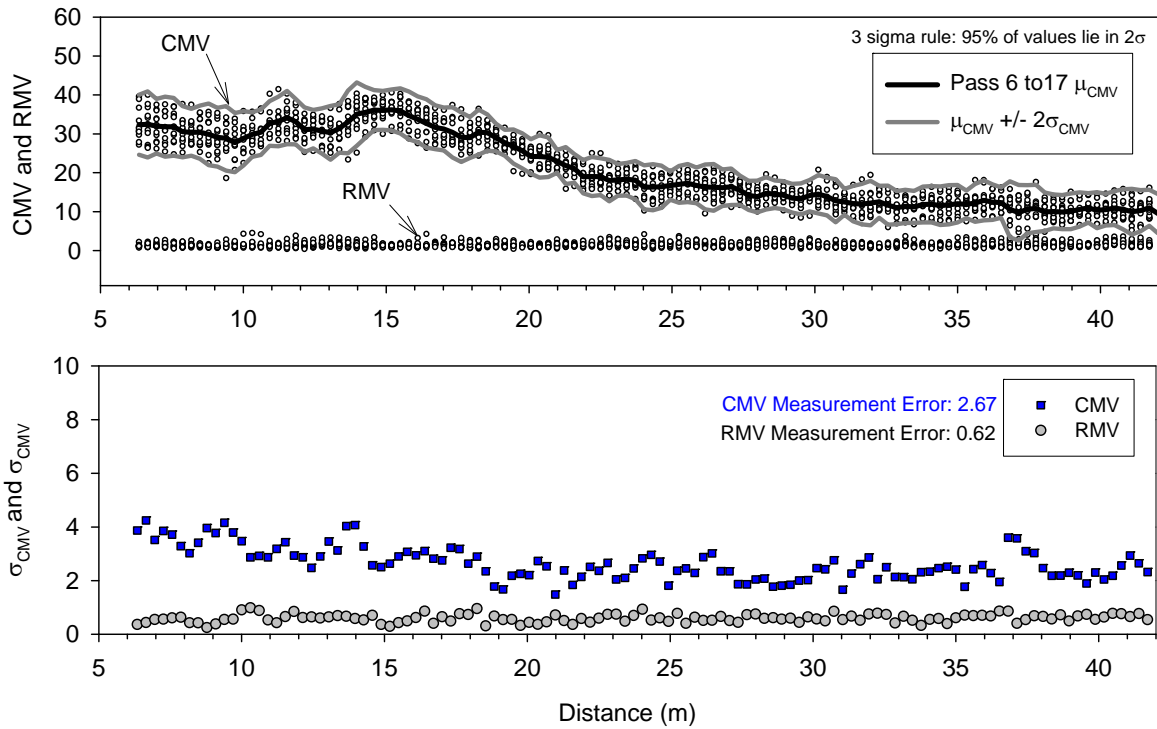


Figure 36. Repeatability analysis for CS 563 CMV/RMV measurement values at $a = 0.85\text{mm}$ and $v = 3.2 \text{ km/h}$ (nominal)

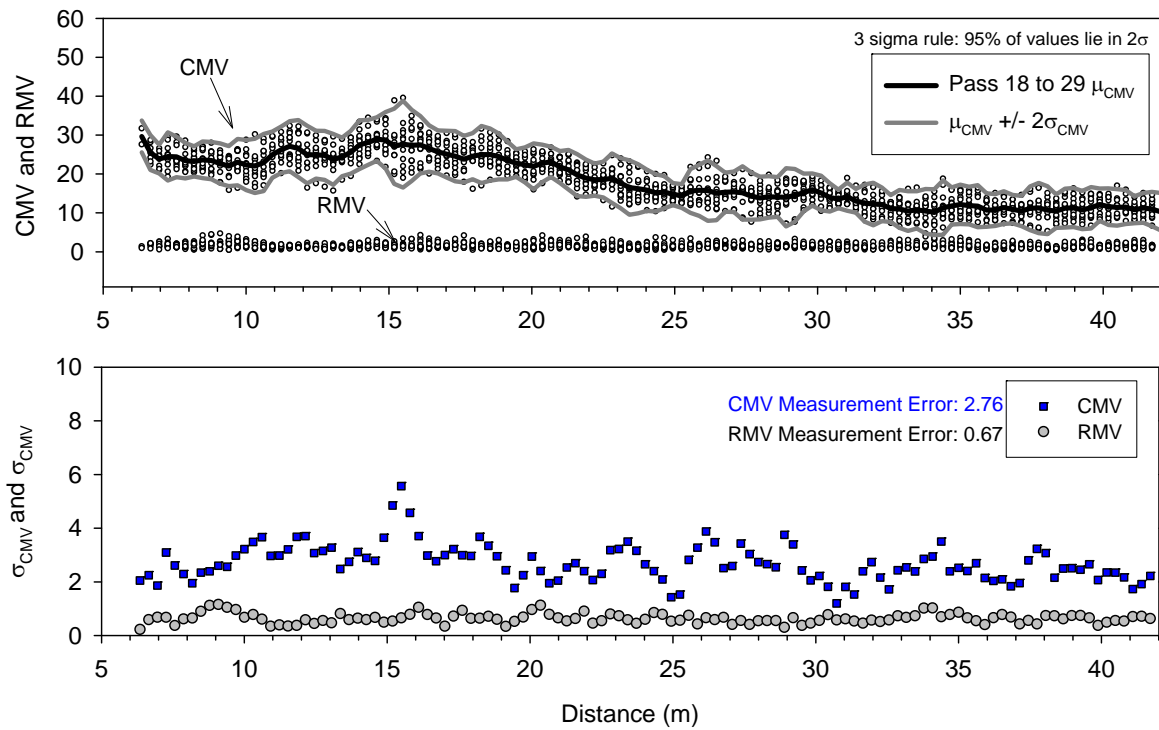


Figure 37. Repeatability analysis for CS 563 CMV/RMV measurement values at $a = 0.85\text{mm}$ and $v = 4.8 \text{ km/h}$ (nominal)

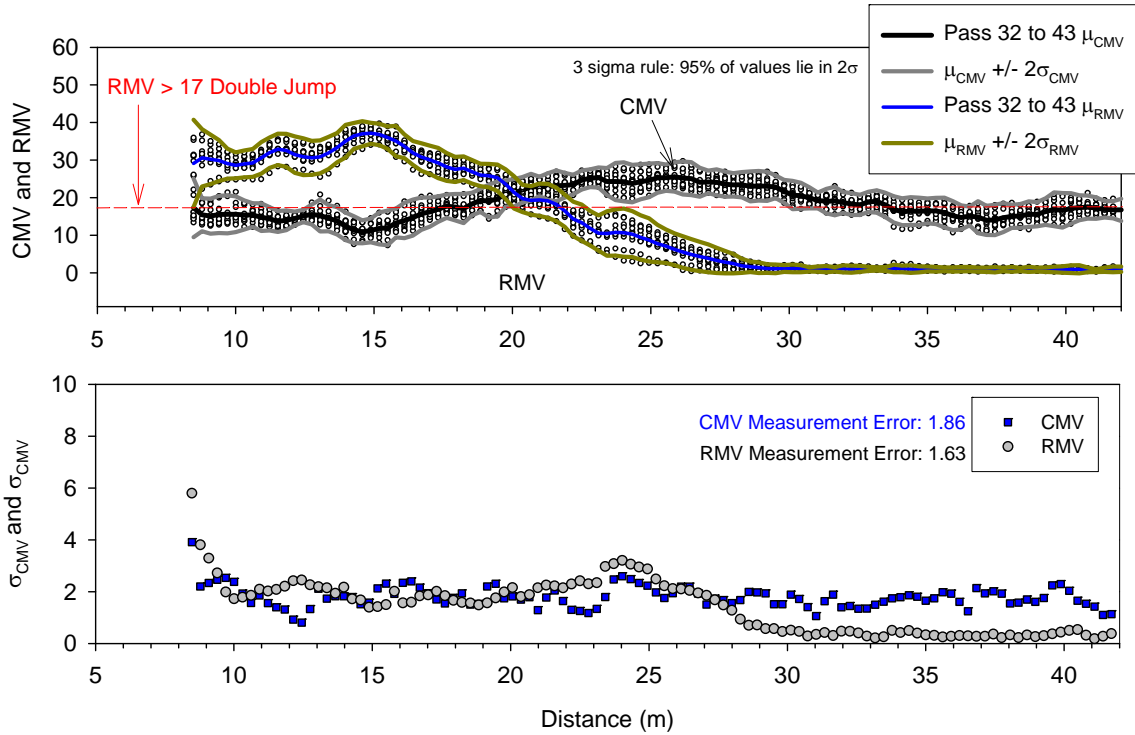


Figure 38. Repeatability analysis for CS 563 CMV/RMV measurement values at $a = 1.70$ mm and $v = 3.2$ km/h (nominal)

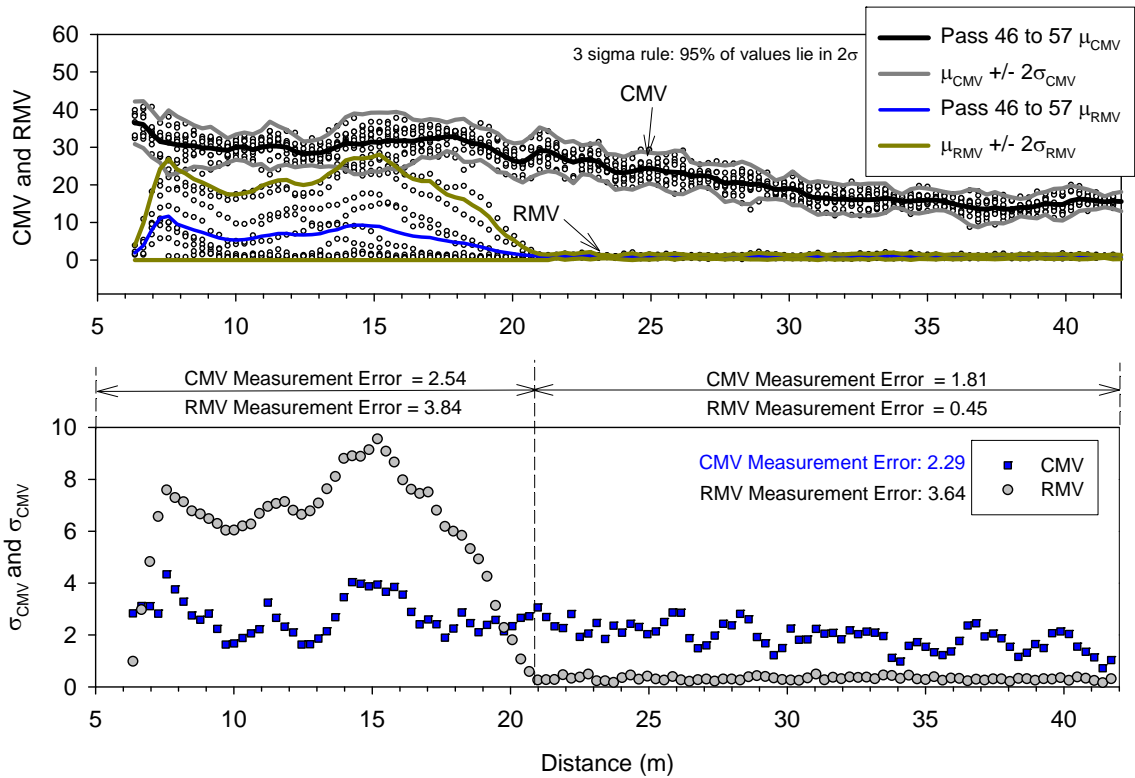


Figure 39. Repeatability analysis for CS 563 CMV/RMV measurement values at $a = 1.70$ mm and $v = 4.8$ km/h (nominal)

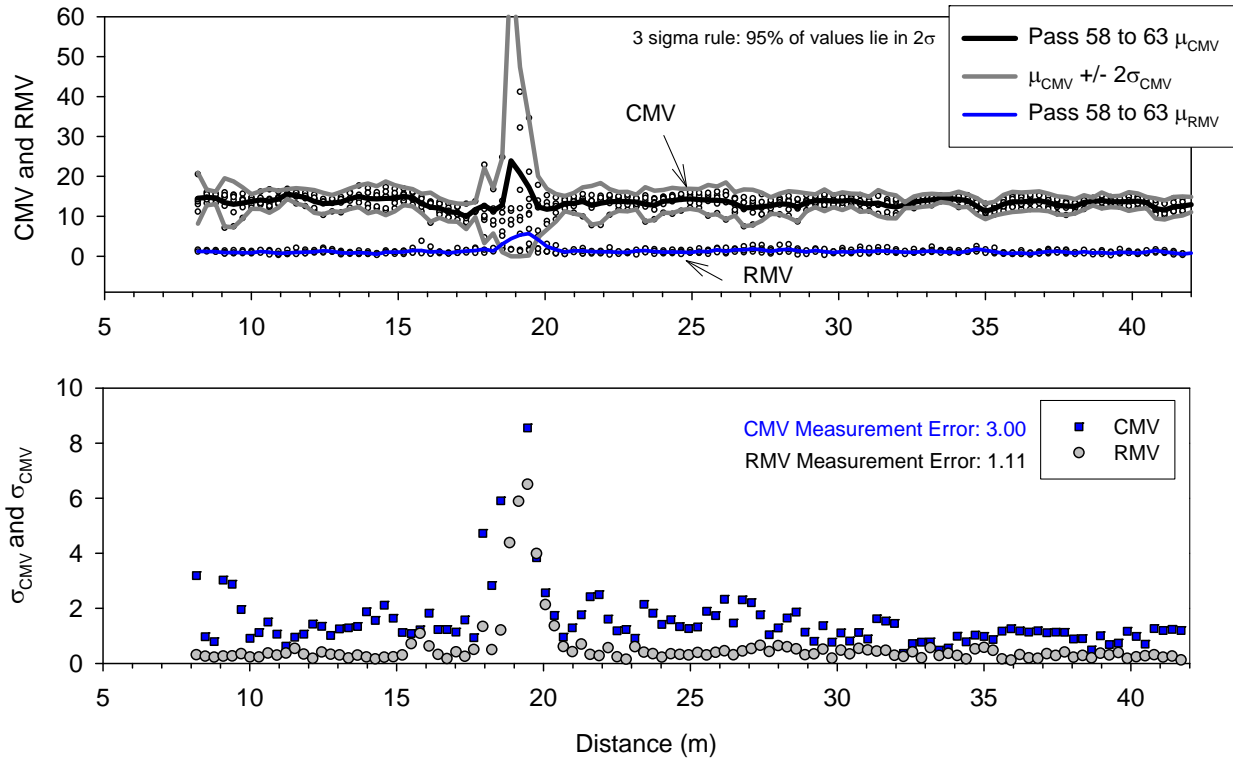


Figure 40. Repeatability analysis for CS 683 CMV/RMV measurement values at $a = 0.85$ mm and $v = 3.2$ km/h (nominal)

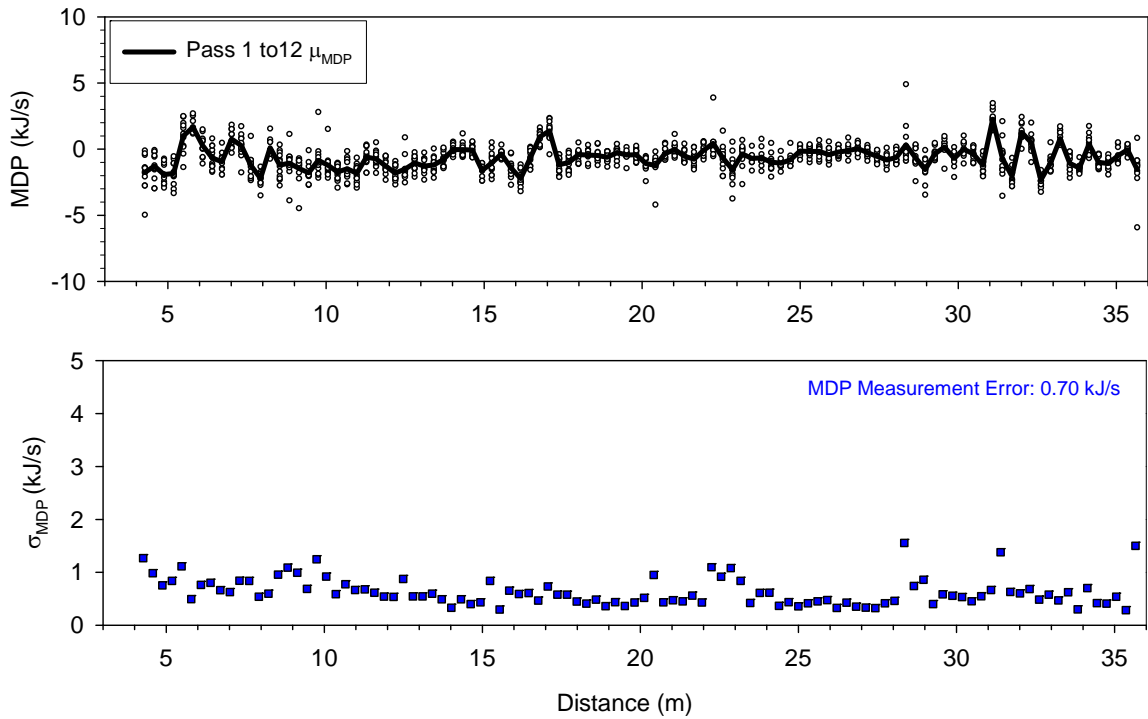


Figure 41. Repeatability analysis for CP 563 MDP measurement values at $a = 0.31$ mm and $v = 3.2$ km/h (nominal)

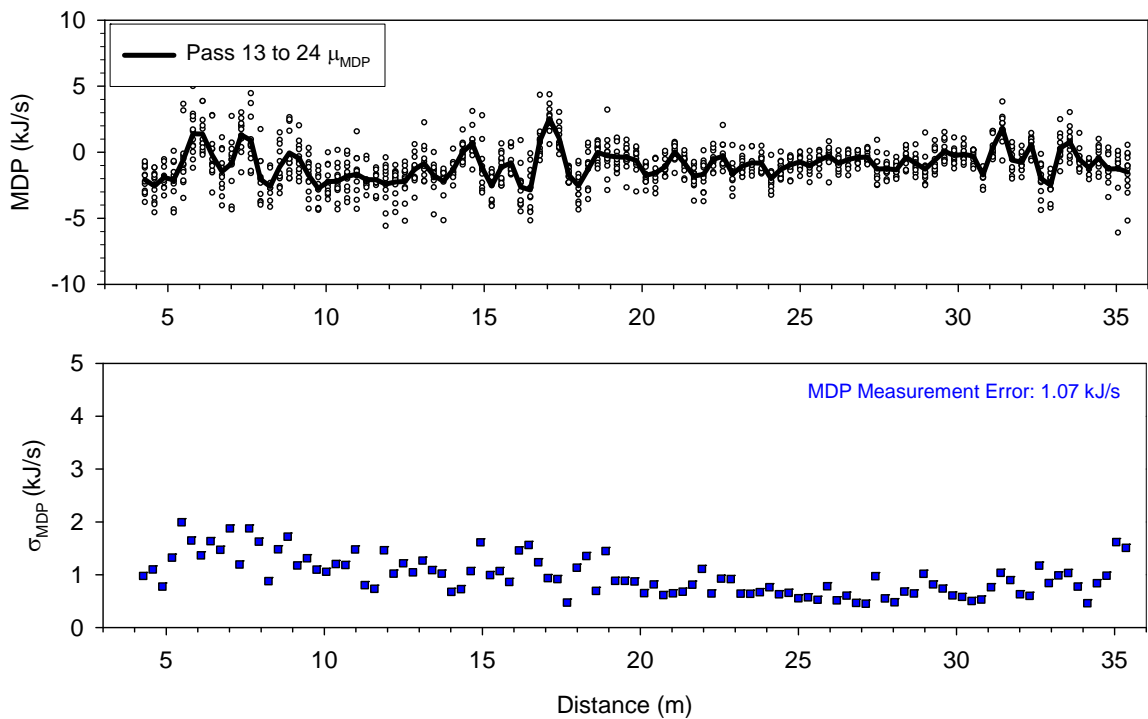


Figure 42. Repeatability analysis for CP 563 MDP measurement values at $a = 0.31$ mm and $v = 4.8$ km/h (nominal)

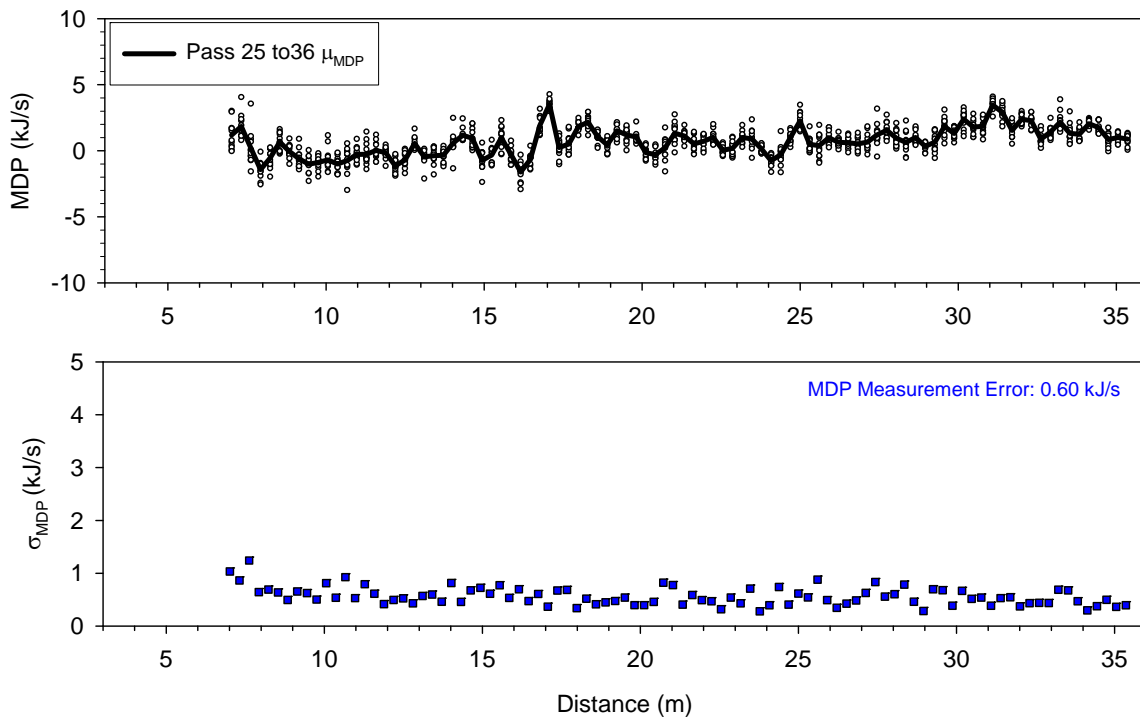


Figure 43. Repeatability analysis for CP 563 MDP measurement values at $a = 1.87$ mm and $v = 3.2$ km/h (nominal)

Summary and Key Conclusions

The precision of roller measurement values CMV, RMV, and MDP from three different machines is quantified in a repeatability and reproducibility context in this study. Repeatability variation refers to the variation observed in repeat measurements made on a test strip under identical conditions. Reproducibility variation refers to the variation observed in repeat measurements on a test strip under changing operating conditions (i.e., change in speed, amplitude, and direction of travel). Some key conclusions from the results and analysis are as follows:

- Data collected from CS 563 roller showed that the CMV data starts to gradually decrease when RMV increases above about 4 (i.e., when roller is double jumping). This is a distinctive feature of CMV and is previously identified in numerical simulations by Adam and Kopf (2004). Increasing RMV (i.e. double jumping) occurs when ground stiffness increases beyond a certain point.
- The relative change in CMV with increasing RMV is important to document when evaluating roller measurement values in any earthwork construction project as it can affect the correlations and target values significantly.
- Double jumping was not noticed when the 563 and 683 rollers were operated at low

amplitude.

- CS-563 machine used on the TH 64 project (White et al. 2008) used RMV of 17 for controlling the amplitude in a variable feedback control mode. RMV of 17 appears to be a significantly higher number as double jumping effects are noticed when RMV increases above 4. Further studies are warranted to check the efficiency of variable feedback control system by reducing the controlling RMV-value to 4.
- Maximum CMV on the CS 563 machine used on this project is about 40.
- On average, CMV measured by the CS683 machine at $a = 0.85$ mm and $v = 3.2$ km/h is about 1.4 times lower than CMV measured by the CS563 machine at similar operating conditions.
- The CMV and RMV measurement values are repeatable between each pass under identical operating conditions. The measurement error associated with CS 563 roller measured CMV is found to vary between 1.7 and 2.8. It is also found that the measurement error when the drum is double jumping is also within these limits (~ 1.9), while it is lower when data from double jump mode is ignored (~ 1.7). The measurement error associated with CS 683 roller measured CMV is about 3.0.
- The CMV and RMV measurement errors at high amplitude are lower compared to low amplitude for the two speeds tested using the CS 563 roller, when data from double jump area is ignored.
- CMV on CP 563 padfoot roller is not repeatable, while MDP data appears to be repeatable between passes made under identical operation parameters.
- The MDP measurement error is found to vary between 0.6 and 1.07, and the error appears to increase when the machine is operated at higher speeds. Careful calibration procedures should help minimize the reproducibility variations associated with increasing speed.
- The MDP values are not reproducible with change in amplitude from 0.31 mm to 1.90 mm.
- Reproducibility variations in CMV and RMV for CS 563 roller are not significant with change in speed from 3.2 km/h to 4.8 km/h at low amplitude setting ($a = 0.85$ mm). Results are also reproducible at high amplitude setting ($a = 1.70$ mm) where there is no double jumping.
- Effect of change in amplitude is significant for CMV and RMV measurement values for the CS 563 roller.
- Effect of change in roller direction is significant for CMV but it is not significant for RMV.

TEST BED STUDIES ON CS 563, CS 683, AND CP 563 ROLLERS WITH DIFFERENT SUBSURFACE CONDITIONS

Three test beds were constructed as part of this project as summarized in Table 8. The test beds were constructed by excavating a 4 feet trench below the existing grade. TB 1 consisted of a concrete pad, TB 2 consisted of a wet and dry subgrade, and TB 3 consisted of a concrete and wet subgrade at the base of the excavation. Seven lifts of CA6-G material were placed and compacted in each test bed. Index properties of the CA6-G and subgrade material are summarized in Table 9.

Both CS 563 and CS 683 smooth drum rollers were used on TB 1, and only CS 563 smooth drum roller was used on TB 2. CP 563 padfoot roller was used on TB 3. Earth pressure cells (EPC’s) were installed in three layers of TBs 1 and 2, to measure the in-ground stresses developed during roller compaction. The initial reading of each EPC measurement has been subtracted because of the uncertainty in its calculation due to temperature fluctuations. Therefore, all the EPC measurements presented below represent only a stress increase under the roller (i.e., excluding overburden geostatic stresses). Following the final roller pass on each lift, in-situ spot tests (Zorn LWD, and DCP) were performed at several locations across the test strip.

Table 8. Summary of test strips

Date	Test Bed (TB)	Roller(s)	Drum	Roller Measurement Value	Subsurface Conditions	Number of CA6-G lifts
05/08/07 05/09/07	1	CS 563 CS 683	Smooth	CMV, RMV	Concrete	7
05/09/07 05/10/07	2	CS 563	Smooth	CMV, RMV	Wet and Dry Subgrade	7
05/29/07 05/30/07	3	CS 563	Padfoot	CMV, RMV, and MDP	Concrete and Wet Subgrade	7

Table 9. Summary of soil index properties

Parameter	Edwards Glacial Till Subgrade	CA6-G Fill Material
Material Description	Sandy lean clay	Clayey Sand to Silty Sand
Maximum Dry Unit Weight (kN/m ³) and Optimum Moisture Content (%)		
Standard Proctor	—	20.9, 9.2%
Modified Proctor	—	21.8, 8.2%
Gravel Content (%) (> 4.75mm)	4	39
Sand Content (%) (4.75mm – 75µm)	20	47
Silt Content (%) (75µm – 2µm)	50	8
Clay Content (%) (< 2µm)	26	6
Liquid Limit, LL (%)	32	22
Plasticity Index, PI	16	7
AASHTO Classification	A-6(10)	A-2-4
Unified Soil Classification (USCS)	CL	SC-SM
Specific Gravity, G _s	2.73	2.70

Description of Test Bed 1

TB 1 was constructed as shown in Figure 44 which had plan dimensions of about 8 ft x 80 ft at the base of the excavation. The test bed was excavated to a depth of about 4 feet below existing grade and a 1 foot thick concrete pad was installed at the base of the test bed. Seven lifts of CA6-G material (loose lift thickness ~ 12 inches) were placed and compacted in the test bed for several roller passes (see Figure 45 and Figure 46). A biaxial geogrid reinforcement of size 10 ft long x 8 ft wide was placed on the test bed on lifts 1 to 6 prior to placing each consecutive lift (see Figure 47). To measure the in-ground stresses during roller compaction passes, semiconductor EPC's were installed on the concrete base, lift 2, and lift 4 as shown in Figure 44. EPC's were installed in orthogonal directions to measure triaxial stress in the ground (σ_x – transverse direction, σ_y – longitudinal direction, and, σ_z – vertical direction).

The fill material was compacted using CS 563 smooth drum for several roller passes in low amplitude, high amplitude, and static settings. In addition, lifts 6 and 7 were compacted using CS 683 roller in low amplitude, high amplitude, and static settings, following the CS 563 roller passes. A summary of roller passes on TB1 is presented in Table 10. Zorn 300-mm plate LWD and DCP tests were performed on each lift after the final static compaction pass at 6 to 9 locations across the test bed. After completing the compaction and testing process on lift 7, the fill material was excavated down to the surface of each underlying layer to perform Zorn LWD and NG tests (Figure 48). These tests were intended to check for improvement in the stiffness of the underlying layers due to the compaction process on the above lifts, and for the effects of confining stresses on the layer stiffness.

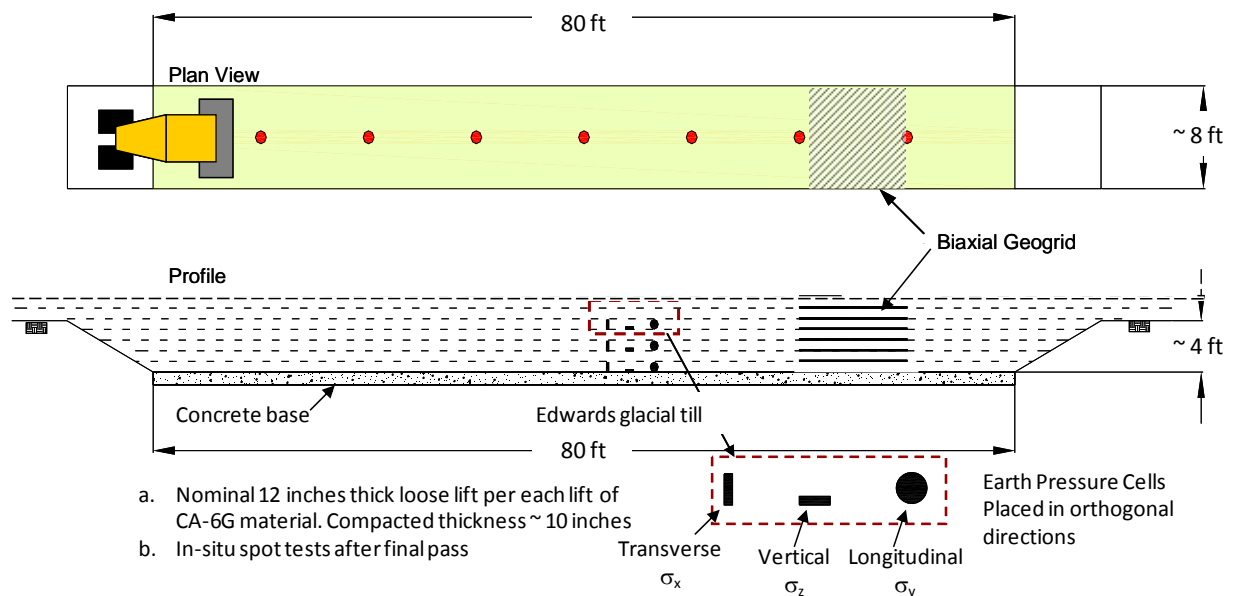


Figure 44. TB 1 plan view and profile with location of in-ground EPCs



Figure 45. Concrete base and lifts 1 to 3 of CA6-G material in TB 1



Figure 46. Lifts 4 to 7 of CA6-G material placed in TB 1



Figure 47. Placement of biaxial Geogrid in TB 1

Table 10. Summary of experimental testing on TB 1 – concrete base

Lift	Roller	Pass	<i>a</i> (mm)	Speed (km/h)	E _{LWD}	DCP [§]	Nuclear Gauge
1	CS 563	1 - 4	0.85	2.6			
		5	1.70	2.6			
		6	Static	2.8	x	x	
		Excavation*	—	—	x		x
2	CS 563	1 - 6	0.85	2.8 to 3.1			
		7 - 8	1.70	2.8			
		9	Static	2.8	x	x	
		Excavation*	—	—	x		x
3	CS 563	1 - 6	0.85	2.8 to 2.9			
		7 - 8	1.70	2.8			
		9	Static	2.8	x	x	
		Excavation*	—	—	x		x
4	CS 563	1 - 6	0.85	2.8 to 3.0			
		7 - 8	1.70	2.8			
		9	Static	2.9	x	x	
		Excavation*	—	—	x		x
5	CS 563	1	Static	2.9			
		2 - 6	0.85	2.8 to 3.1			
		7 - 8	1.70	2.8			
		9	Static	2.9	x	x	
		Excavation*	—	—	x		x
6	CS 563	1	Static	2.8			
		2 - 6	0.85	2.9 to 3.0			
		7 - 8	1.70	2.8			
		9	Static	2.8	x	x	
	CS 683	10 - 13	0.85	2.9			
		14	Static	2.8			
Excavation*	—	—	x		x		
7	CS 563	1 - 6	0.85	2.9 to 3.0			
		7 - 9	1.70	2.9			
		10	Static	2.8	x	x	
	CS 683	11 - 13	0.85	2.9			
		14	1.70	2.9			
		15	Static	2.9			

*Tests were conducted on top of each lift by excavating down after compacting all seven layers of CA6-G material

§DCP tests on lift 6 were performed for a maximum penetration depth of about 6 feet



Figure 48. Process of excavation to the top of each underlying lift to perform LWD and NG testing

Roller-Integrated Compaction Measurements and EPC Measurements

Roller-integrated CMV and RMV raw data plots for each roller pass and compaction growth curves for lifts 1 to 7 are presented in Figure 49 to Figure 57. Each compaction lift was compacted using CS 563 roller at different amplitude settings. CS 683 roller was used on lifts 6 and 7 after CS 563 roller passes.

Lift 1 on this test bed was placed on concrete base, and as expected high CMV values were

measured on this lift (Figure 49). Average CMV of about 37 and 41 were measured at low amplitude (pass 4) and high amplitude (pass 5) settings. During high amplitude operation on pass 5, double jumping occurred in a portion of the test bed which is evidenced by an increase in RMV and a sudden drop in CMV (this effect of decrease in CMV during double jump is discussed in previous chapter of this report). The compaction growth curve shows that the CMV measurement values increased on average from about 13 on pass 1 to about 41 on pass 5.

CMV measurement values on lift 2 also showed an increase with increasing passes up to pass 6 (Figure 50). On average, CMV increased from about 7 to 19 from pass 1 to 6 compacted at low amplitude. No considerable increase in CMV is noted for passes 7 and 8. CMV measurements on lifts 3 to 6 did not show much increase in compaction (Figure 51 to Figure 57). CMV measurements at different passes on these lifts were in the range of 4 to 10. On lift 7, CMV measurements showed an increase from about 7 to 13 from pass 1 to pass 8. No apparent difference in CMV is noted in the area where biaxial geogrid was placed along the test bed.

CMV measurements by the CS 683 machine on lifts 6 and 7 showed higher values (~ 13 to 16 on lift 6 and ~ 15 to 20 on lift 7) compared to measurements by the CS 563 machine.

Vertical and horizontal stress increase in the ground during each compaction pass for lifts 1 to 7 are included in Figure 49 to Figure 57. EPC's in this test bed were installed at three positions along the vertical profile: (a) on top of concrete base (position 1), (b) on top of lift 2 (position 2), and (c) on top of lift 4 (position 3). Figure 49 and Figure 50 show readings from EPC's located at position 1, Figure 51 and Figure 52 show readings from EPC's located at positions 1 and 2, and Figure 53 to Figure 57 show readings from EPC's located at positions 1, 2, and 3.

A summary of peak horizontal and vertical stresses developed under the roller at low amplitude, high amplitude, and static settings is presented in Figure 58, Figure 59, Figure 60, respectively. Stress distribution curves interpreted by hand for peak vertical stress increase under CS 563 and 683 machines are presented in these figures. As expected, comparison between these figures reveals that the peak stresses increase with increasing amplitude. One way to interpret the measurement influence depth of the roller is to use the stress distribution curves and find the depth at which the vertical stress increase has decayed to a certain percentage of the value at the surface. If 10% of maximum stress at the surface is considered as a threshold, the data indicates the measurement influence depth at both high and low amplitude settings is in the range of about 0.6 to 0.7 m from the surface. Using this criterion, the measurement depth does not appear to vary with increasing vibration amplitude. Further, this interpretation is purely a function of interpreted contact stresses under the drum.

A better way to develop further insights in to quantifying measurement influence depth is to perform a detailed laboratory study combined with numerical studies on the response of multi-layered soils. Using the in-ground stress measurements from this test bed, laboratory stress path tests could be conducted to better quantify the stress-strain characteristics of the fill material.

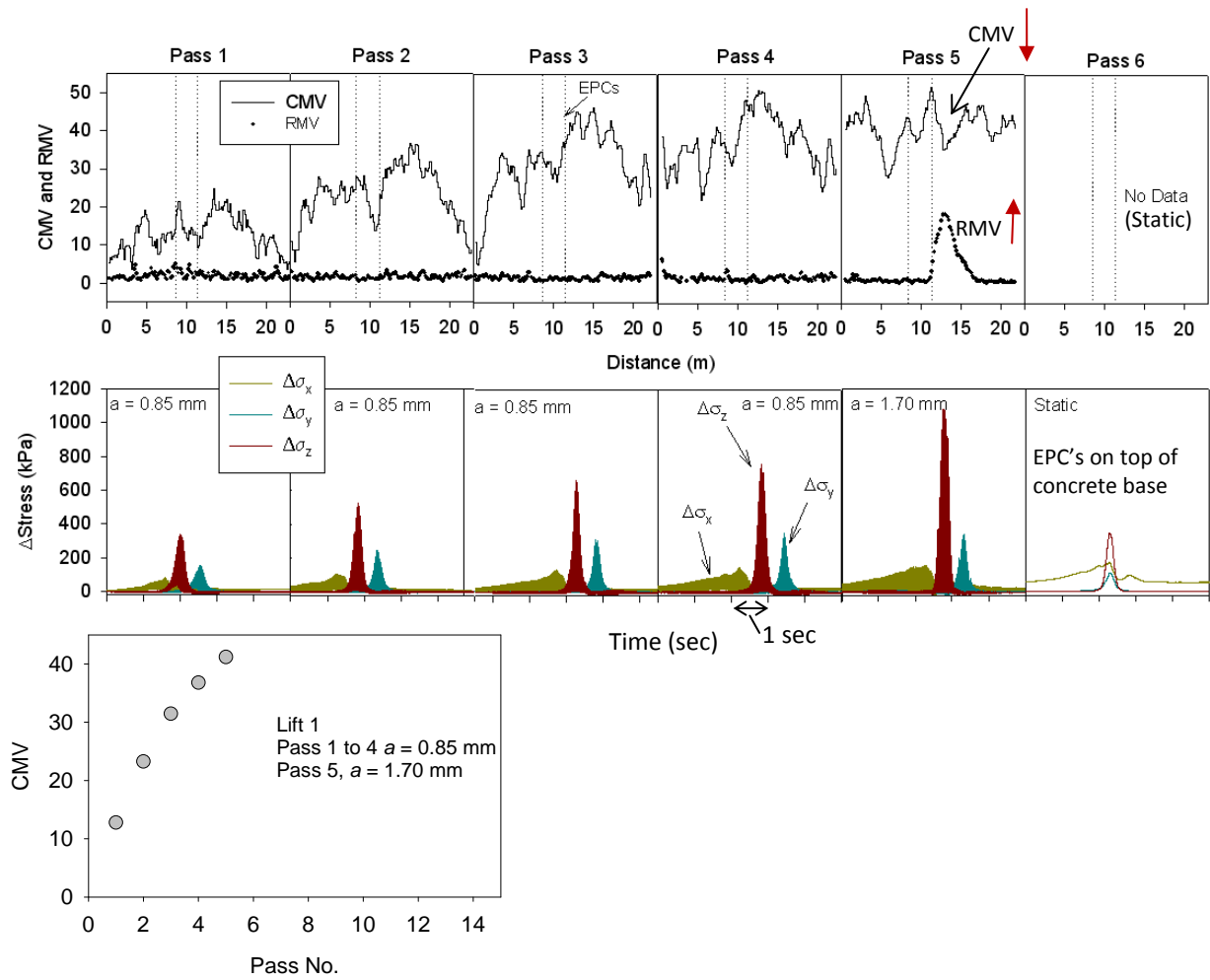


Figure 49. CMV and in-ground stress measurements for CS 563 roller passes – lift 1

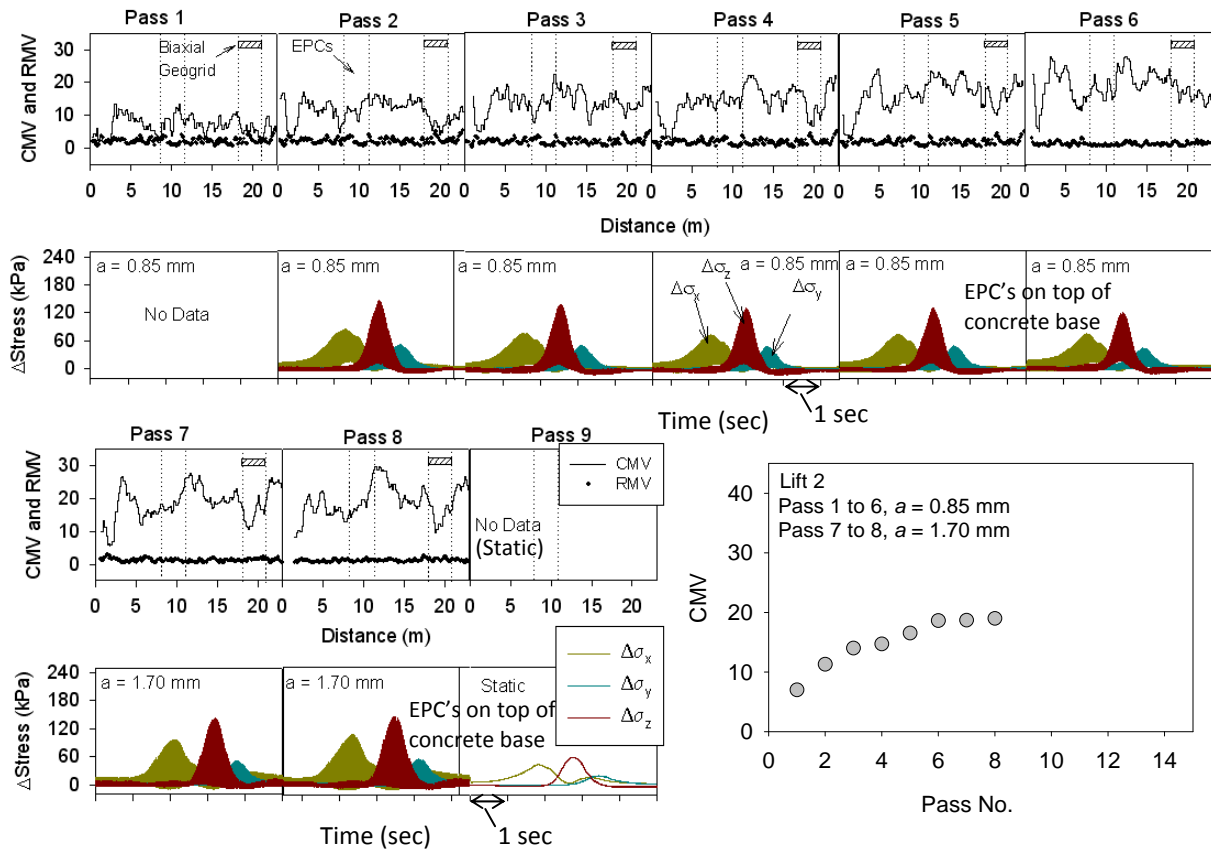


Figure 50. CMV and in-ground stress measurements for CS 563 roller passes – lift 2

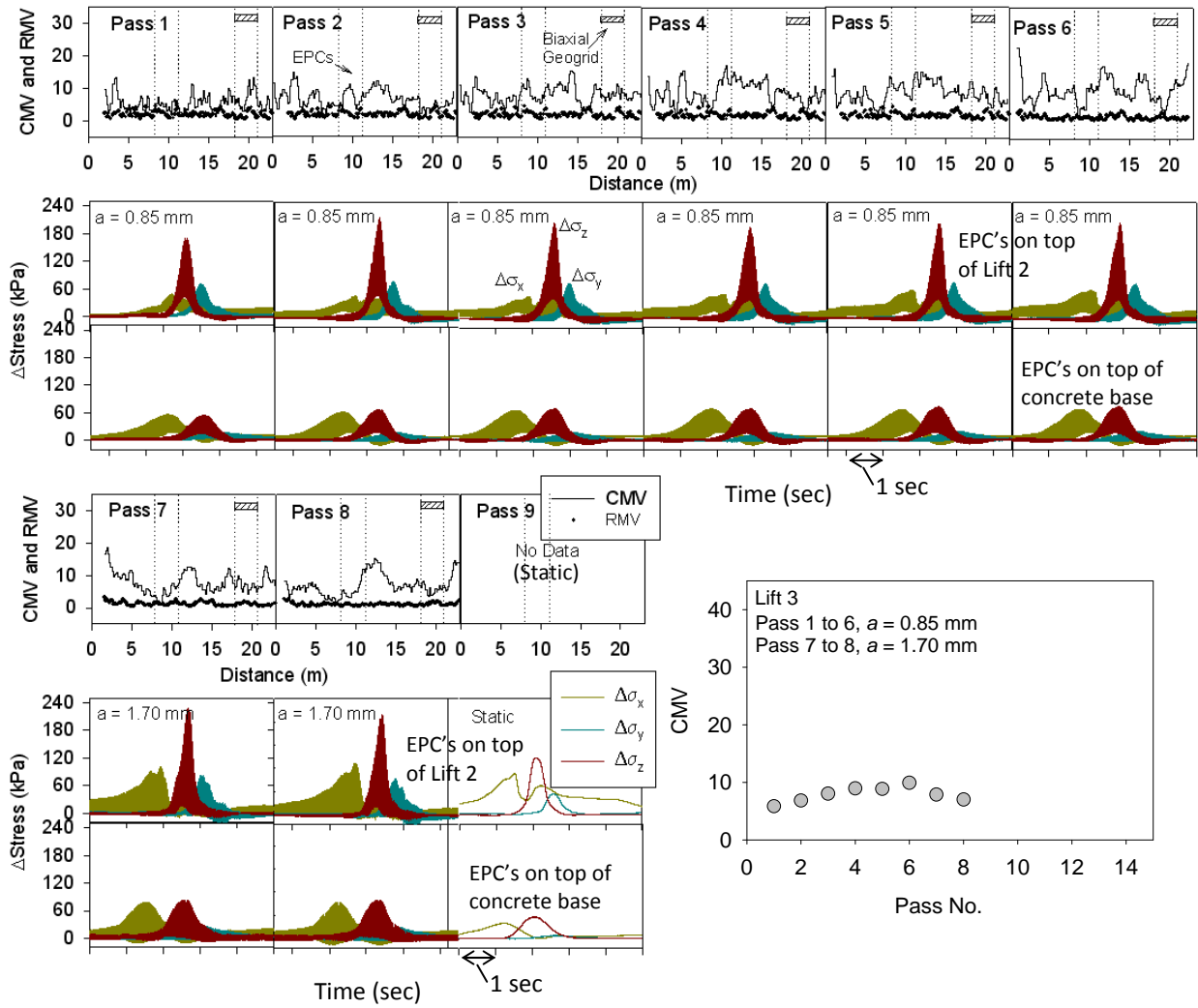


Figure 51. CMV and in-ground stress measurements for CS 563 roller passes – lift 3

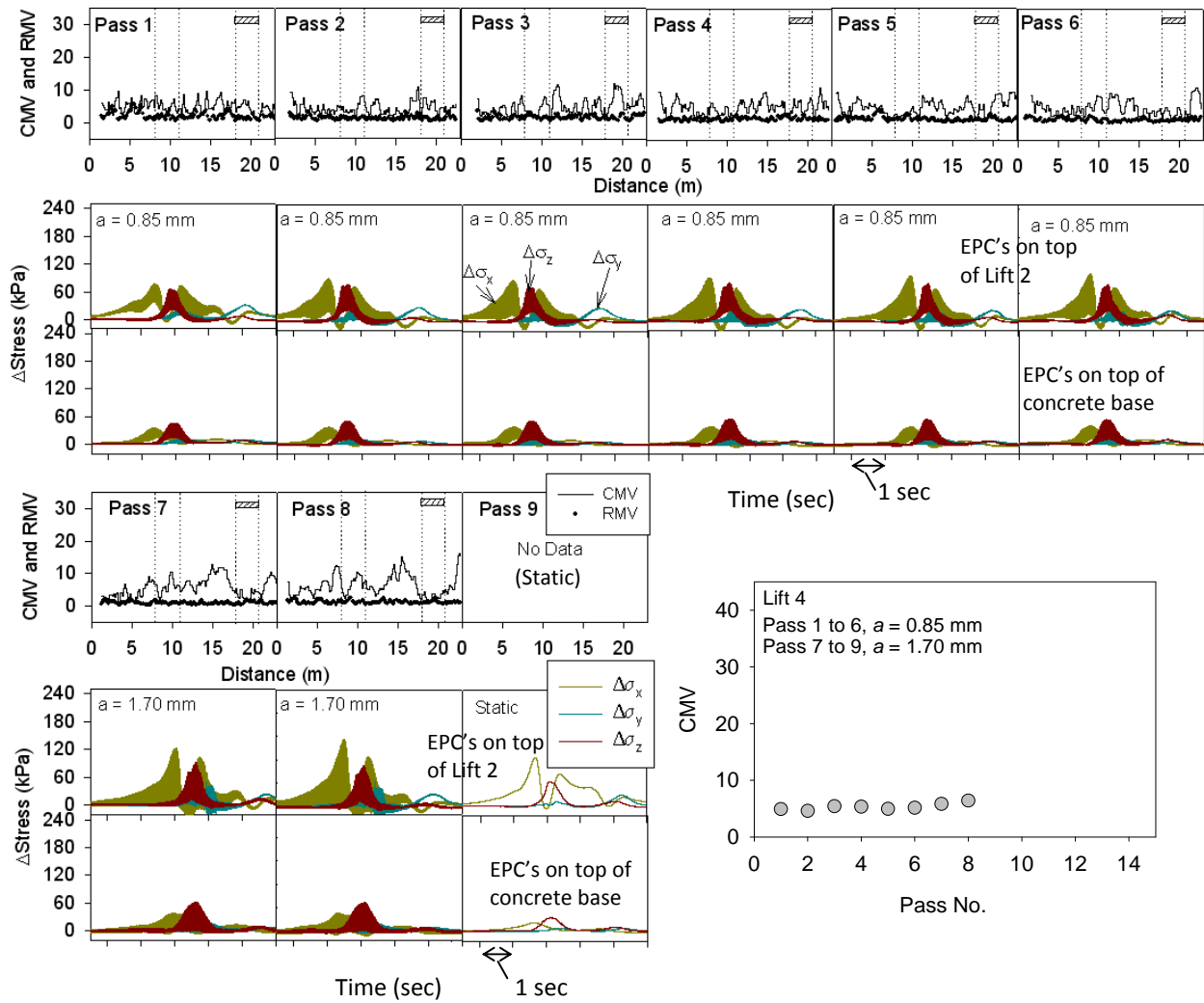


Figure 52. CMV and in-ground stress measurements for CS 563 roller passes – lift 4

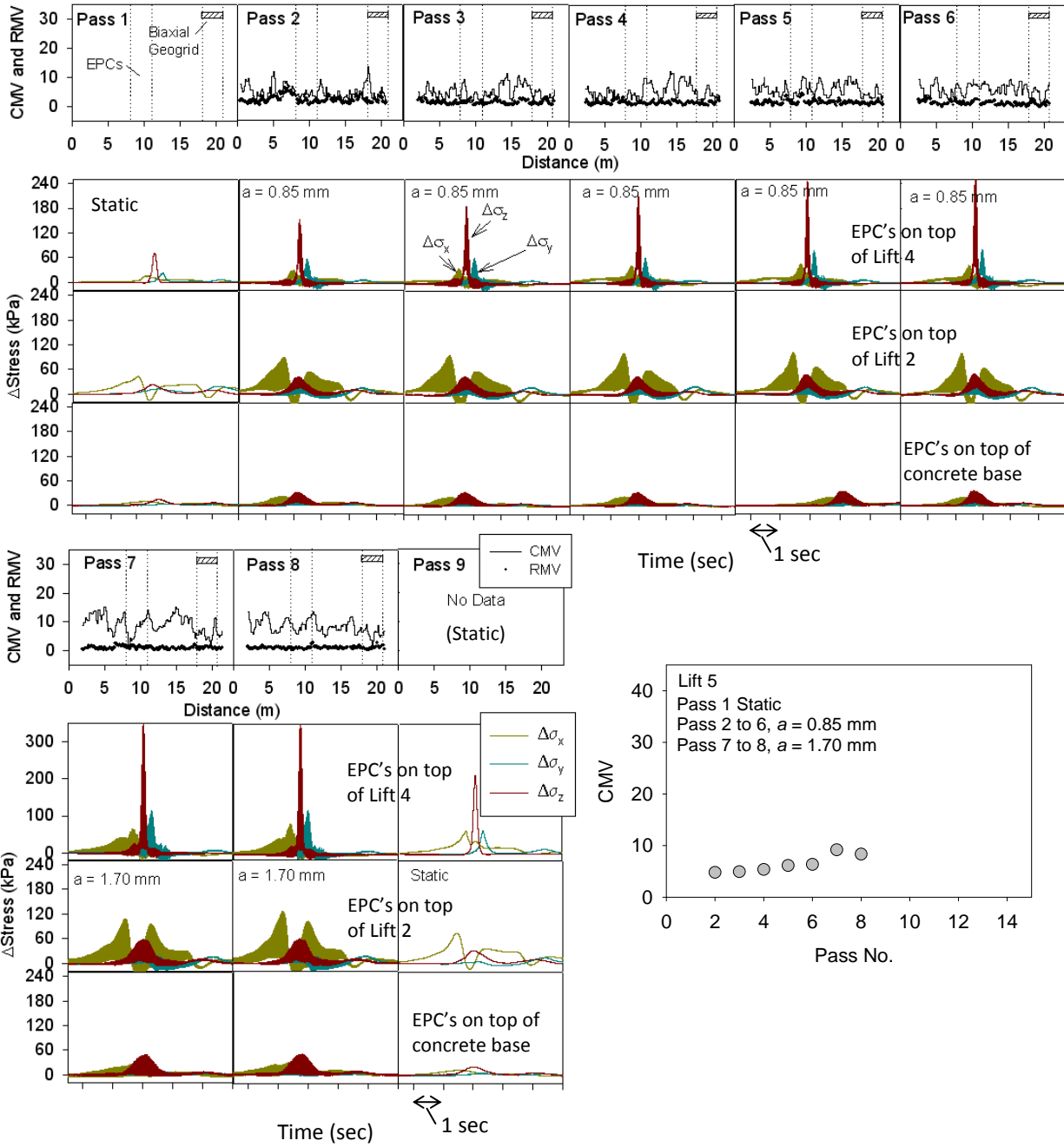


Figure 53. CMV and in-ground stress measurements for CS 563 roller passes – lift 5

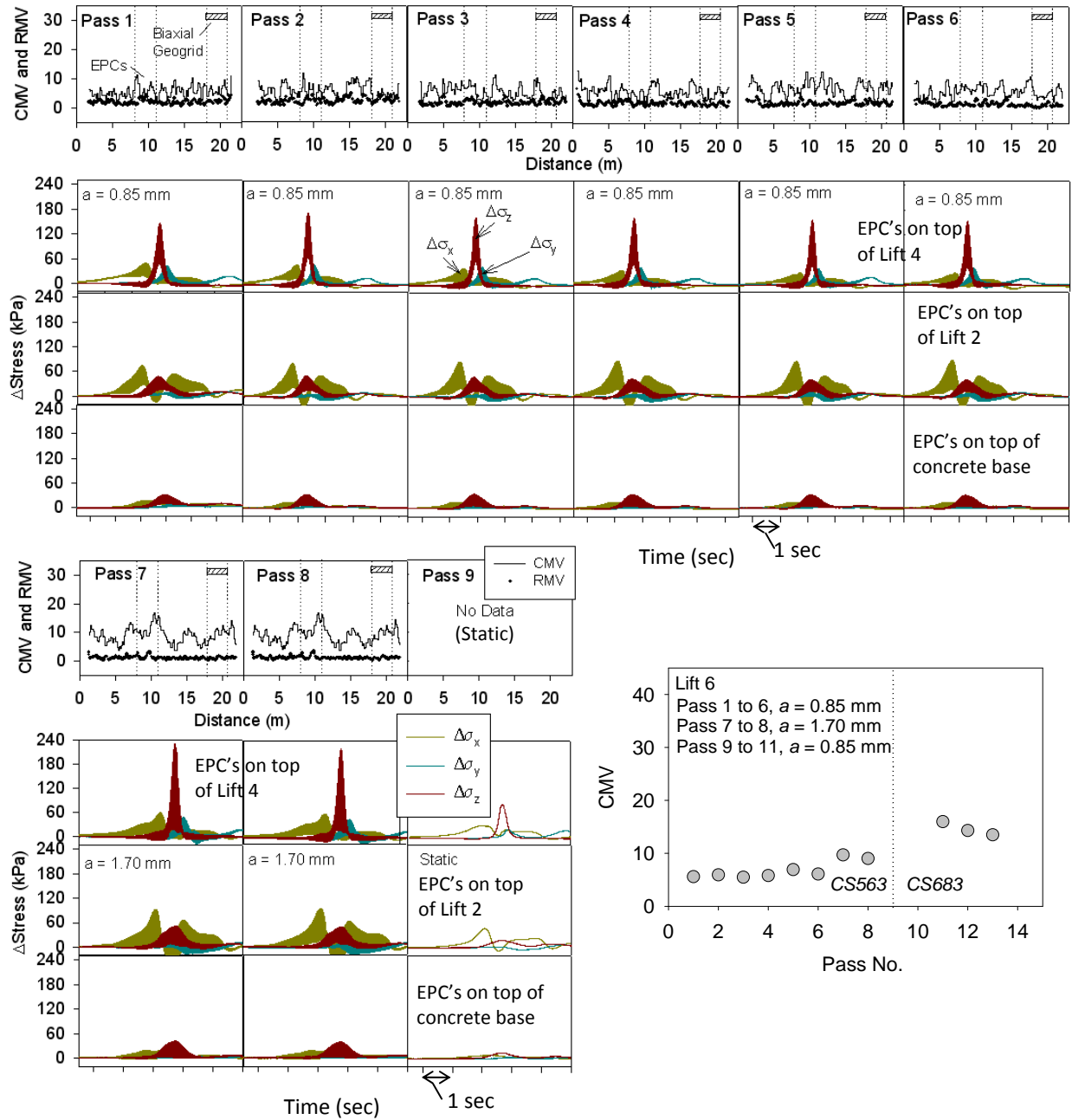


Figure 54. CMV and in-ground stress measurements for CS 563 roller passes – lift 6

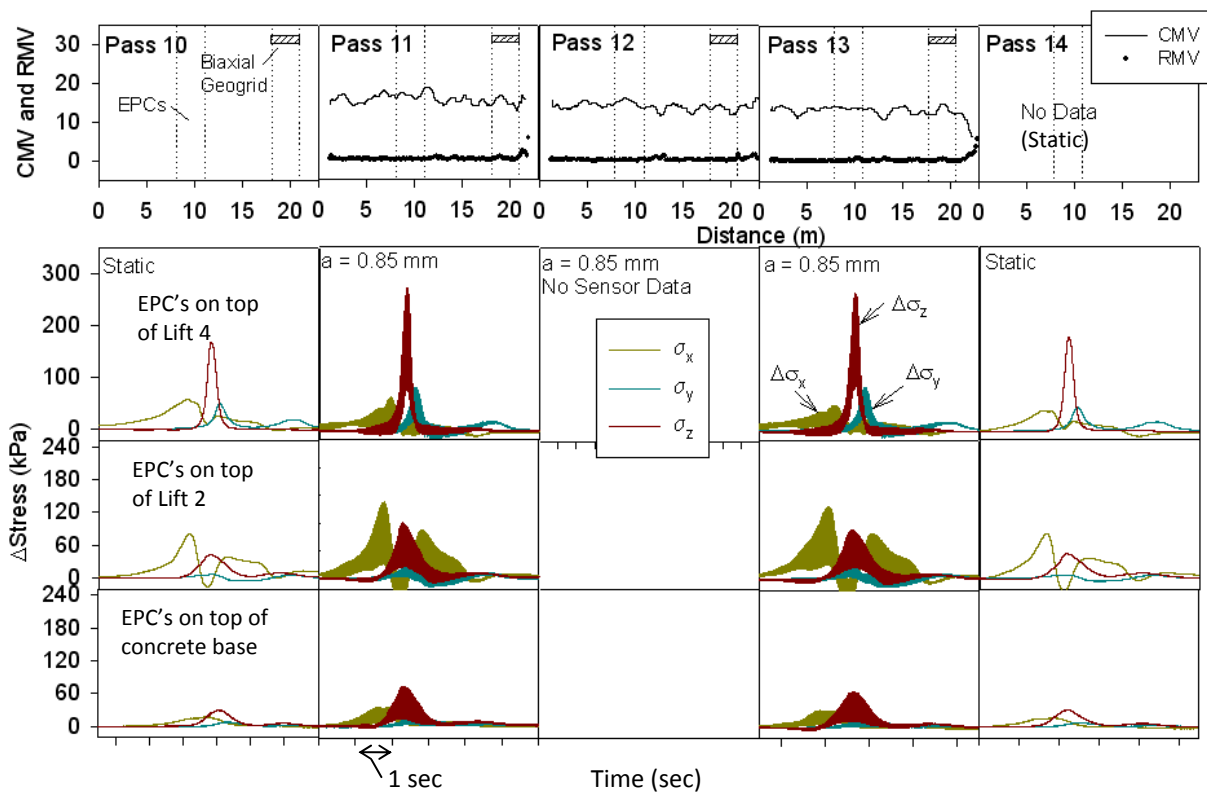


Figure 55. CMV and in-ground stress measurements for CS 683 roller passes – lift 6

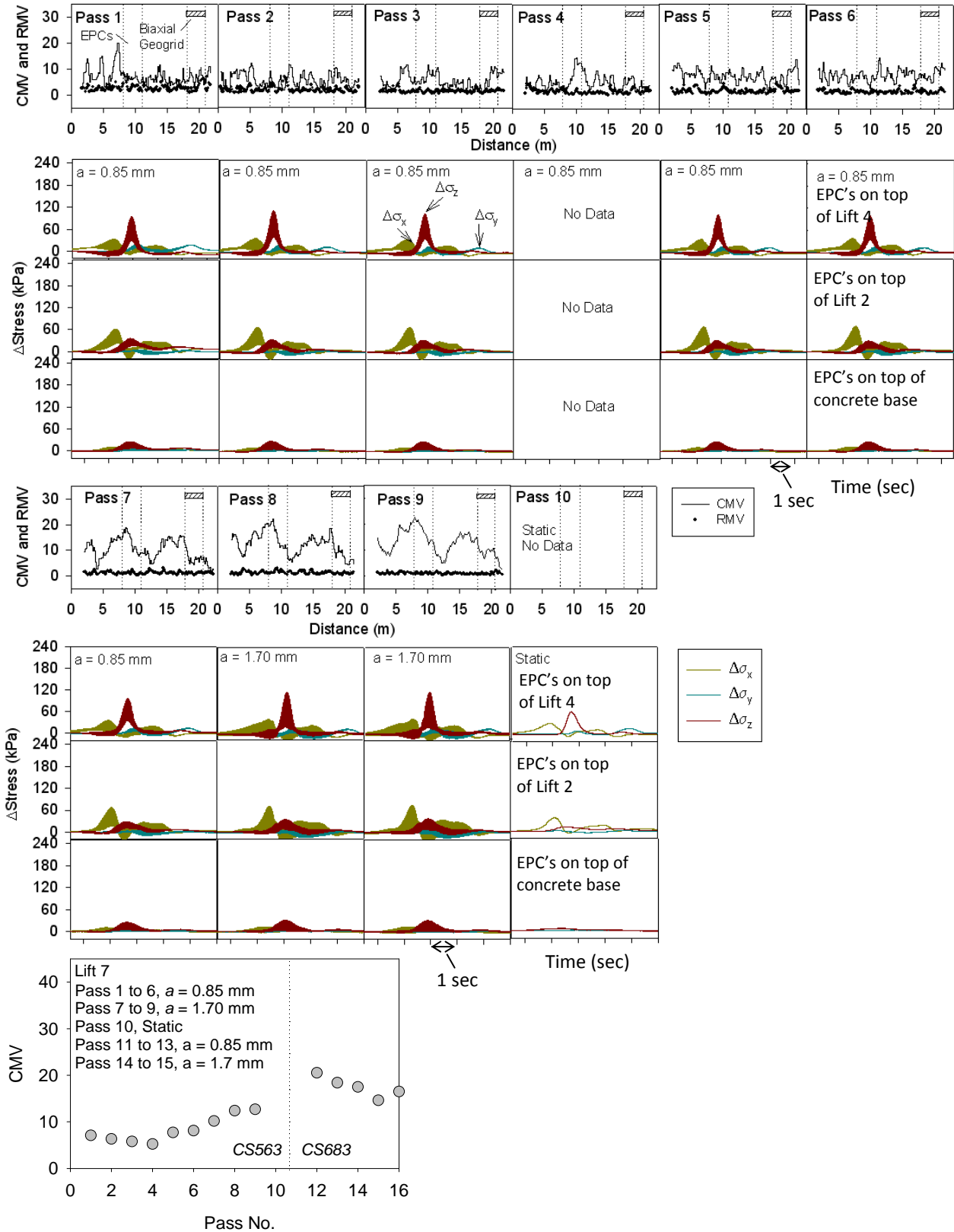


Figure 56. CMV and in-ground stress measurements for CS 563 roller passes – lift 7

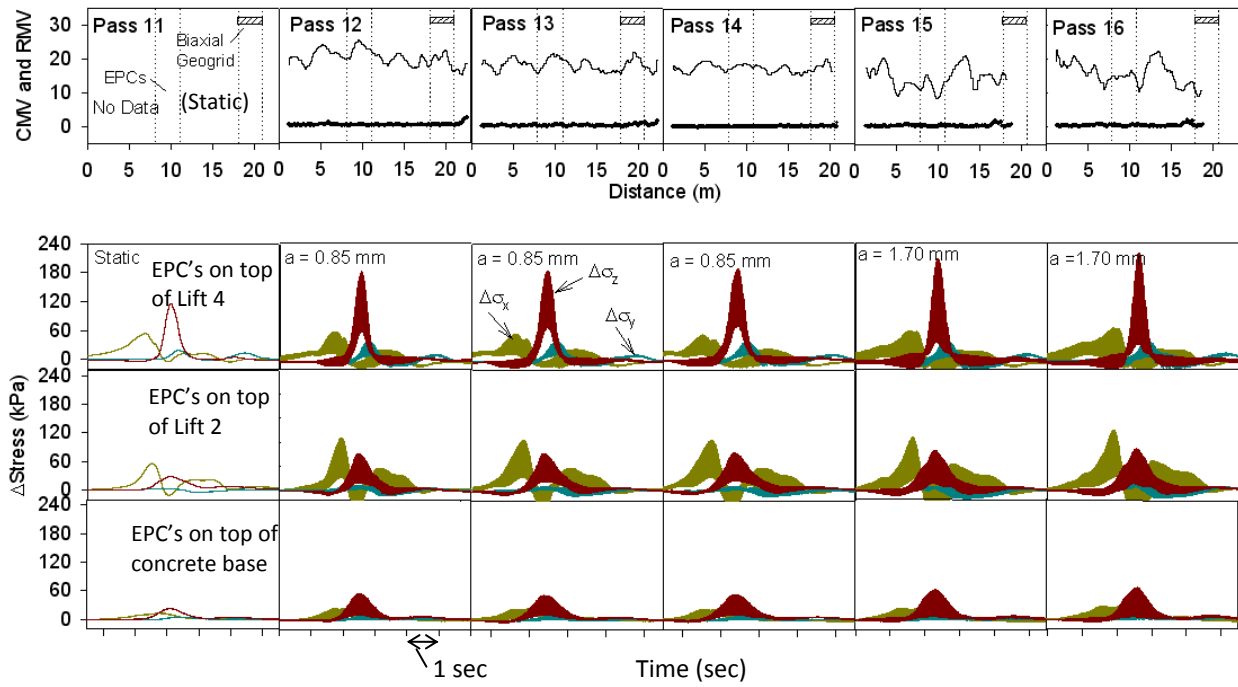


Figure 57. CMV and in-ground stress measurements for CS 683 roller passes – lift 7

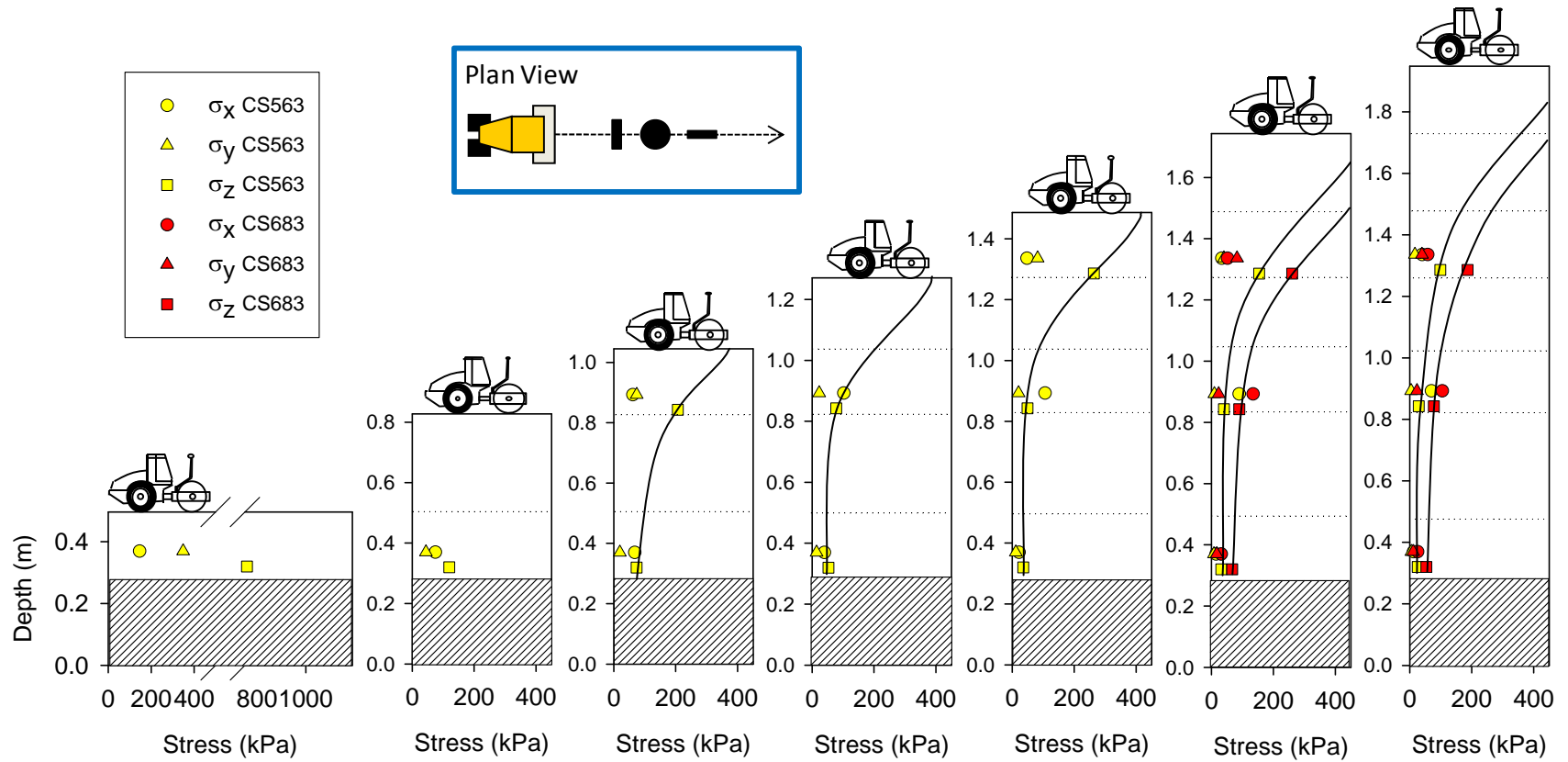


Figure 58. Stress distribution under the roller at a = 0.85 mm - TB 1

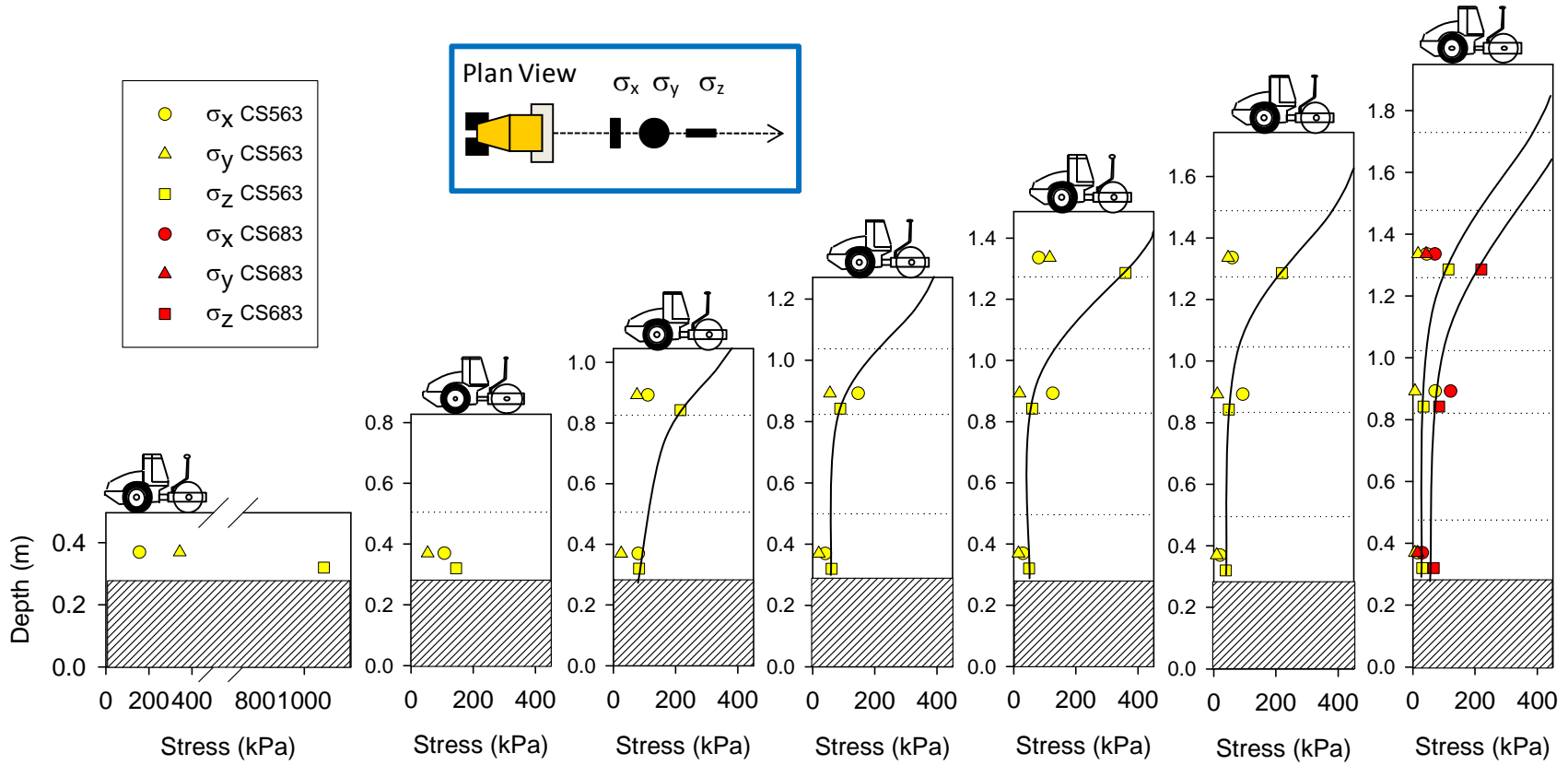


Figure 59. Stress distribution under the roller at a = 1.70 mm – TB 1

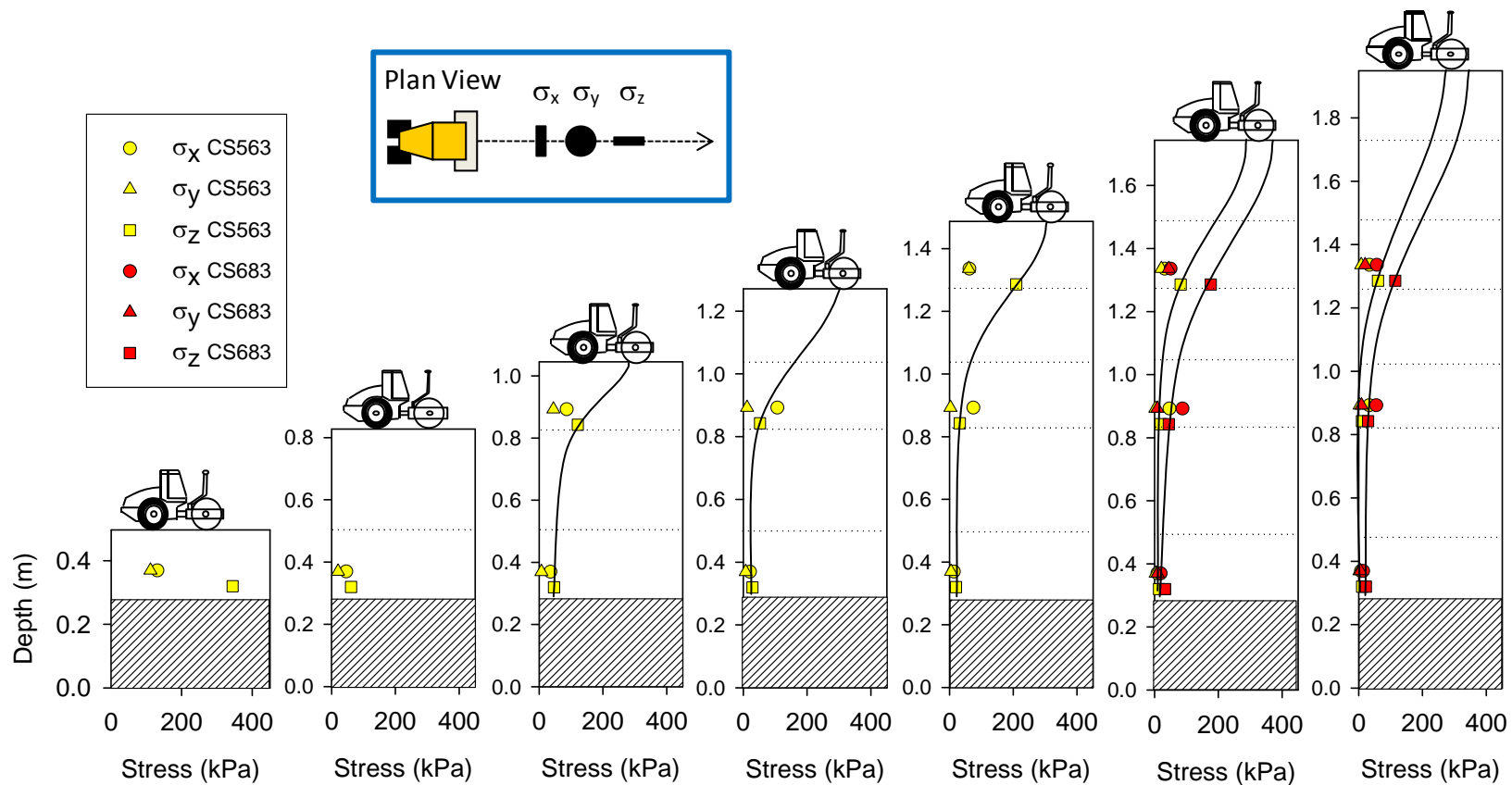


Figure 60. Stress distribution under the roller in static mode – TB 1

CMV Comparison to In-Situ Soil Properties

Figure 62 and Figure 61 present CMV measurement values on lifts 1 to 7 for pass 9 in comparison with E_{LWD} and CBR (calculated from DCP) values, respectively. CMV measurement values are shown as solid lines while E_{LWD} and CBR data are shown as discrete points. Except for measurements on lift 2, E_{LWD} measurements did not match well with CMV measurements. CBR measurements matched well with CMV for lifts 6 and 7, while they did not match well with measurements on lifts 1, 2, 3, and 4.

Figure 63 presents average CMV values for pass 1 and 9 as a compaction growth on each lift. It appears that the CMV measurements at pass 9 plateau at approximately 0.8 m above the surface of the concrete base. Further, it is clear that for lift 1 and 2 the underlying stiff concrete layer helps significantly in achieving better compaction. Also shown in Figure 63 are E_{LWD} and CBR_{300} quality assurance (QA) measurements taken on each compaction lift after pass 9, which did not show much variation along the profile. However, the post-construction QA E_{LWD} measurements performed in the excavation showed an increase in E_{LWD} values on each lift by about 2 to 2.5 times. This increase in modulus is partially attributed to possible densification of underlying layers during compaction of the layers above, and partially to the effect of increasing confining stress with depth that increase the stiffness of granular materials. The later effect is well known and according to Lambe and Whitman (1969) increase in confining stress (σ_c) increases the elastic modulus of granular materials by σ_c^n where n varies of 0.4 to 1.0. The possibility of post-construction densification of the underlying layers can be seen from the difference in elevation at test location 4 during compaction and in excavation. Further, the DCP-CBR profiles shown in Figure 64 show a significant increase in CBR as the layer above is placed and compacted. This is an important aspect of compaction of granular materials and their behavior which is not well documented in literature.

Figure 64 also compares CBR profiles to average CMV measurement values at seven test locations on each compaction lift. The average CMV-values were determined by averaging the measurement values over a width of approximately 3 m which is half way between each test location. Interestingly, the average CMV measurement values follow closely along the 2-m DCP-CBR profile from tests performed on lift 6.

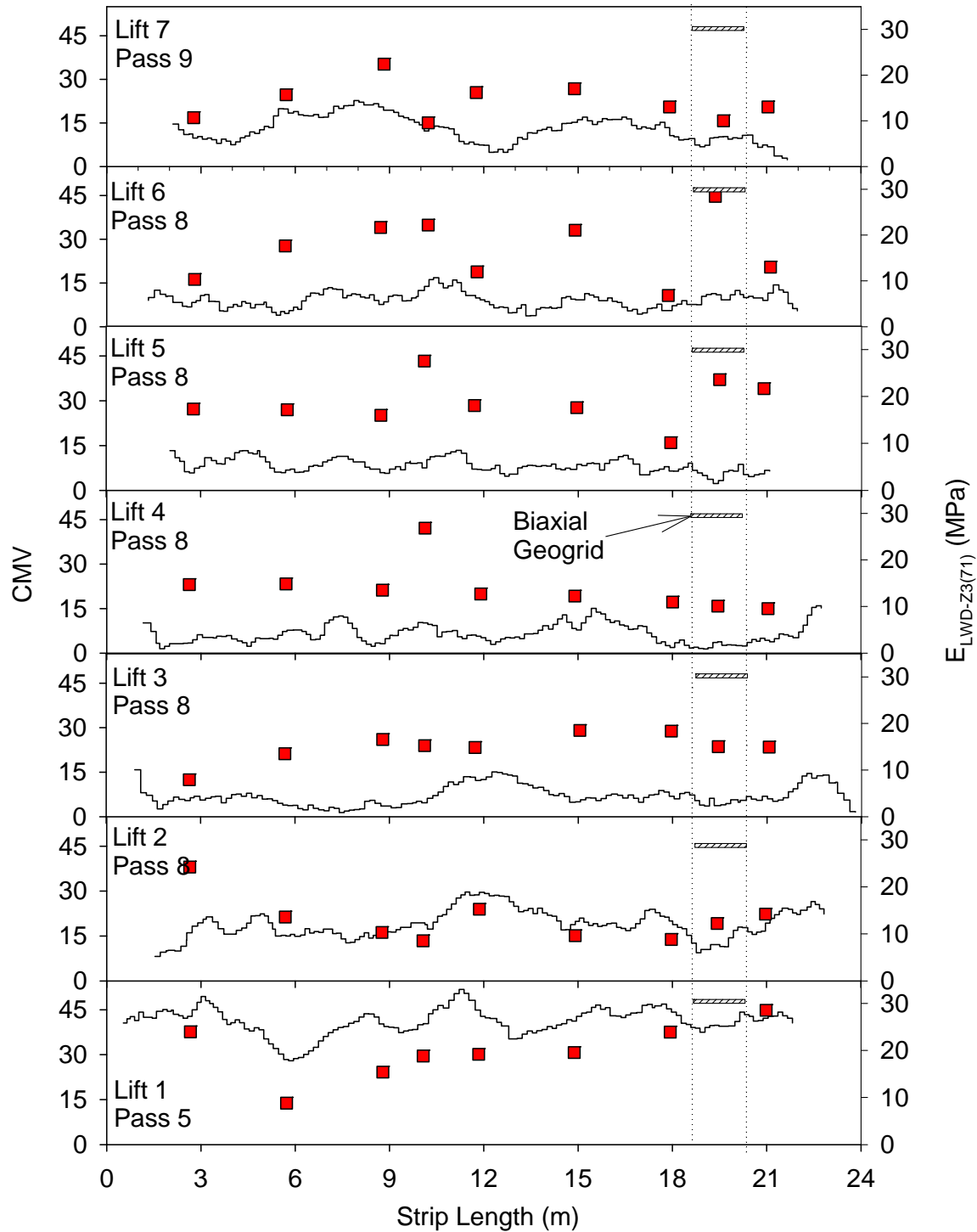


Figure 61. CMV and E_{LWD} measurement values after final pass on each lift – TB 1

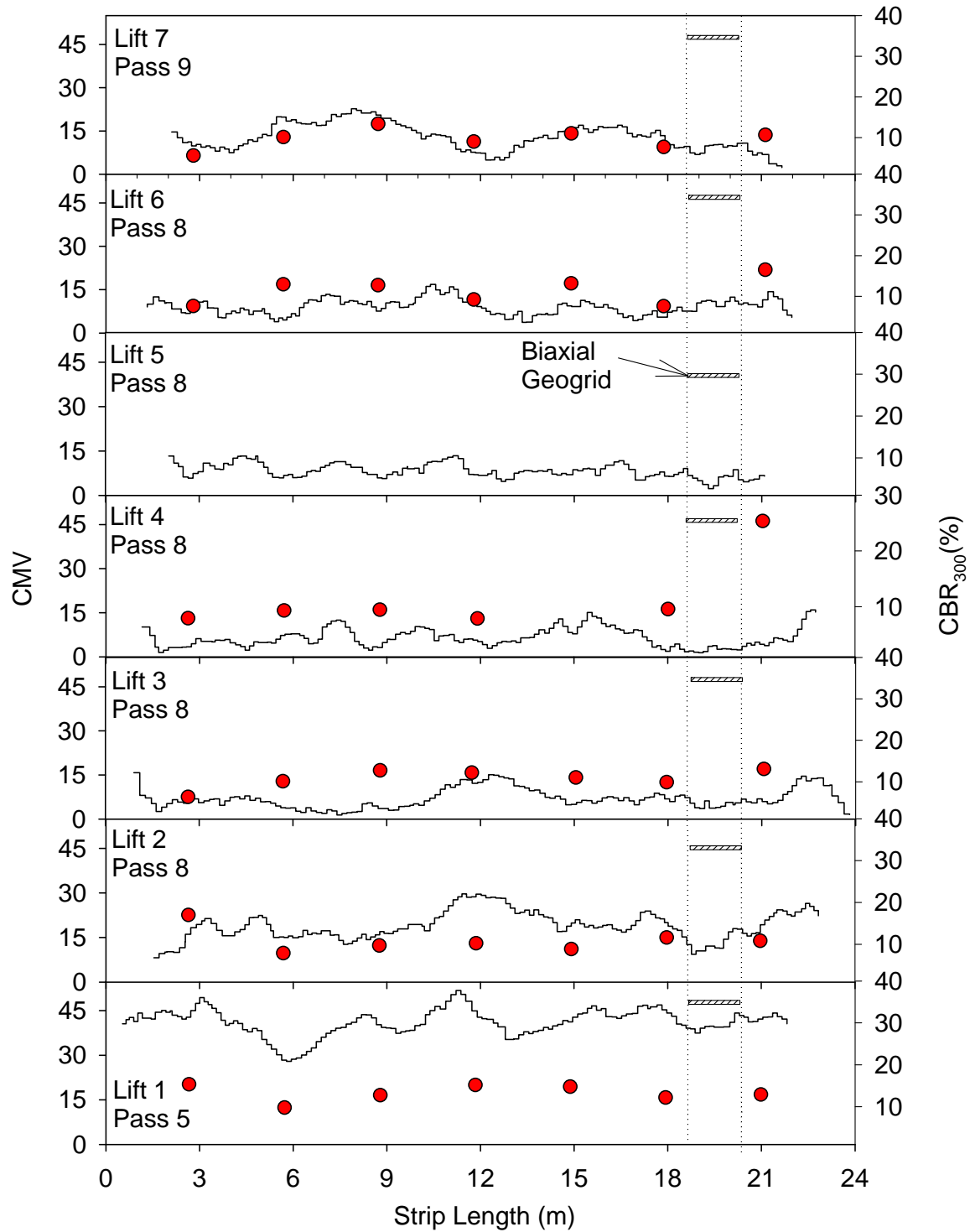


Figure 62. CMV and CBR measurement values after final pass on each lift – TB 1

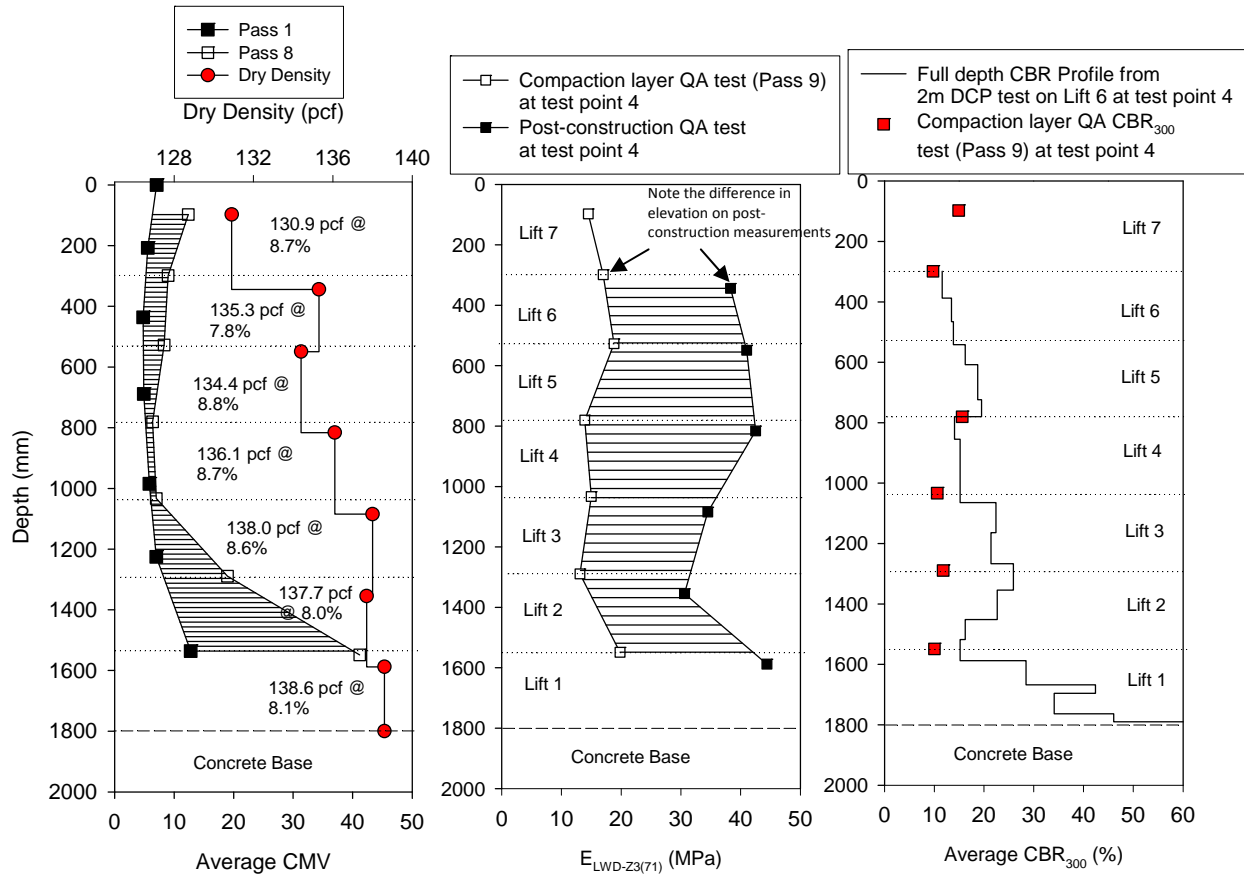


Figure 63. CMV, E_{LWD}, and CBR comparison – TB 1

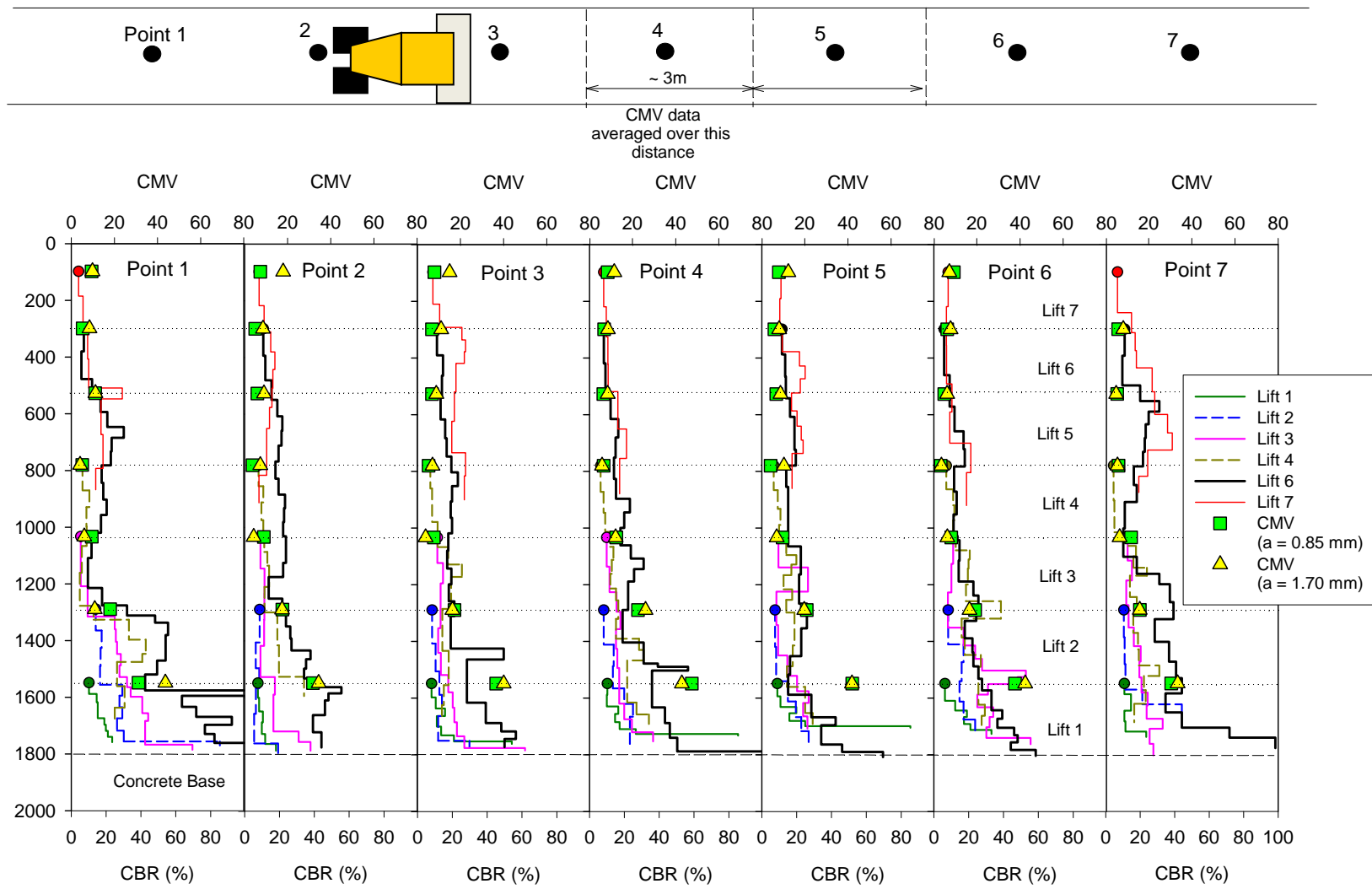


Figure 64. DCP-CBR profiles on each lift at seven points along the test bed with comparison to CMV measurements on each lift

Description of Test Bed 2

TB 2 was constructed as shown in Figure 65 with plan area of about 8 ft x 100 ft at the base of the excavation. The test bed was excavated to a depth of about 4 feet below existing grade. Following excavation, about half of the test bed was scarified and saturated to a depth of about 1 foot below the excavation to create a soft layer. The process of preparing the wet subgrade is shown in Figure 66. Seven lifts of CA6-G material (loose lift thickness ~ 12 inches) were then placed and compacted in the test bed for several roller passes (see Figure 67 and Figure 68). A biaxial geogrid reinforcement of size 10 ft long x 8 ft wide was placed along the soft subgrade portion of the test bed on lifts 1 to 6 prior to placing each consecutive lift (see Figure 69). To measure the in-ground stresses during roller compaction passes, semi-conductor EPC's were installed on the soft subgrade layer, lift 2, and lift 4 as shown in Figure 65. EPC's were installed in orthogonal directions to measure triaxial stress in the ground (σ_x , σ_y , and, σ_z).

The fill material was compacted using CS 563 smooth drum for several roller passes in low amplitude, high amplitude, and no amplitude (static) settings. A summary of roller passes on TB1 is presented in Table 11. Roller-integrated CMV, RMV, and MDP were continuously measured during the compaction process. Zorn 300-mm plate LWD and DCP tests were performed on each lift after the final static compaction pass at 9 to 10 locations across the test bed. After completing the compaction and testing process on lift 7, the fill material was excavated down to the surface of each underlying lift to the soft subgrade layer. Zorn LWD and NG tests were performed in the excavation on top of each lift. These tests were intended to check for improvement in the stiffness of the underlying layers due to the compaction process on the above lifts, and for the effects of confining stresses on the layer stiffness.

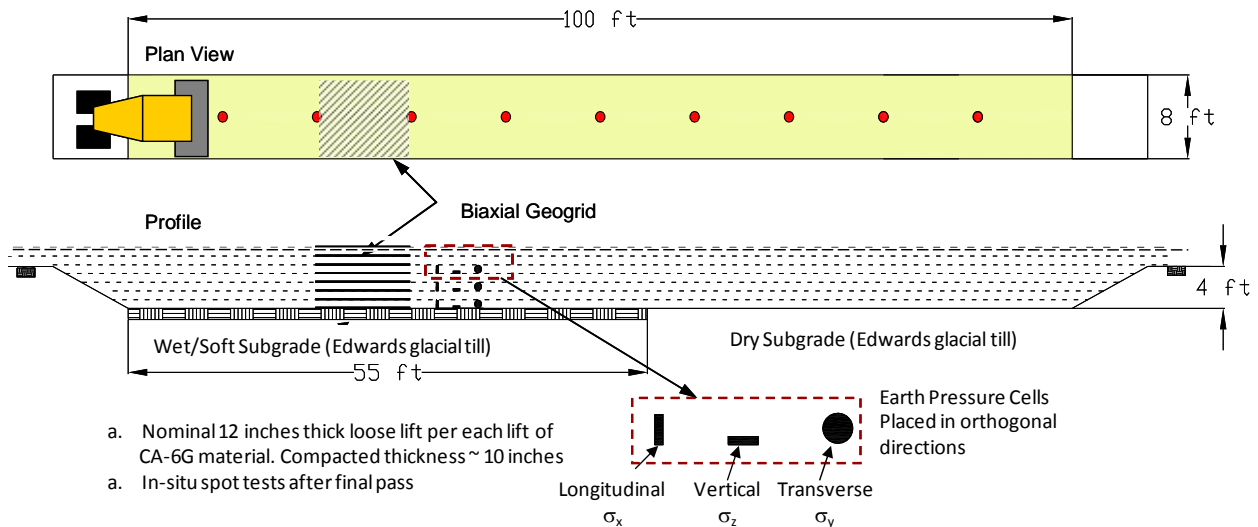


Figure 65. TB 2 plan view and profile with in-ground EPC's



Figure 66. Preparation of wet subgrade portion of TB 2



Figure 67. Wet/dry subgrade and lifts 1 to 3 of CA6-G material placed in TB 2



Figure 68. Lifts 4 to 7 of CA6-G material placed in TB 2



Figure 69. Placement of geogrid layer on soft subgrade

Table 11. Summary of experimental testing on TB 2 – wet/dry subgrade

Lift	Pass	<i>a</i>	Speed (mph)	E_{LWD}	DCP[§]	Nuclear Gauge
1	1 - 2	Low	2			
	3	Static	2	x	x	
	Excavation*	—	—	x		x
2	1 - 6	Low	2			
	7 - 8	High	2			
	9	Static	2	x	x	
	Excavation*	—	—	x		x
3	1 - 6	Low	2			
	7 - 8	High	2			
	9	Static	2	x	x	
	Excavation*	—	—	x		x
4	1 - 6	Low	2			
	7 - 8	High	2			
	9	Static	2	x	x	
	Excavation*	—	—	x		x
5	1 - 6	Low	2			
	7 - 8	High	2			
	9	Static	2	x	x	
	Excavation*	—	—	x		x
6	1 - 6	Low	2			
	7 - 8	High	2			
	9	Static	2	x	x	
	Excavation*	—	—	x		x
7	1 - 6	Low	2			
	7 - 8	High	2			
	9	Static	2	x	x	
	Excavation*	—	—	x		x

*Tests were conducted on top of each lift by excavating down after compacting all seven layers of CA6-G material

§DCP tests on lift 6 were performed for a maximum penetration depth of about 6 feet (~2m)

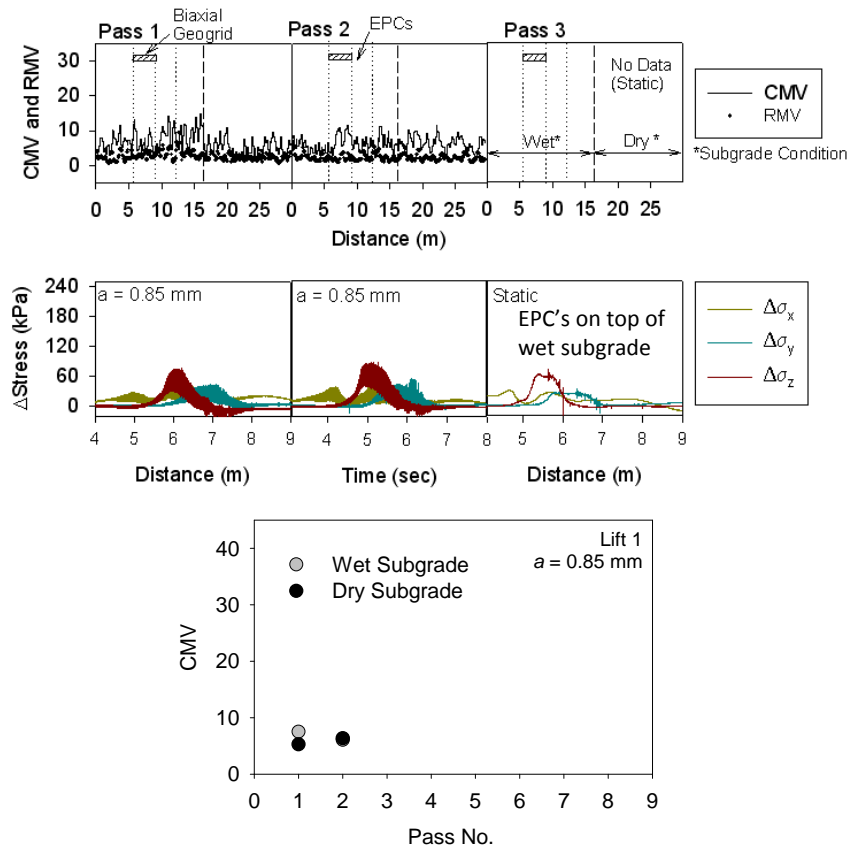


Figure 70. CMV and in-ground stress measurements for CE 563 roller passes – lift 1

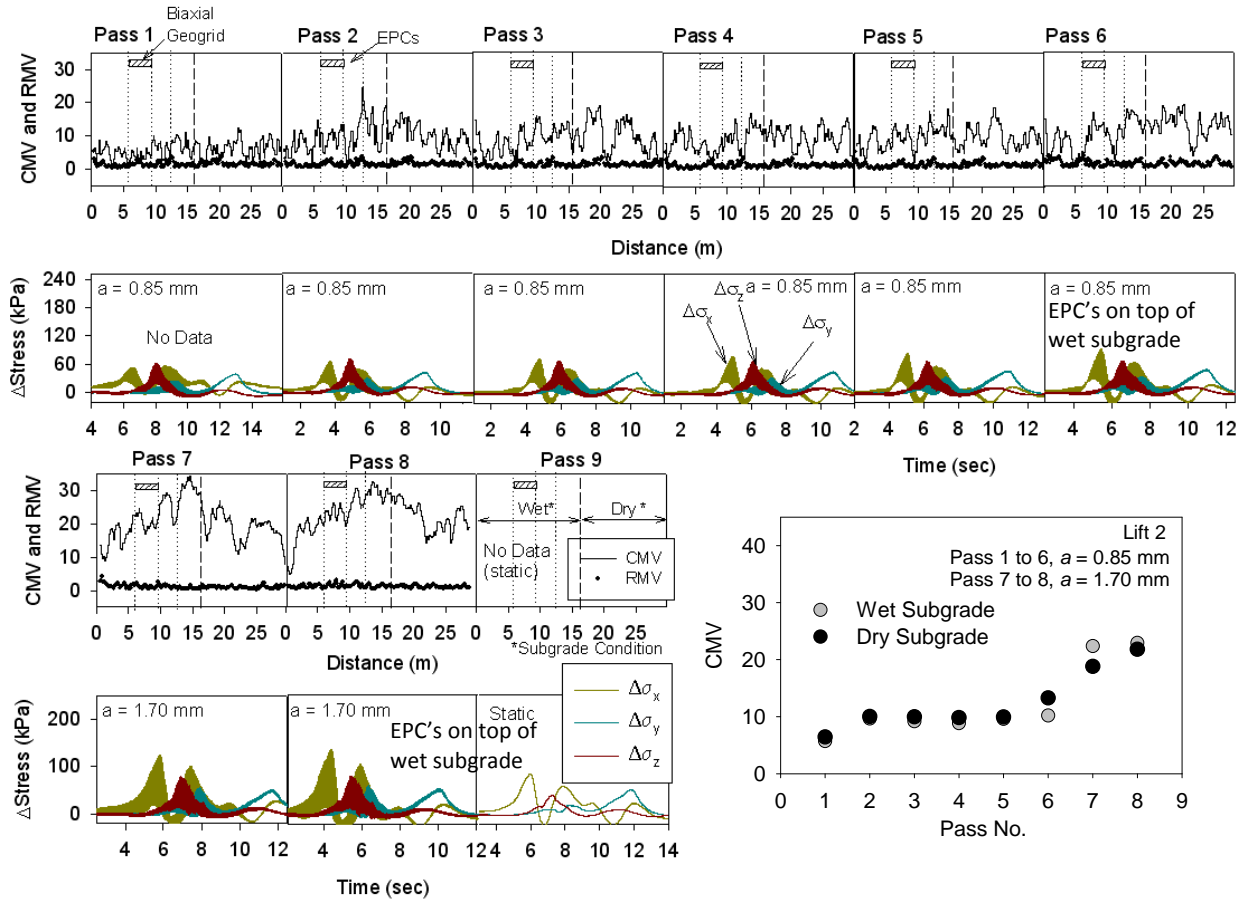


Figure 71. CMV and in-ground stress measurements for CS 563 roller passes – lift 2

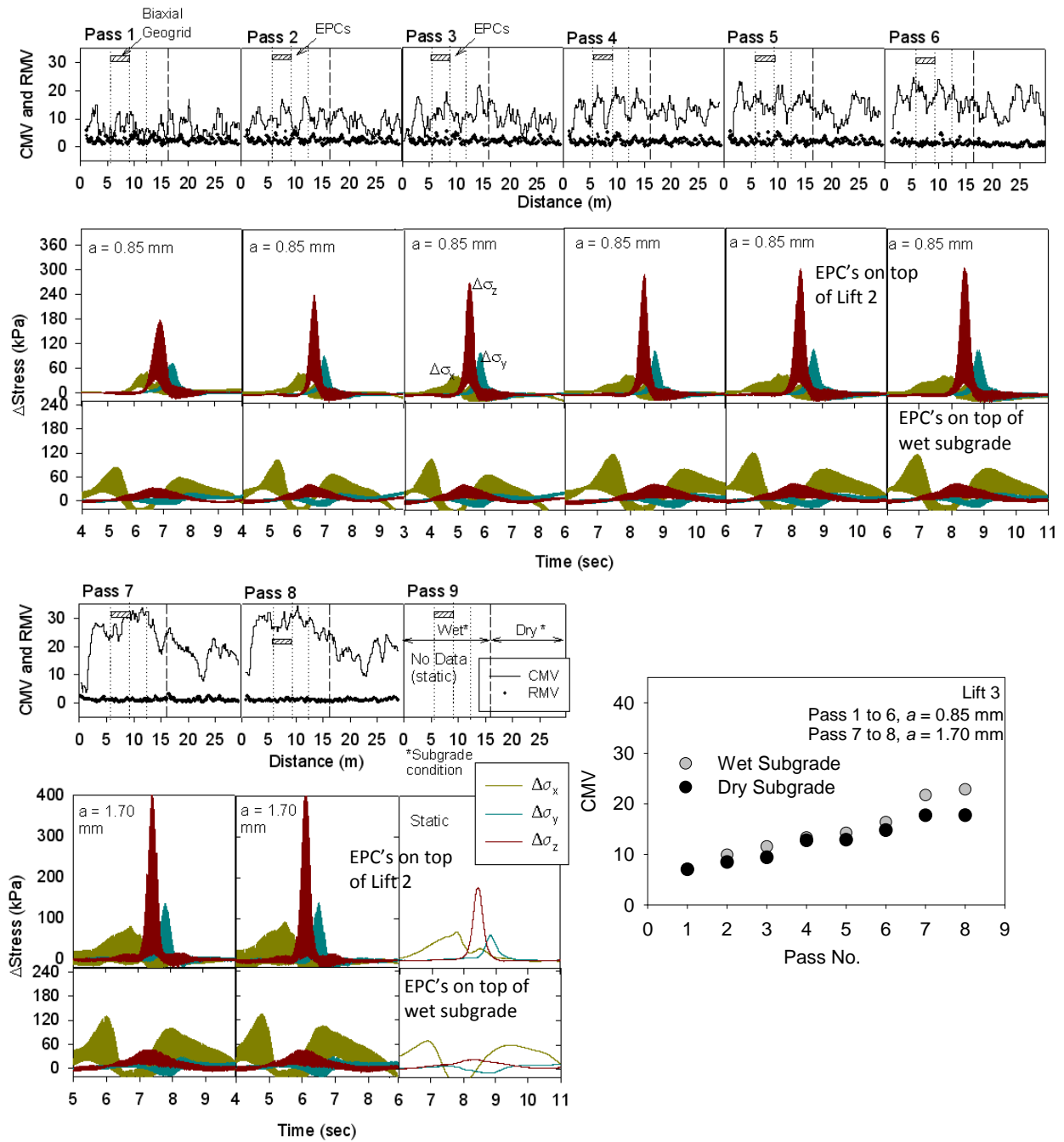


Figure 72. CMV and in-ground stress measurements for CS 563 roller passes – lift 3

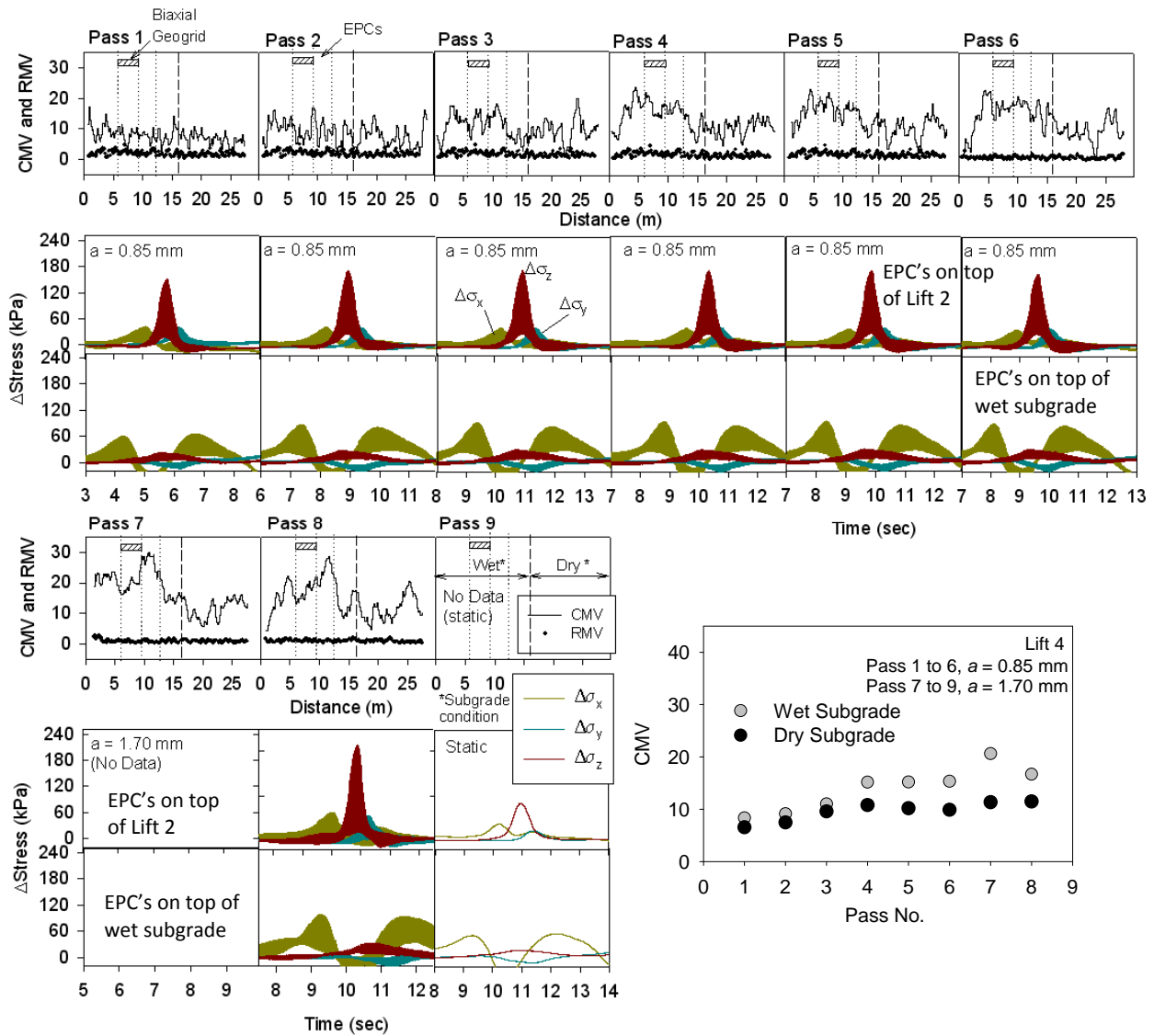


Figure 73. CMV and in-ground stress measurements for CS 563 roller passes – lift 4

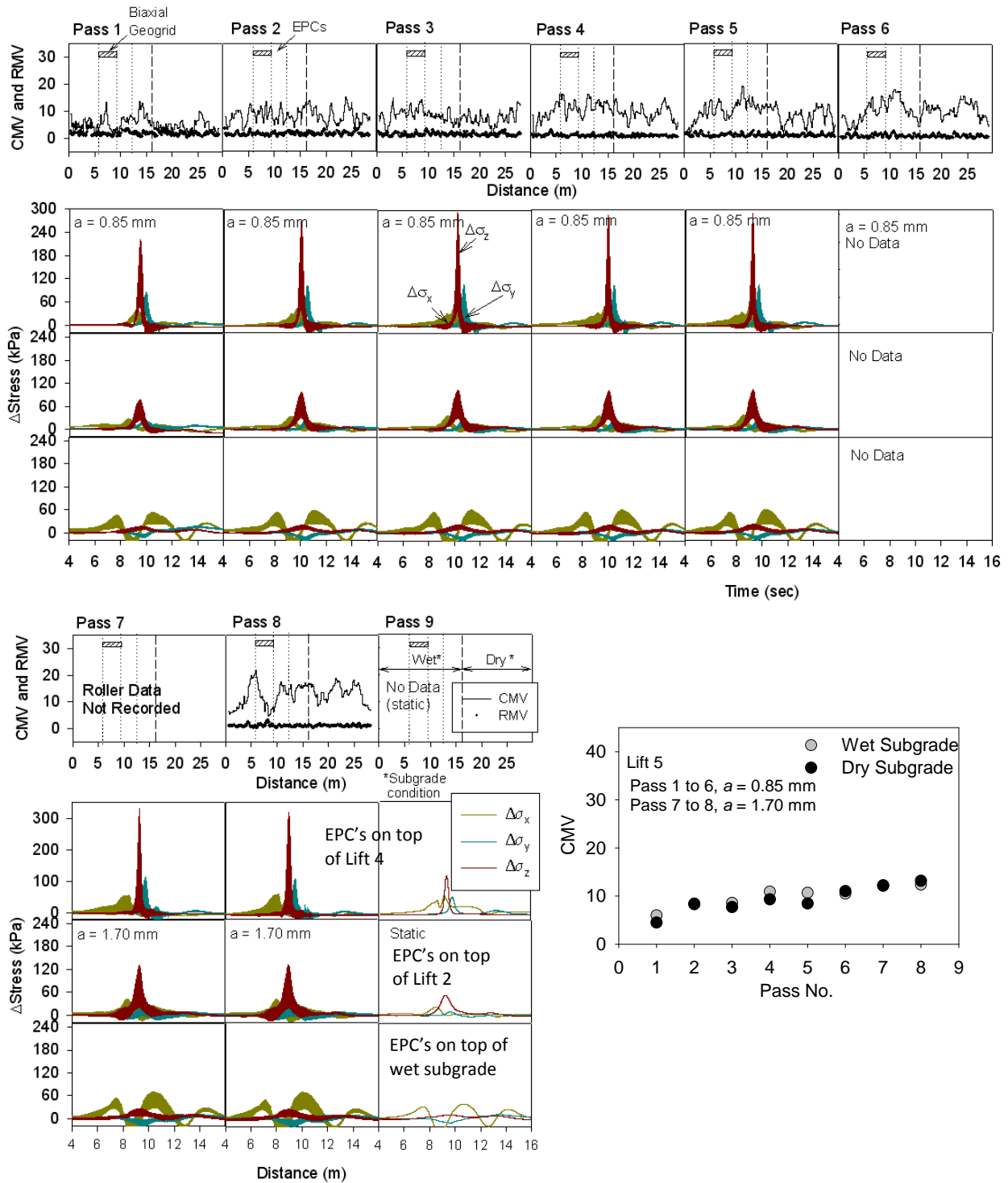


Figure 74. CMV and in-ground stress measurements for CS 563 roller passes – lift 5

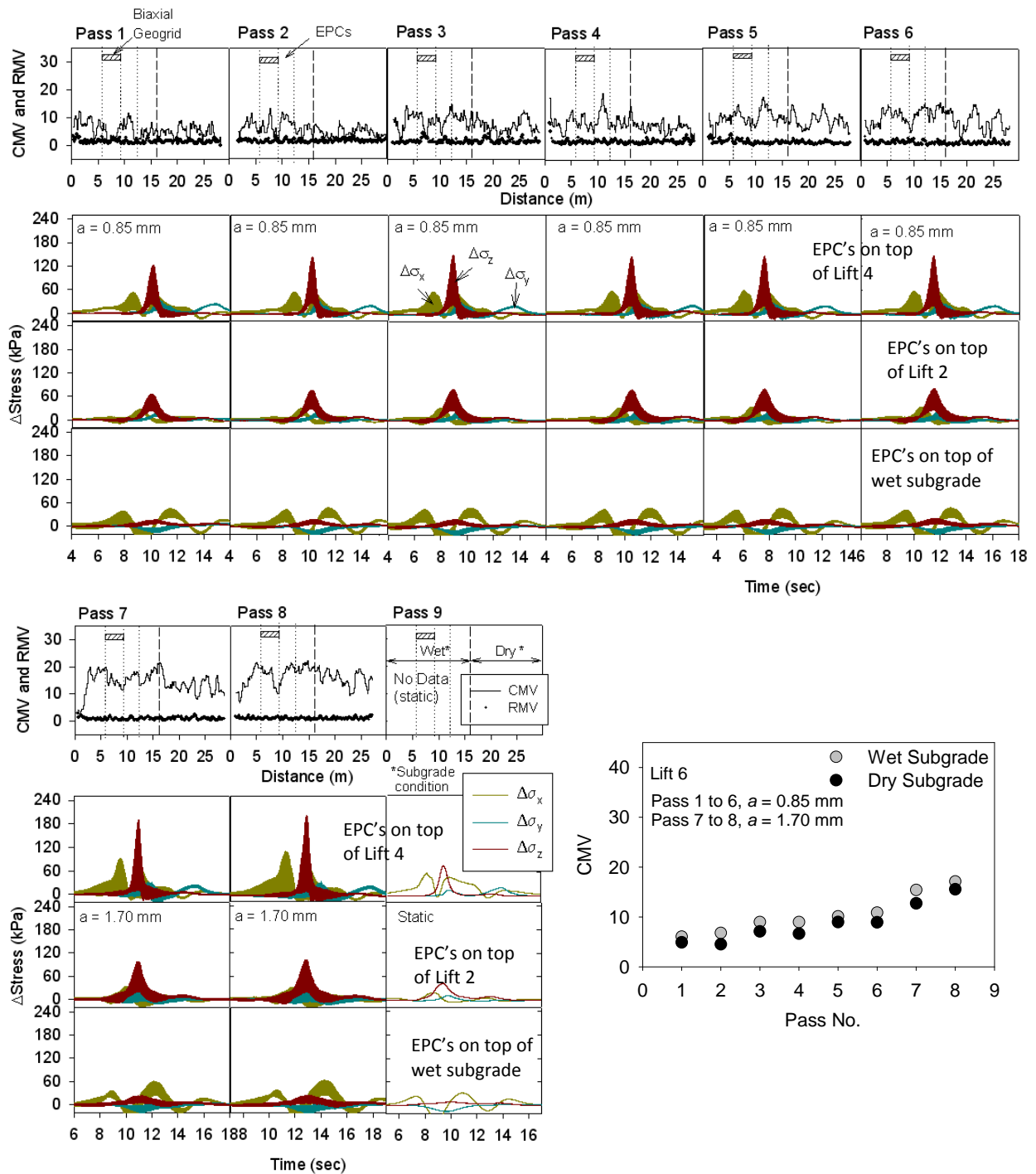


Figure 75. CMV and in-ground stress measurements for CS 563 roller passes – lift 6

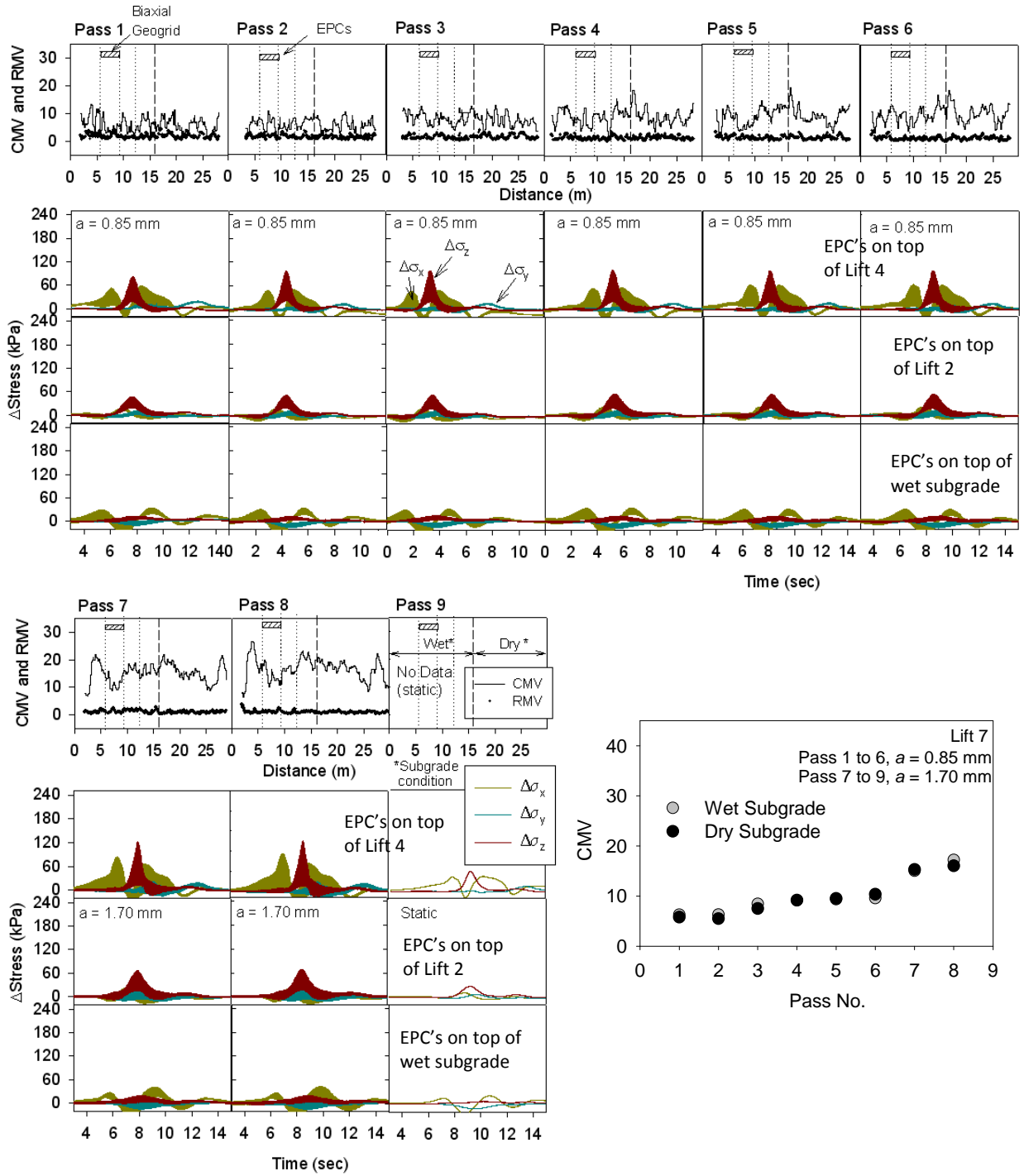


Figure 76. CMV and in-ground stress measurements for CS 563 roller passes – lift 7

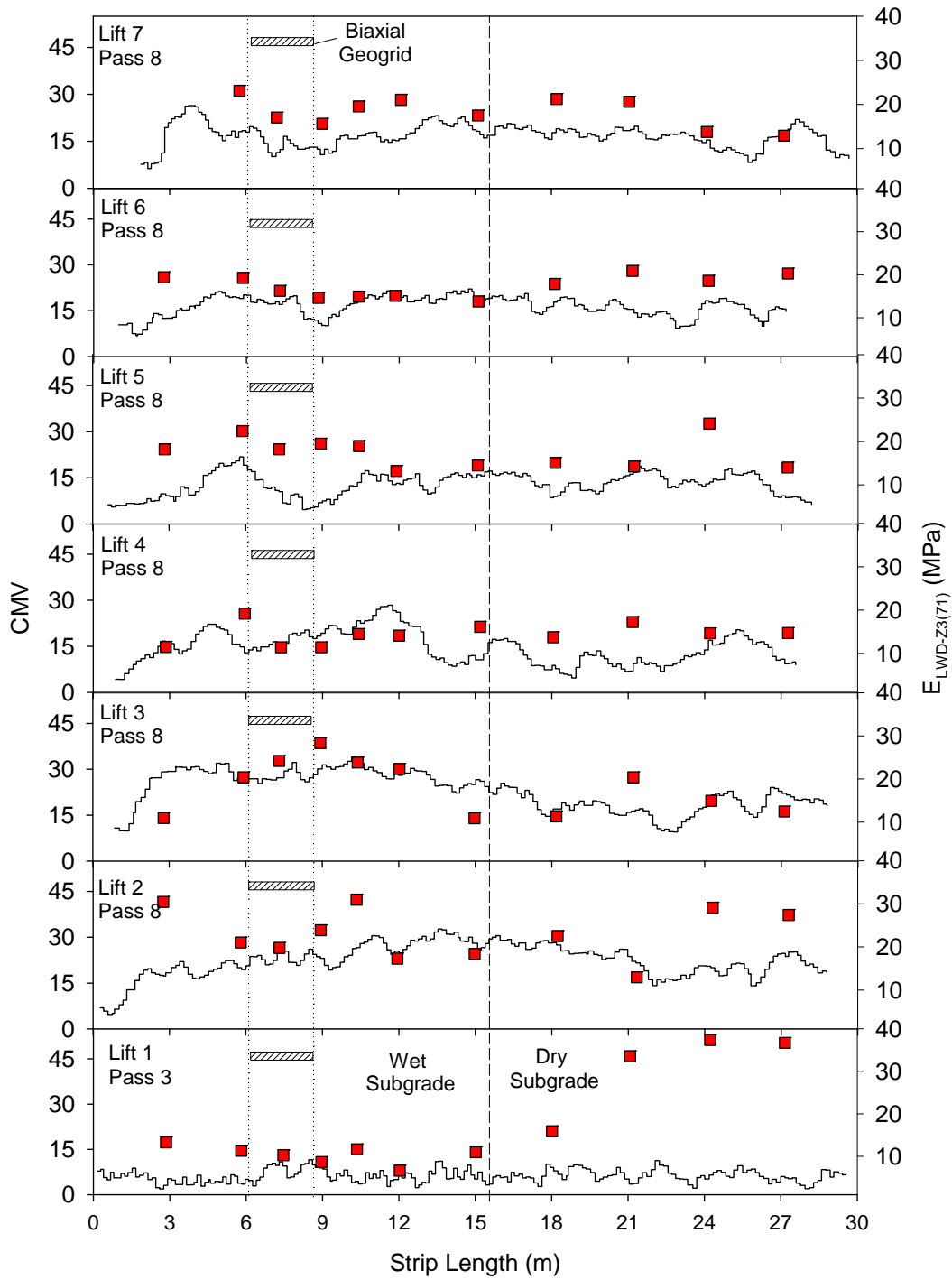


Figure 77. CMV and E_{LWD} measurement values after final pass on each lift – TB 2

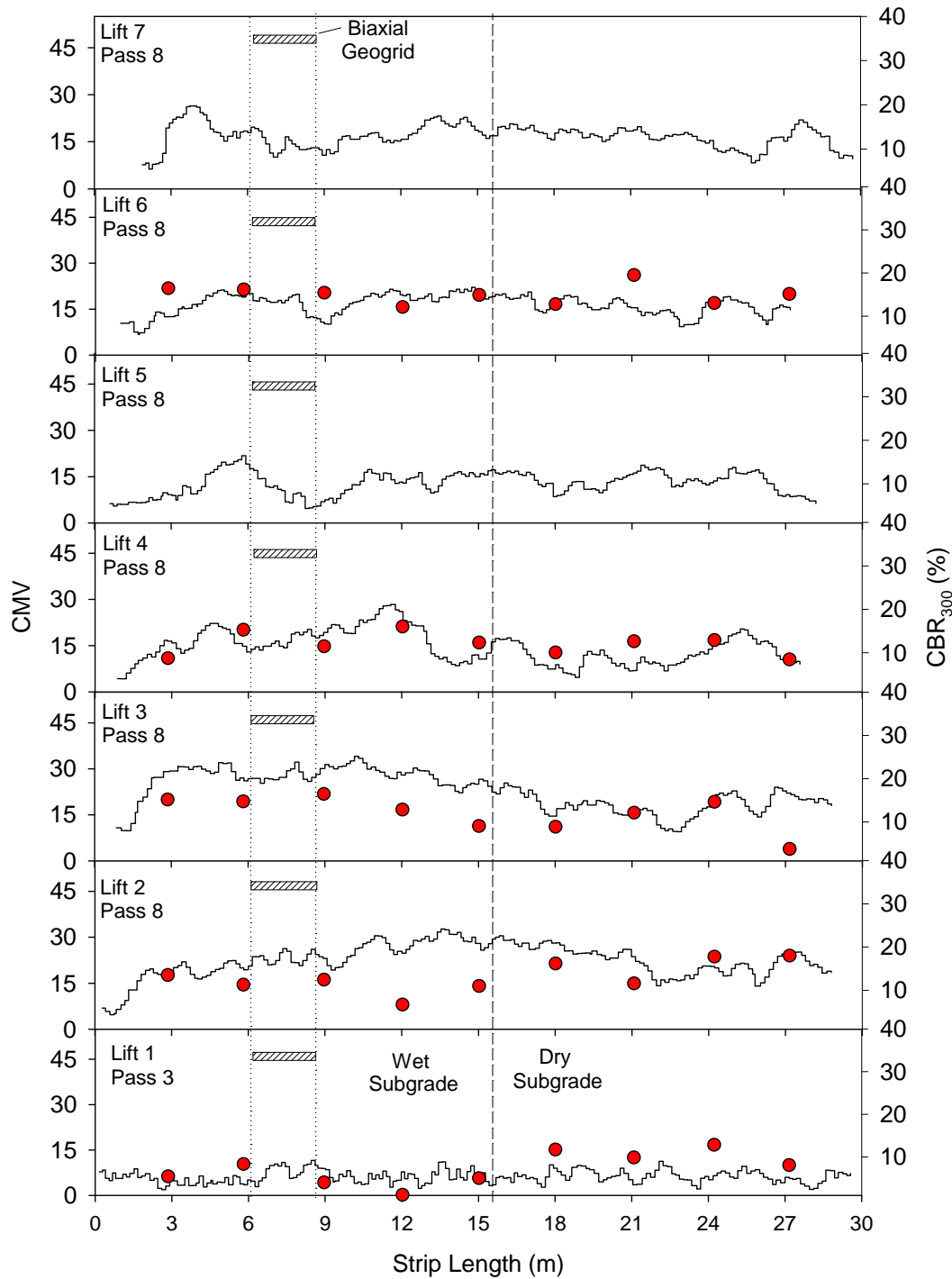


Figure 78. CMV and CBR measurement values after final pass on each lift – TB 2

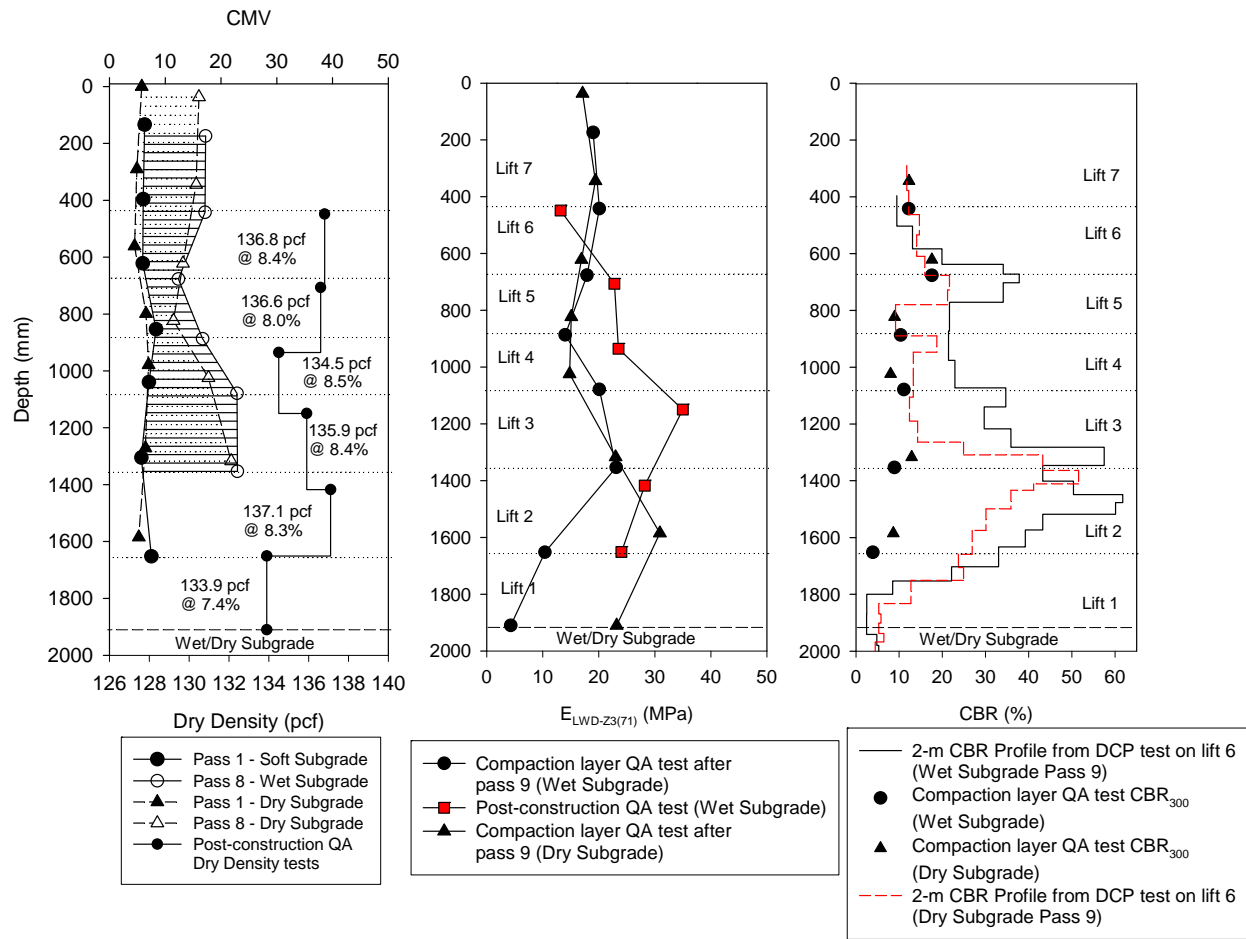


Figure 79. CMV, E_{LWD} , and CBR comparison – TB 2

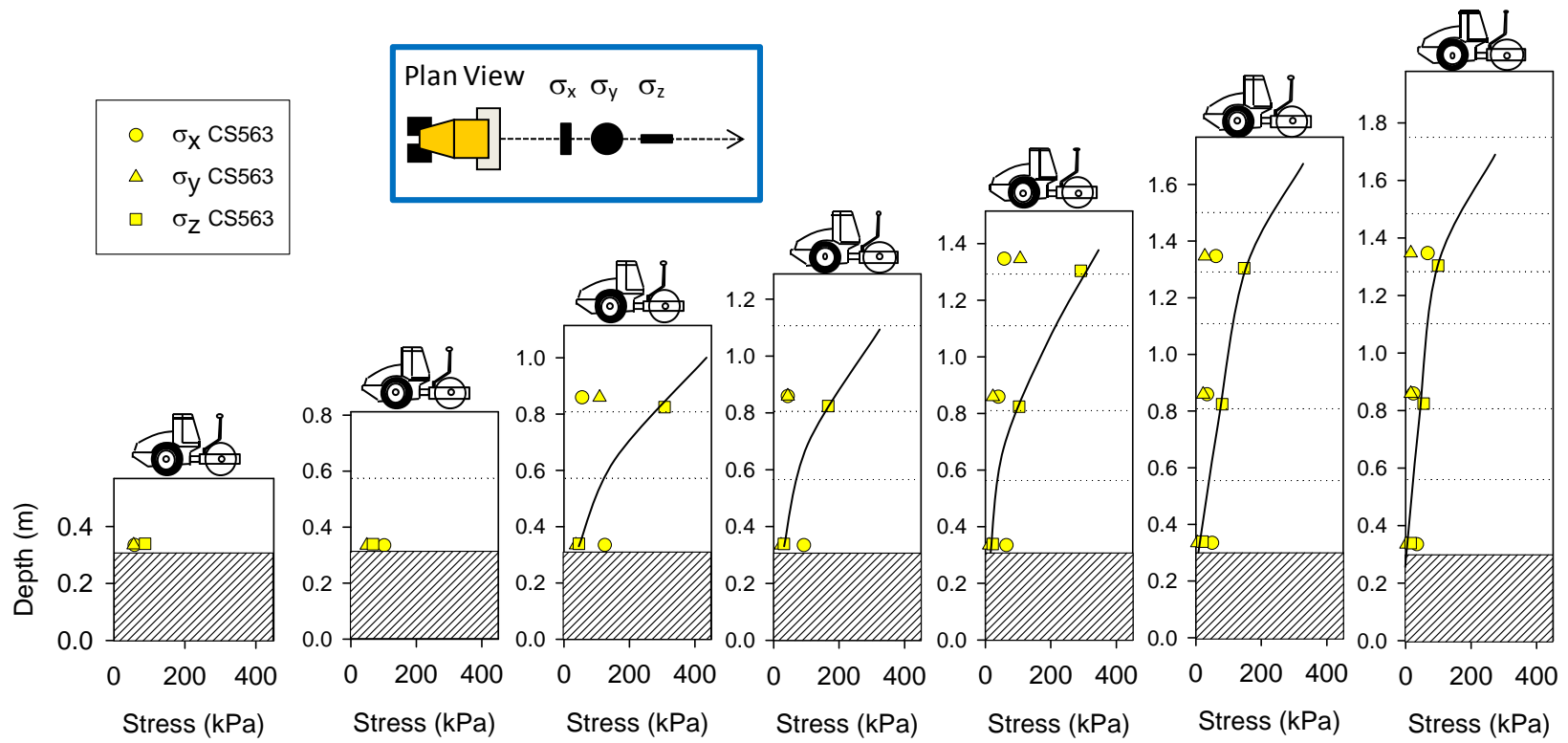


Figure 80. Stress distribution under the roller at a = 0.85 mm – TB 2

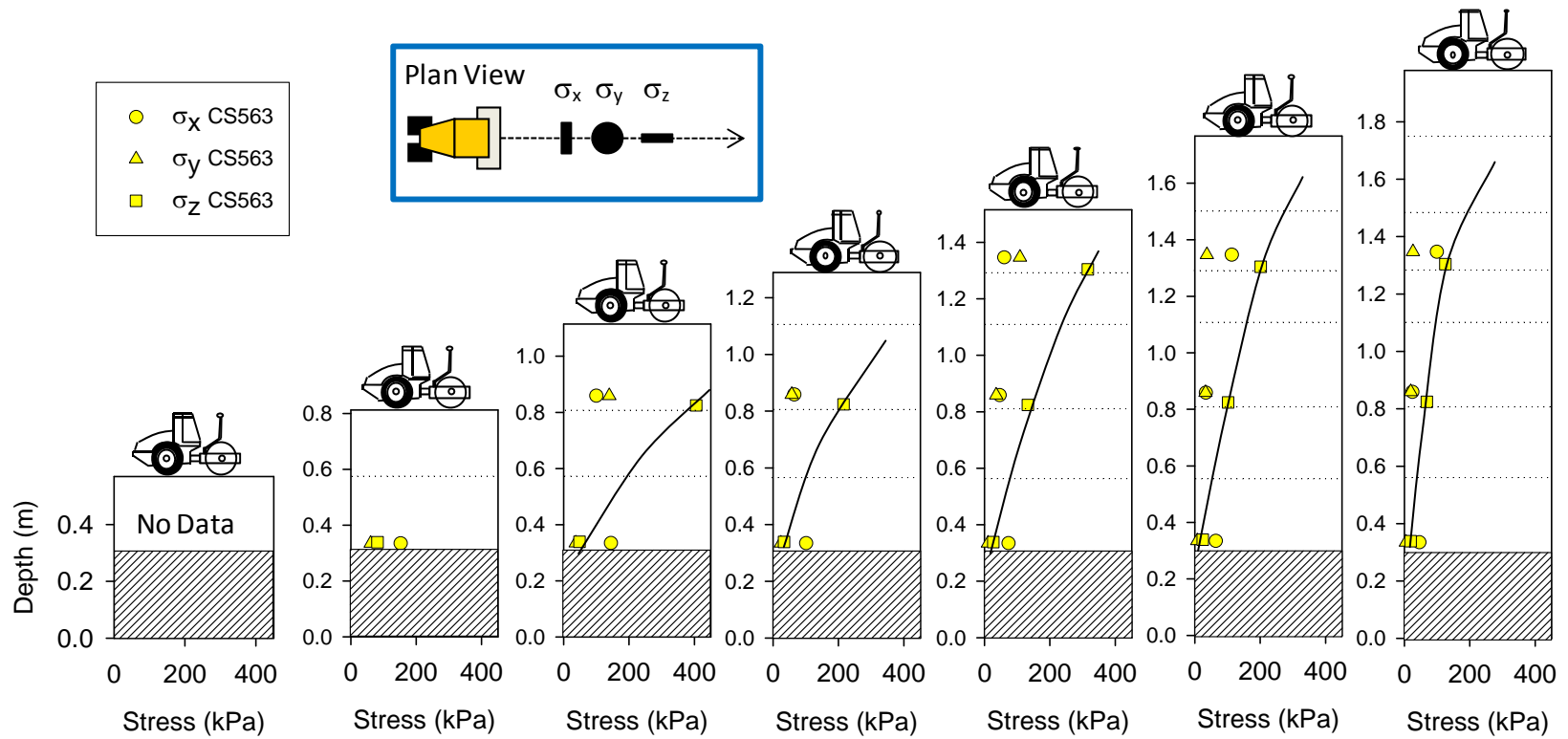


Figure 81. Stress distribution under the roller at a = 1.70 mm – TB 2

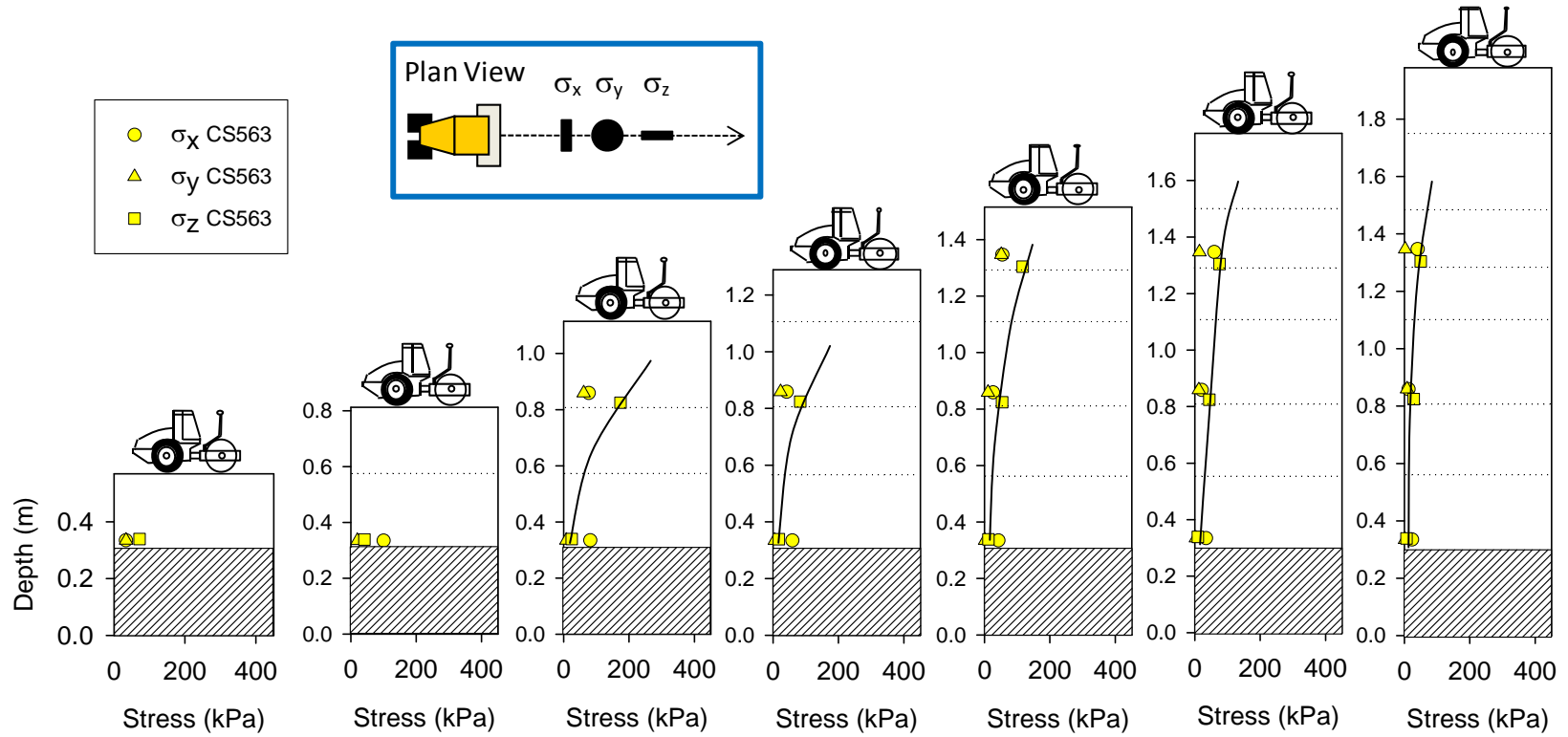


Figure 82. Stress distribution under the roller in static mode – TB 2

Description of Test Bed 3

TB 3 was constructed as shown in Figure 83 which had plan dimensions of approximately 8 ft x 80 ft at the base of the excavation. The test bed was excavated to a depth of about 4 feet below existing grade. Following excavation, about half of the test bed was scarified and moisture conditioned to a depth of about 0.3 m below the excavation to create a soft/wet subgrade layer. A 0.3 m thick concrete layer was continued in the remaining half of the excavation to create a stiff layer. Seven lifts of CA6-G material (loose lift thickness ~ 0.3 m) were then placed and compacted using CS 563 padfoot roller for several roller passes in low amplitude, high amplitude, and static settings (Figure 84 and Figure 85). A summary of roller passes is presented in Table 12. During roller operation at low and high amplitude settings the amplitude output on the display appeared variable. Further, when the roller was operated in static setting the machine was vibrating at low amplitude (measured as 0.31 mm). Roller-integrated CMV, RMV, and MDP were continuously monitored during the compaction process.

Zorn 300-mm plate LWD and full-depth DCP tests (~ 1 m depth) were performed on each lift after the final static compaction pass at six locations along the test strip. LWD tests were performed by excavating down to the bottom of the padfoot penetration. After completing tests on the final lift, the fill material was excavated down to the surface of each underlying lift as shown in Figure 86 at two locations along the test strip (one location above the concrete base and the other location above the soft subgrade). LWD tests were performed in the excavation on top of each lift. These tests were intended to check for improvement in the stiffness of the underlying layers due to compaction of the lifts placed above, and for the effects of confinement on the layer stiffness.

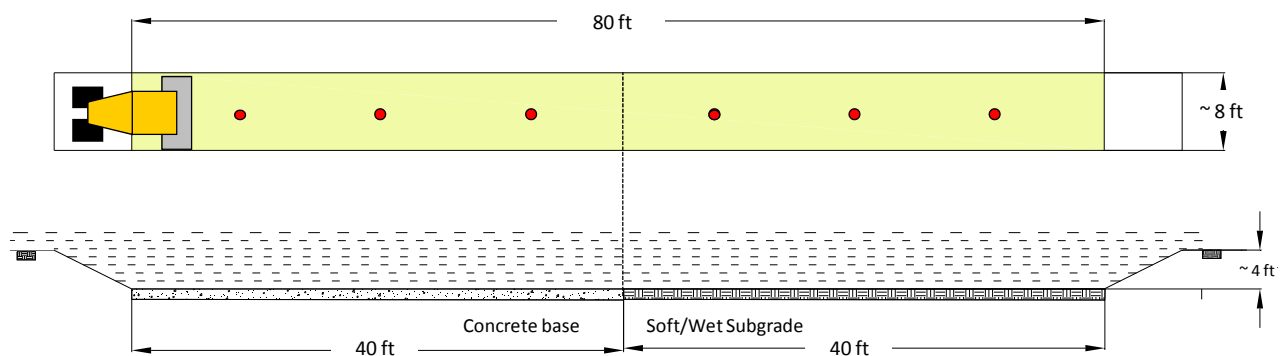


Figure 83. TB 3 plan view and profile with location of in-ground EPCs

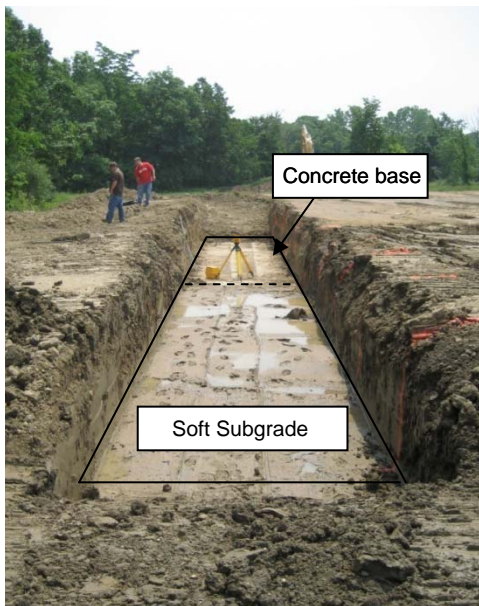


Figure 84. Concrete and soft/wet subgrade base and lifts 1 to 3 of CA6-G material placed in TB 3



Figure 85. Lifts 4 to 7 of CA6-G material placed in TB 3

Table 12. Summary of experimental testing on TB 3 – concrete/soft subgrade

Roller	Lift	Pass	Amplitude setting	Speed (km/h)	E _{LWD-Z3}	DCP
CS563	1	1 - 6	Low	4.6 to 4.8		
		7 - 8	High	4.2 to 4.5		
		9	Static	5.1	x	x
		Excavation*	—	—	x	
	2	1 - 6	Low	3.0 to 3.3		
		7 - 8	High	3.1		
		9	Static	3.3	x	x
		Excavation*	—	—	x	
	3	1 - 6	Low	3.0 to 3.3		
		7 - 8	High	3.1 to 3.2		
		9	Static	3.1	x	x
		Excavation*	—	—	x	
	4	1 - 6	Low	3.0 to 3.4		
		7 - 8	High	3.0 to 3.2		
		9	Static	3.6	x	x
		Excavation*	—	—	x	
	5	1 - 6	Low	2.9 to 3.7		
		7 - 8	High	3.3 to 3.5		
		9	Static	3.5	x	x
		Excavation*	—	—	x	
	6	1 - 6	Low	3.0 to 3.6		
		7 - 8	High	3.3 to 3.5		
		9	Static	3.7	x	x
		Excavation*	—	—	x	
	7	1 - 6	Low	3.3 to 3.8		
		7 - 8	High	3.0 to 3.3		
		9	Static	3.4	x	x

*Tests were conducted on top of each lift by excavating down after compacting all seven layers of CA6-G material



Figure 86. Process of excavation to the top of each underlying lift to perform LWD testing

Roller-Integrated Compaction Measurements

Roller-integrated MDP, CMV, and RMV raw data plots for each roller pass on lifts 1 to 7 are presented in Figure 87 to Figure 90, respectively. Screen shots of MDP measurements from the Caterpillar viewer program for pass 9 on lifts 1 to 7 are shown in Figure 91. CMV and RMV measurements on this machine were not repeatable. In addition, the amplitude output when roller was operated at low and high amplitude settings did not appear to be representative. The influence of these uncertainties makes the CMV and RMV results from this test bed difficult to interpret, therefore, this information was not further analyzed. Only MDP data is further analyzed and discussed in this report.

Repeatability and reproducibility analysis presented in the earlier chapter indicated that amplitude influences the MDP measurement values. Despite this effect, MDP data on lift 1 shows a clear distinction between the differences in the underlying subgrade support at all passes. MDP values range between 2 to 10 kJ/s in the area underlain by concrete base and 20 to 38 kJ/s in the area underlain by soft/wet subgrade for lift 1. This difference is also visually noted (Figure 87) with significant rutting in the area underlain by soft/wet subgrade. Figure 92 shows pass 9 MDP measurements on lifts 1 through 7. MDP measurements on lift 2 through 7 show “bridging” of the underlying soft subgrade layer. This is further discussed and statistically quantified in the following section of this report.

Average MDP compaction growth curves for all lifts are presented in Figure 93. These curves generally showed a decrease in MDP with increasing compaction with similar trends for a given pass between the soft subgrade and concrete base areas. The MDP growth curves showed some irregular trends which are possible due to: (a) roller off-tracking from the previous pass path as noted in a field study by Newman and White (2008) and (b) variations in amplitude between passes. Figure 94 shows roller paths for each pass on lifts 1 to 7 which do not indicate any roller off-tracking. Therefore, the influence of the variable vibration amplitude between passes is believed to have contributed to the variations in MDP growth curves. The average MDP values on pass 9 ($a = 0.31$ mm) were consistently higher than the average MDP values at higher amplitude settings for all lifts. This is consistent with the observations in the earlier repeatability and reproducibility analysis chapter. The higher MDP values with increasing amplitude are

believed to be related to the mechanical performance of the roller and/or roller-soil interaction. Higher dynamic forces applied during high amplitude vibration will likely cause greater drum sinkage which increases the rolling resistance and consequently the MDP. It is not known if more power is needed to propel the machine at higher amplitudes and if amplitude should be considered in the calibration process.

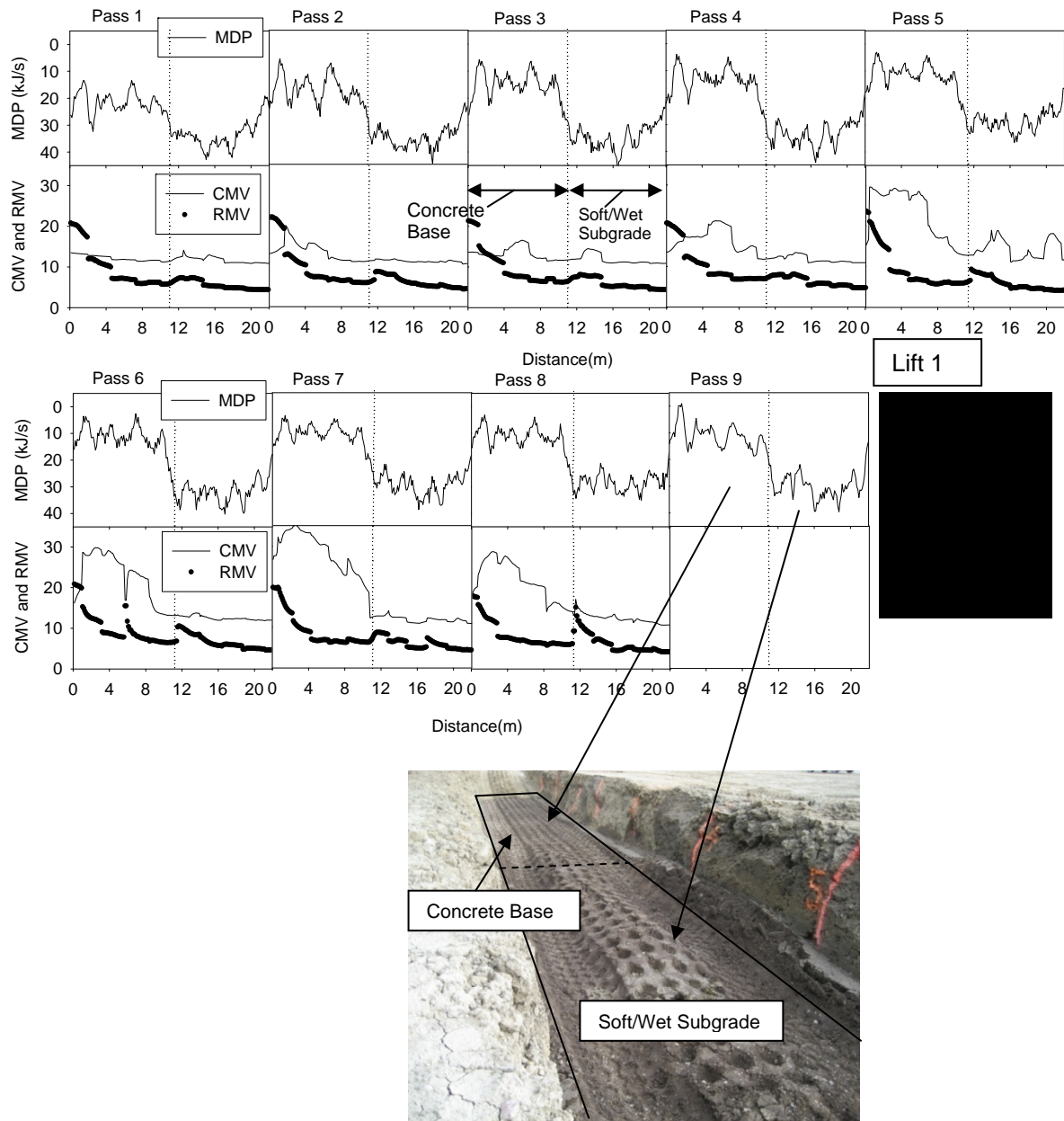


Figure 87. Raw data plots of MDP, CMV, and RMV measurements on lift 1 (picture showing the rutting observed on lift 1 after pass 9)

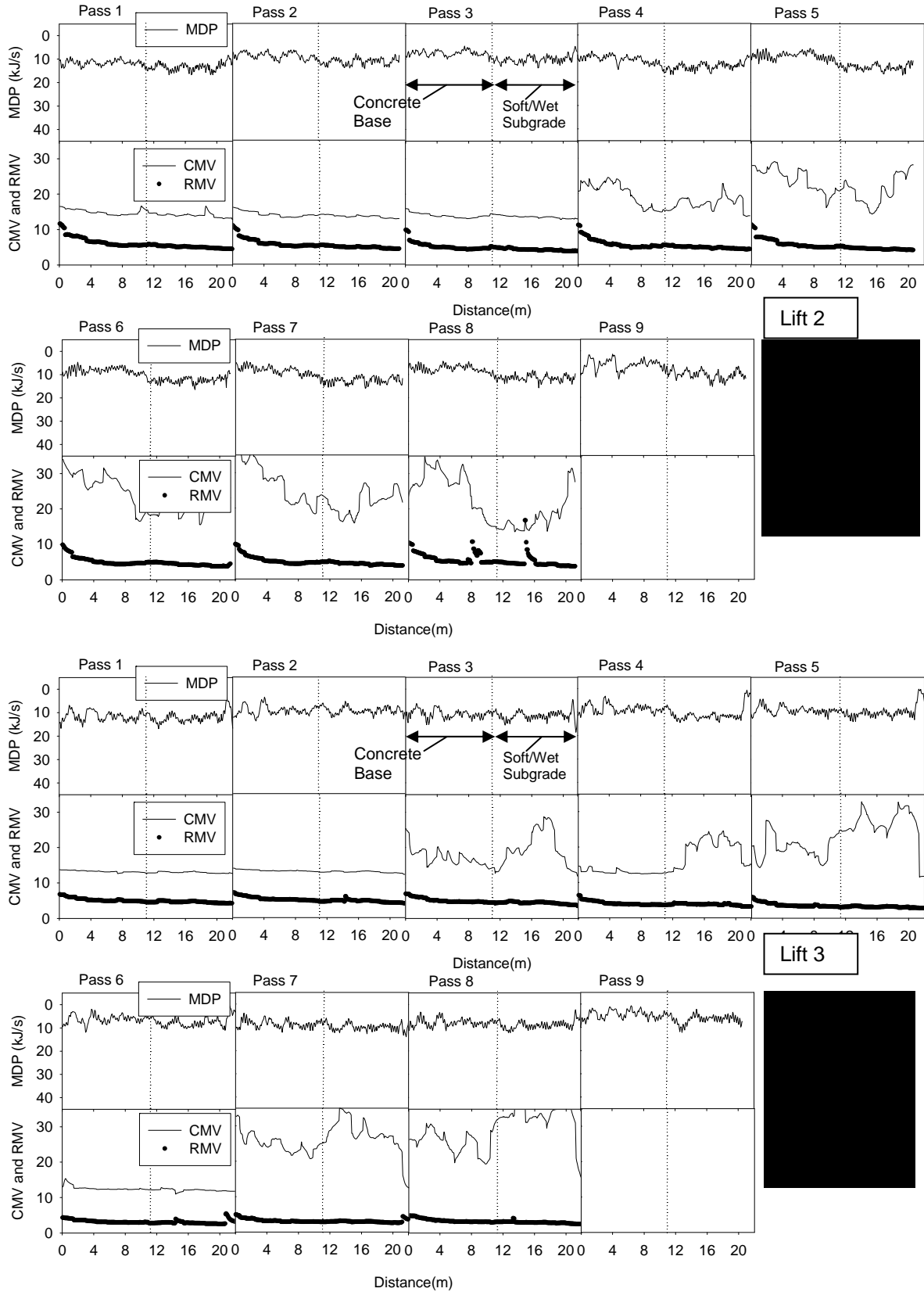


Figure 88. Raw data plots of MDP, CMV, and RMV measurements on lifts 2 and 3

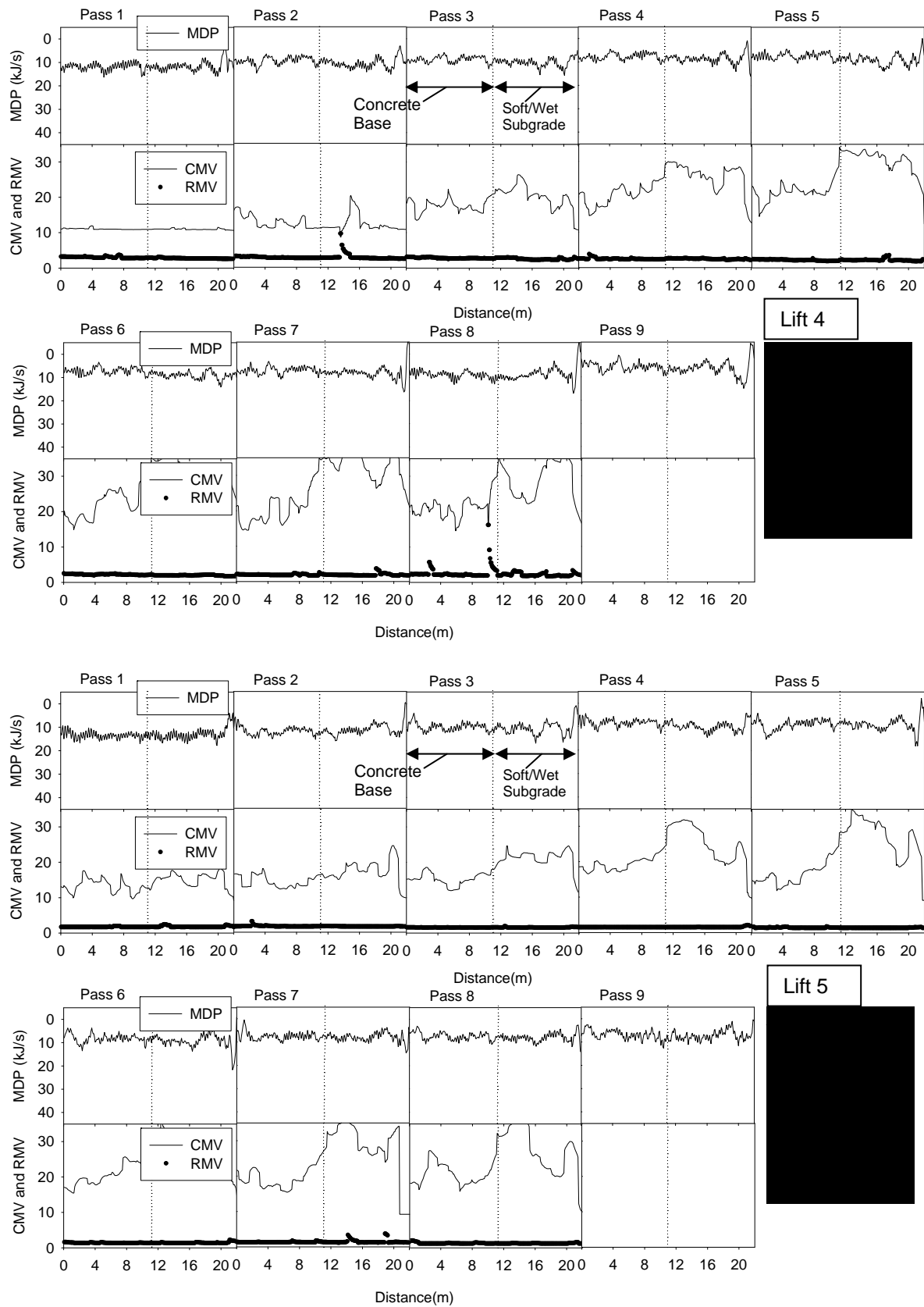


Figure 89. Raw data plots of MDP, CMV, and RMV measurements on lifts 4 and 5

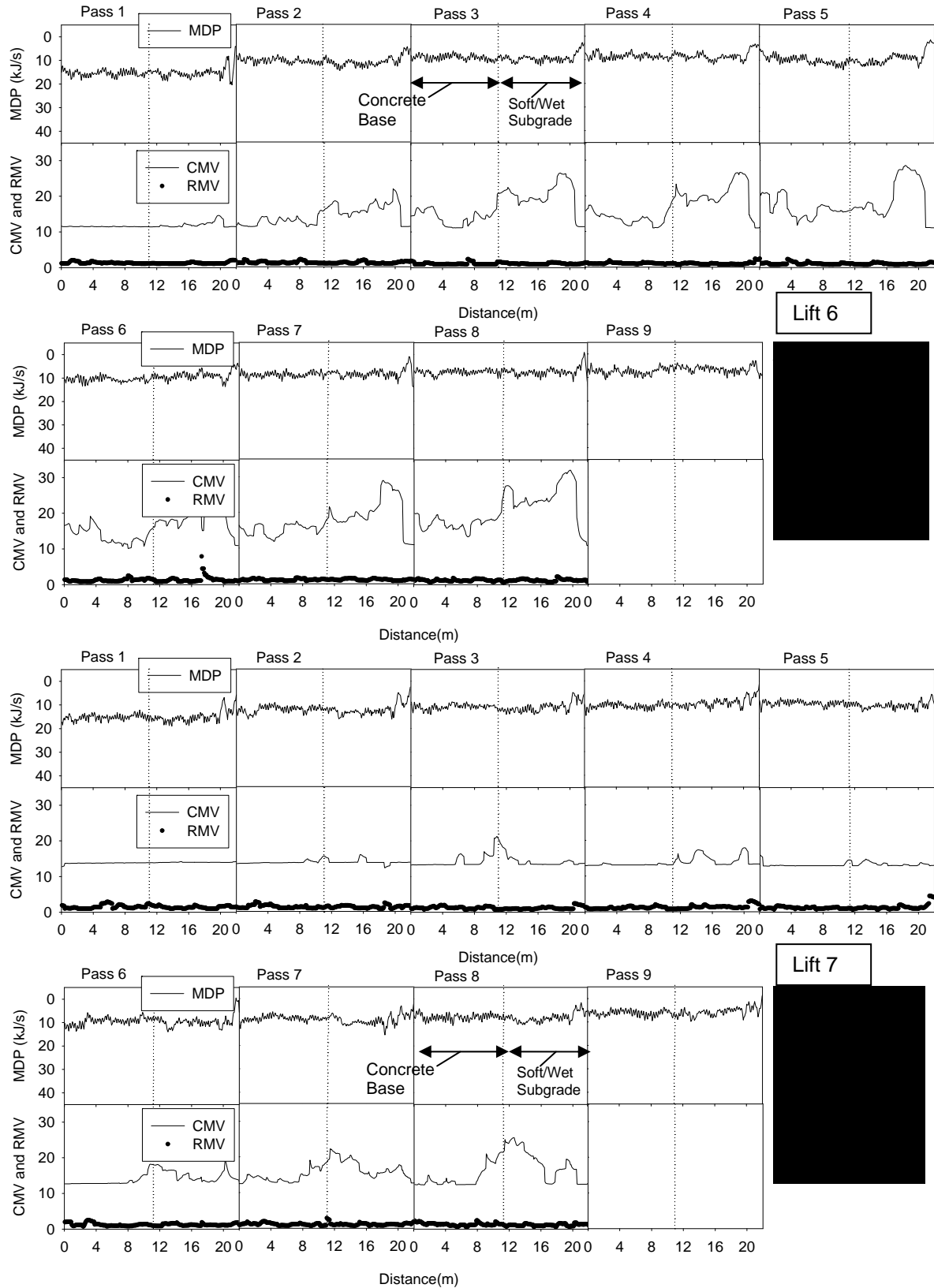


Figure 90. Raw data plots of MDP, CMV, and RMV measurements on lifts 6 and 7



Figure 91. Caterpillar viewer program screen shots of MDP final static pass on each lift – TB 3 (color)

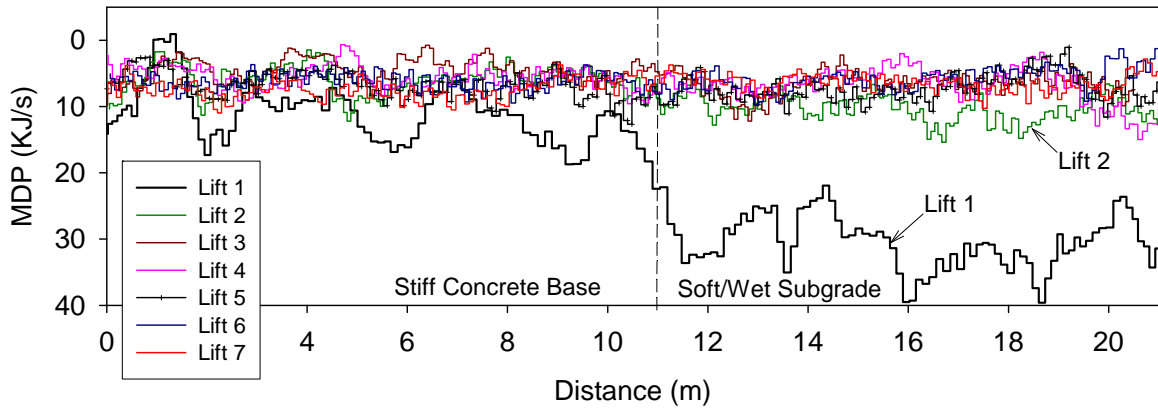


Figure 92. Pass 9 MDP measurements on lifts 1 to 7 – TB 3 (color)

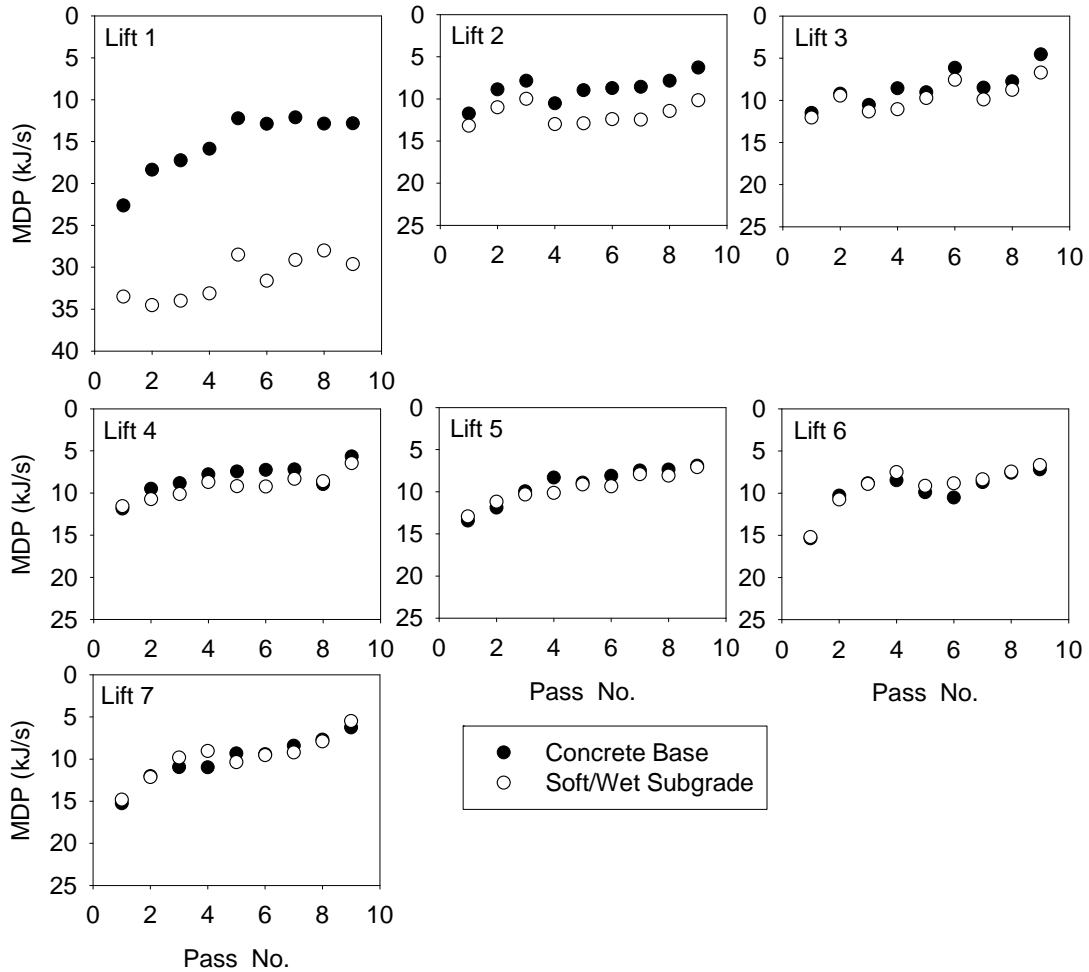


Figure 93. MDP compaction growth curves – TB 3

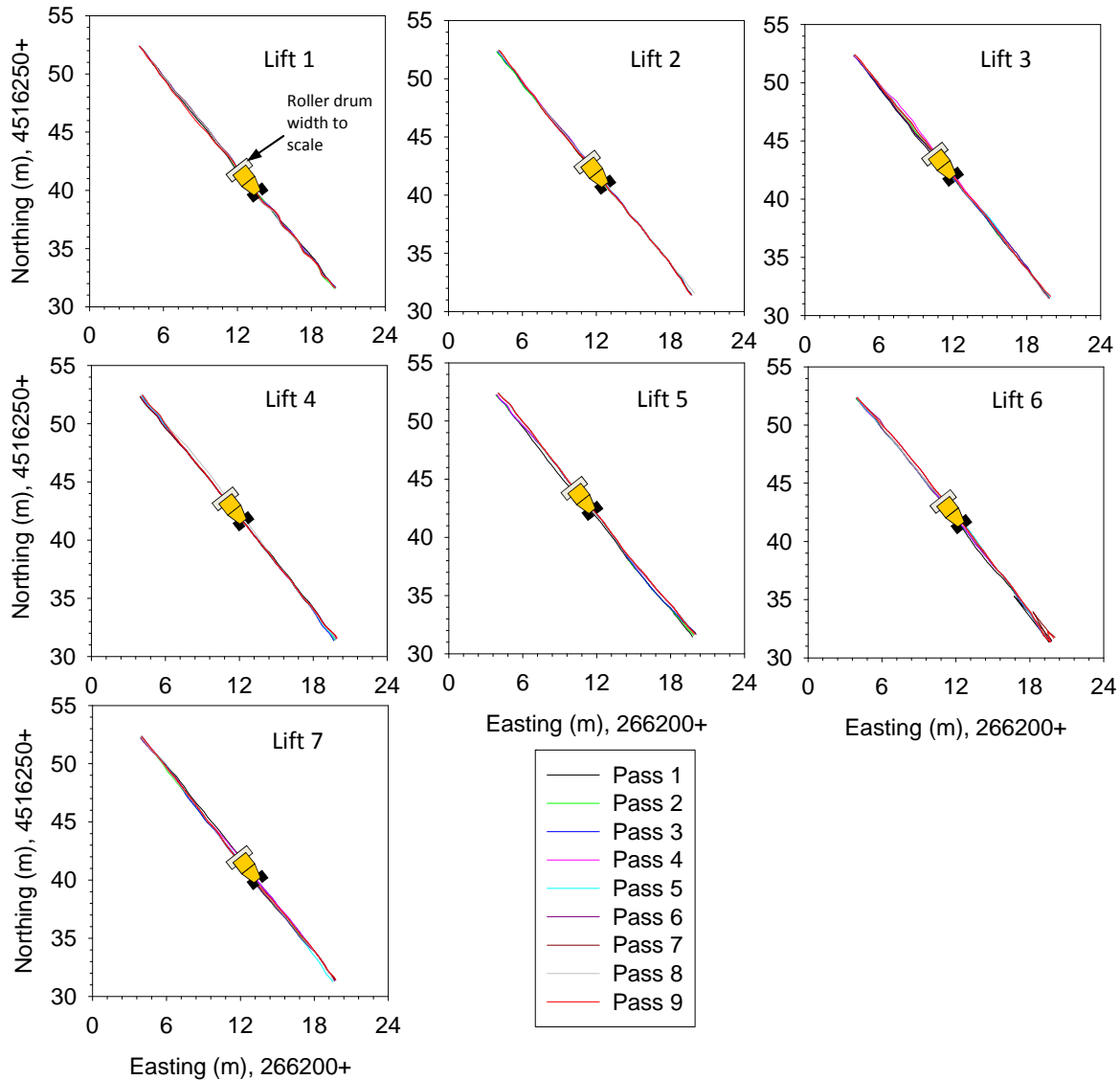


Figure 94. GPS position of roller drum during compaction passes on each lift – TB 3 (color)

MDP Comparison to In-Situ Soil Properties

Figure 95 and Figure 96 present MDP values on lifts 1 to 7 for pass 9 in comparison with E_{LWD} and CBR (calculated from DCP) values, respectively. MDP values are shown as solid lines while E_{LWD} and CBR data are shown as discrete points (note that the CBR values represent the properties of only the compaction layer (300 mm penetration depth), while the MDP and E_{LWD} values may be influenced by stiffness of the underlying layers). Both CBR and E_{LWD} measurement values matched reasonably well with MDP measurement values on all lifts. Regression relationships between MDP, CBR, and E_{LWD} measurements are presented in Figure 97. These relationships showed R^2 values > 0.7 , however, significant scatter is observed in these relationships.

Figure 98 presents average MDP, E_{LWD} and CBR values on each lift for the soft subgrade and concrete base areas. The MDP plot shows compaction growth from pass 1 to 9 separately for the portion of the test bed underlain by concrete base and soft subgrade. It is clear that for lifts 1 and 2, stiff underlying support with concrete base helps achieve significantly better compaction compared to soft subgrade support. The average MDP measurements over both concrete base and soft subgrade appear to converge and plateau at approximately 0.9 m to 1.0 (lift 4) above the bottom of the excavation. For pass 9, the ratio of average MDP in the area underlain by soft subgrade to average MDP in the area underlain by concrete base at 0.3-m elevation (lift 1) was about 2.3. The ratio at elevations 0.6- (lift 2), 0.8- (lift 3), and 1.1-m (lift 4) decreased to approximately 1.6, 1.5, and 1.1, respectively.

E_{LWD} and CBR_{300} quality assurance (QA) measurements taken on each compaction lift after pass 9 on the soft subgrade and concrete base areas are shown in Figure 98. Similar to MDP, E_{LWD} and CBR_{300} measurements over concrete base and soft subgrade areas appear to converge and plateau at approximately 0.9 and 1.0 m (lift 4) above the bottom of the excavation. The ratio of average E_{LWD} in the area underlain by concrete base to the average E_{LWD} in the area underlain by the soft/wet subgrade at about 0.3 m elevation (on lift 1) was about 3.7. The ratio at elevations 0.6-, 0.8-, and 1.1-m decreased to approximately 1.9, 1.2, and 1.0, respectively. Similarly, the ratio of average CBR in the area underlain by concrete base to the area underlain by soft/wet subgrade at 0.3-m elevation was about 8.7, and measurements at elevations 0.6-, 0.8-, and 1.2-m decreased the ratio to about 1.8, 1.4, and 1.1, respectively.

Also presented in Figure 98 are the post-construction QA E_{LWD} measurements performed in the excavation. The excavation was performed to the surface of each underlying layer to perform LWD test at two locations along the test bed (one in the concrete base area and the other in the soft subgrade area). The results show the E_{LWD} values in the concrete base area increased by about 2 times on lift 6 to about 4 times on lift 1, while the values in the soft/wet subgrade area increased by about 1.5 times on lift 5 to 13 times on lift 1. This increase in modulus is partially attributed to possible densification of underlying layers during compaction of the layers above, and partially to the effect of increasing confining stress with depth that increase the stiffness response of granular materials. The later effect is well known and according to Lambe and Whitman (1969) increase in confining stress (σ_c) increases the elastic modulus of granular materials by σ_c^n where n varies of 0.4 to 1.0. While no density tests were available from this test bed to confirm the underlying layer densification, the DCP-CBR profiles in Figure 98 show a significant increase in CBR as the layer above is placed and compacted (for e.g. see increase in lift 1 CBR from lift 2 CBR profile). This is an important aspect of compaction of granular materials and their behavior which is not well documented in literature.

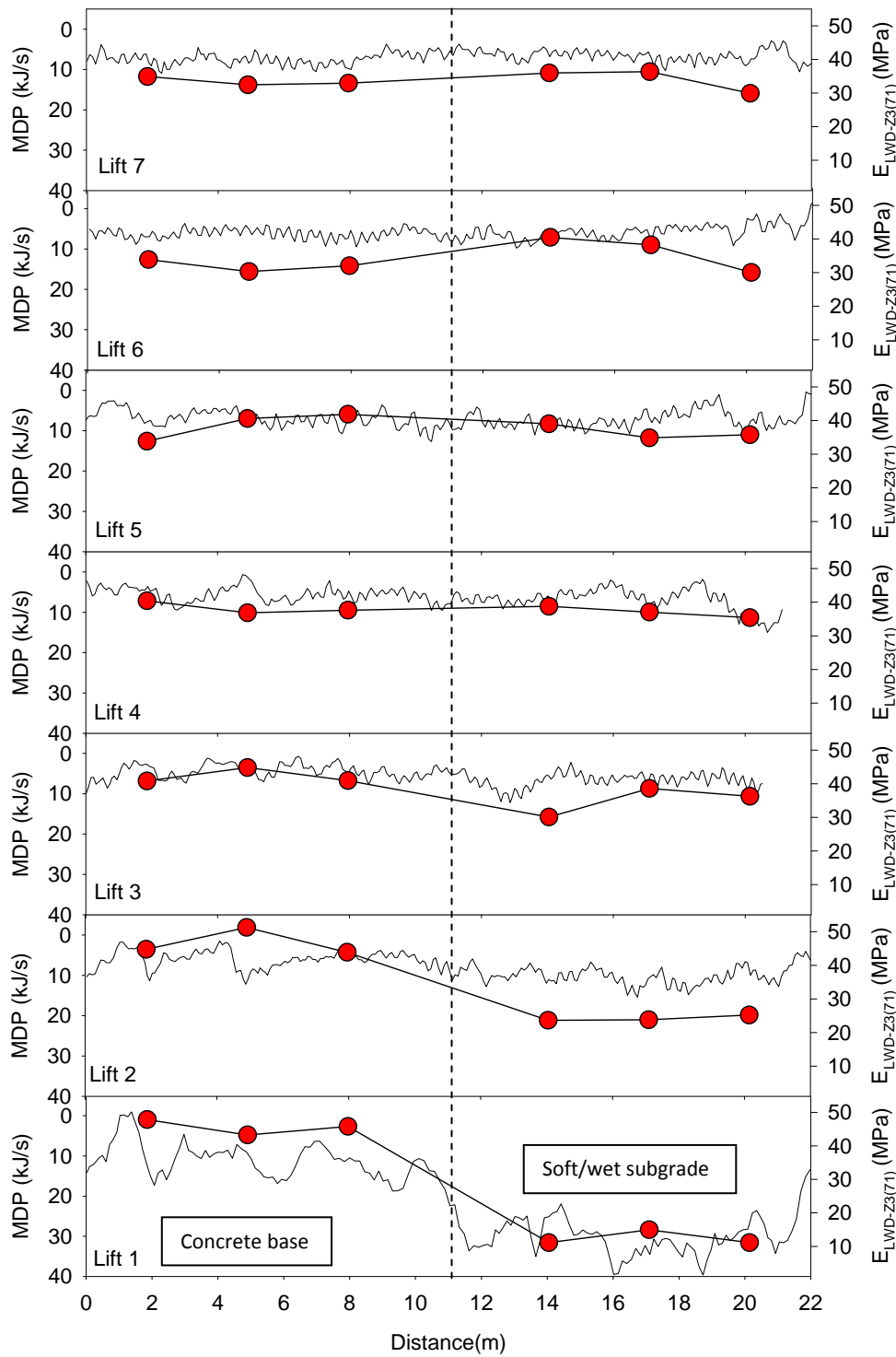


Figure 95. MDP and E_{LWD} comparison plot after final pass on each lift – TB 3

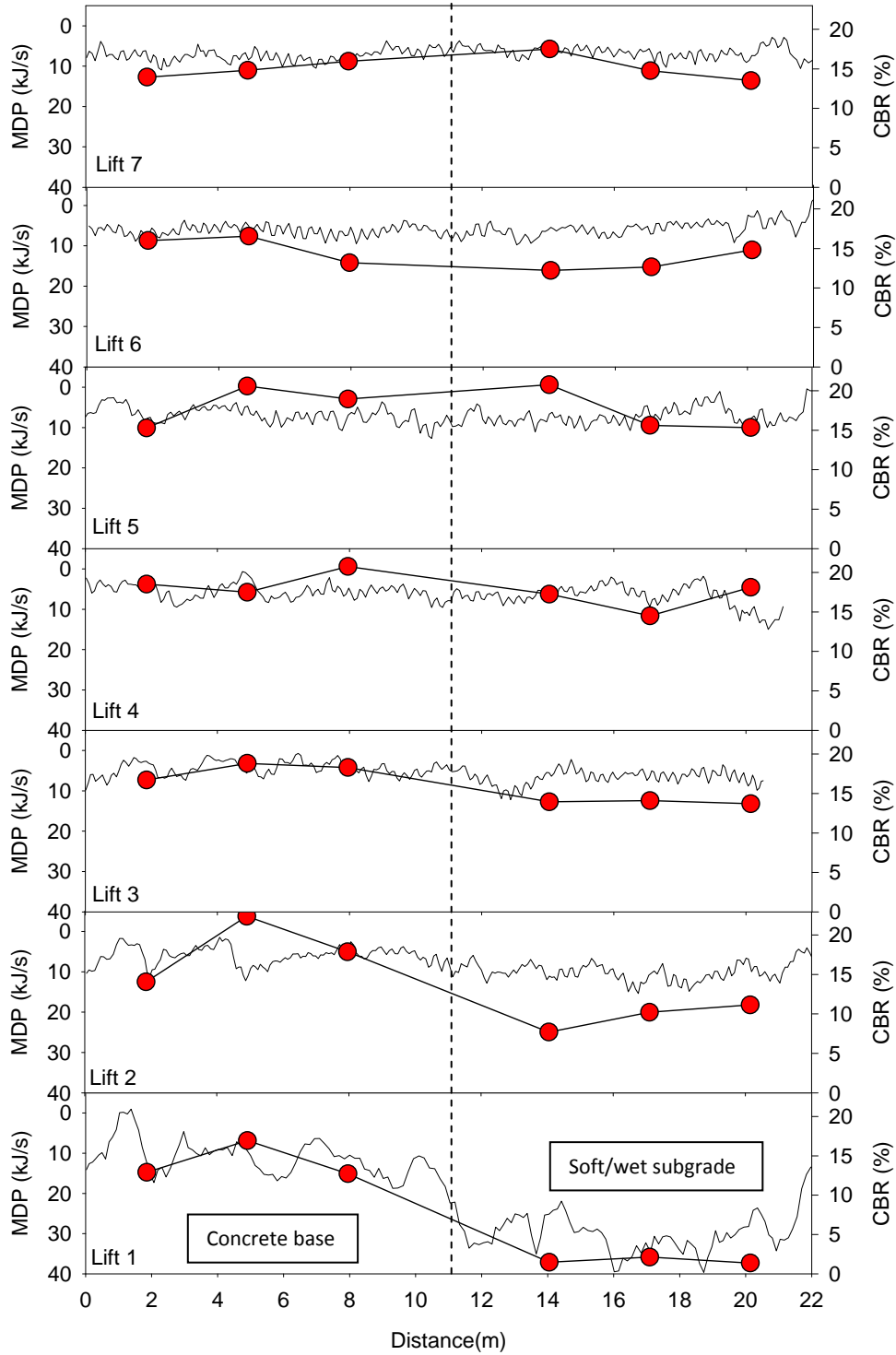


Figure 96. MDP and CBR comparison plot after final pass on each lift – TB 3

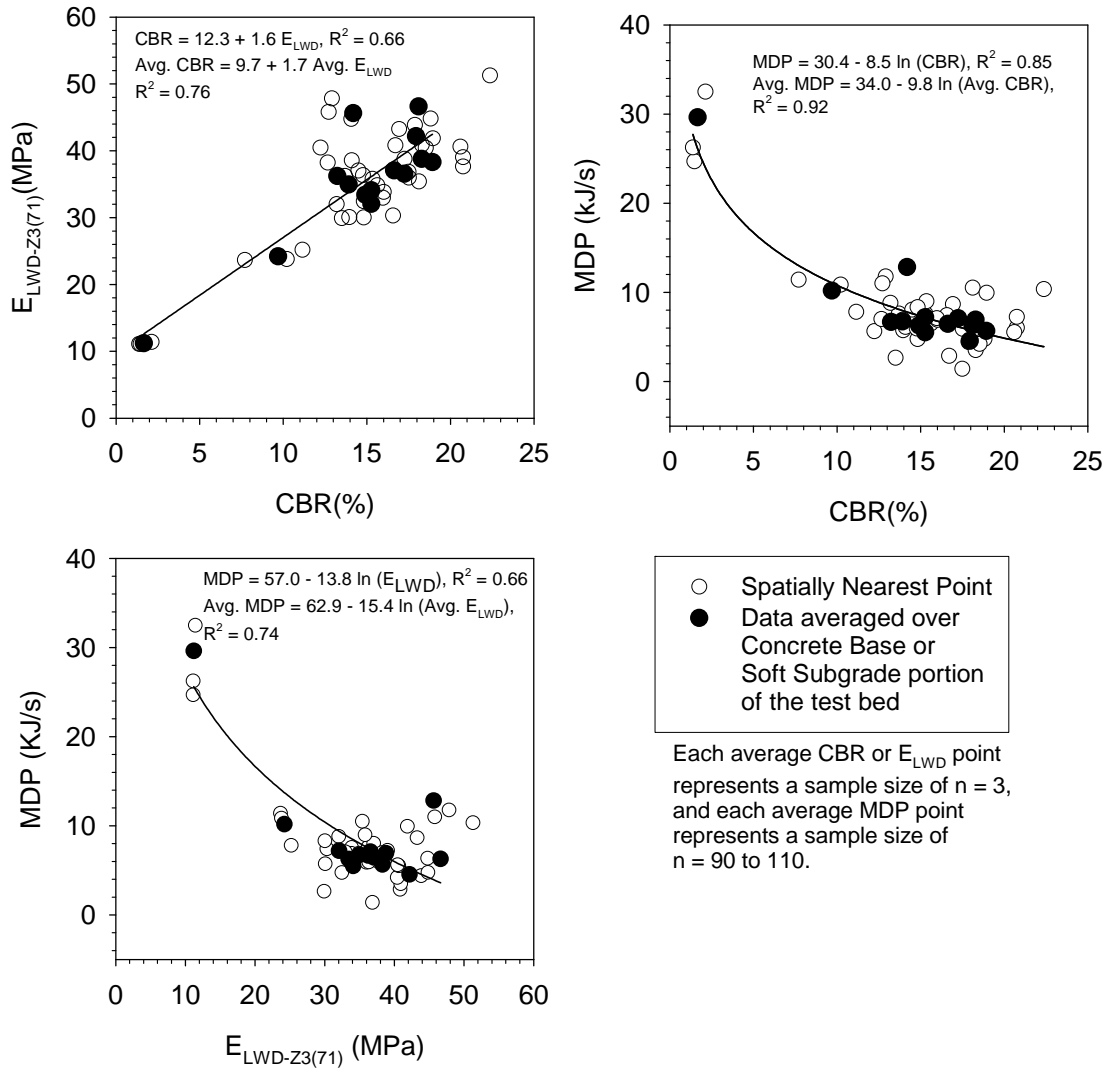


Figure 97. Relationships between CBR, E_{LWD} , and MDP from TB 3

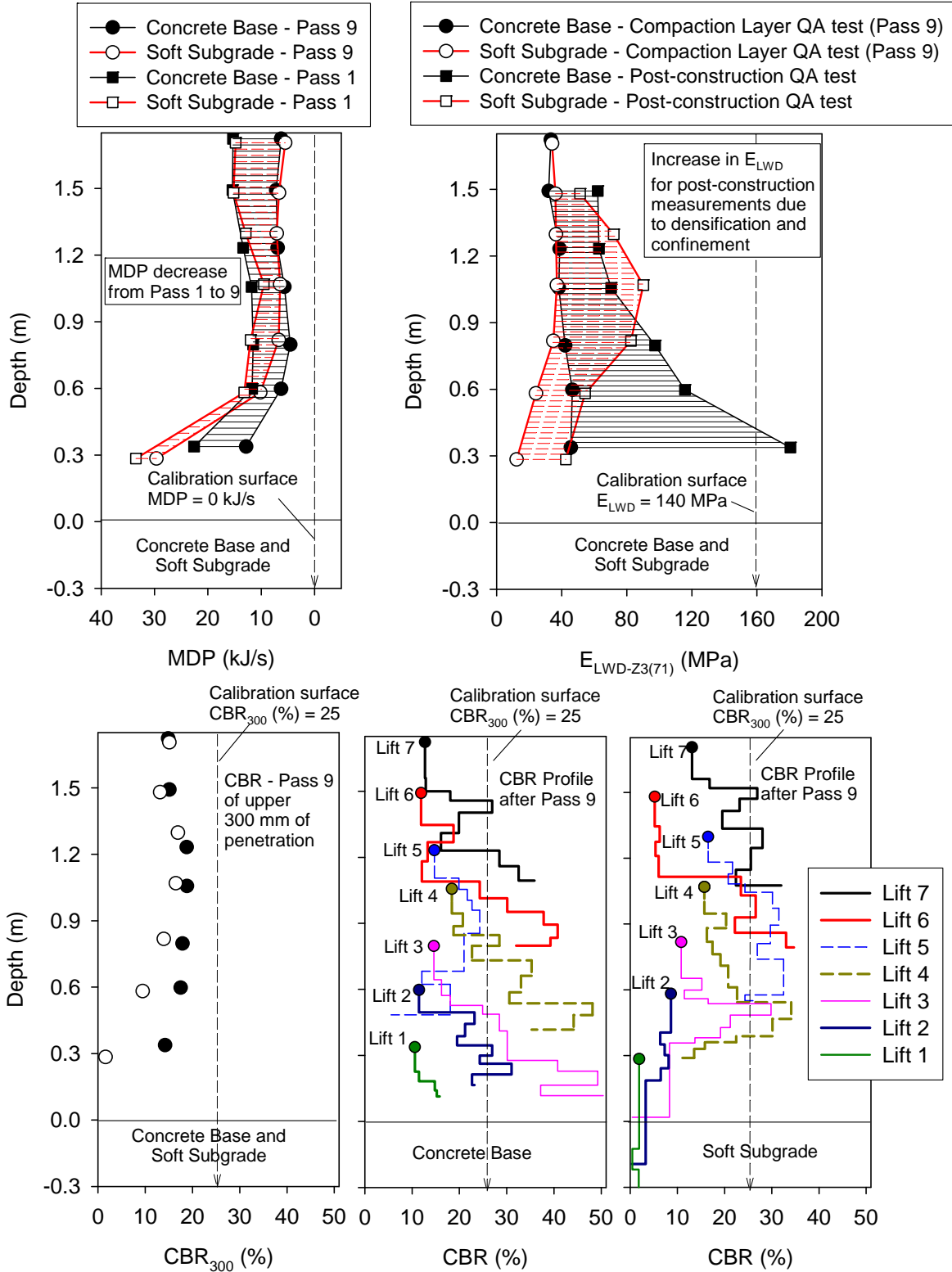


Figure 98. Average MDP, E_{LWD} , and CBR measurement values on all compaction lifts – TB3

Statistical Analysis on Influence of Support Conditions

Statistical analysis was performed to assess the influence of underlying layers on MDP and E_{LWD} values measurements. The analysis is performed by incorporating measurement values of the underlying layers into a linear regression model to predict measurement values at the surface. The significance of the underlying layer properties are selected based on statistical p - and t -values. The criteria for identifying the significance of a parameter included: p -value < 0.05 = significant, < 0.10 = possibly significant, > 0.10 = not significant, and t -value < -2 or $> +2$ = significant. The p -value indicates the significance of a parameter and the t -ratio value indicates the relative importance (i.e., higher the absolute value greater the significance). The t - and p -values from the analysis are summarized in Table 13.

Analysis on MDP measurements indicates that for lifts 2, 3, 4, and 5, MDP measurements on the immediate underlying layer are statistically significant. For lifts 6 and 7, the effect of underlying layers is not statistically significant. Further, the statistical significance of the underlying layers seems to decrease as additional lifts are placed in the test bed, which is evidenced by the decreasing t -value in Table 13. For example, the influence of lift 1 on lift 2 MDP is greater compared to the effect of lift 2 on lift 3 MDP, and so on. This quantifies the effect of “bridging” of the soft subgrade layer. Interestingly, as the t -values decrease, the variability (COV) of MDP measurements along the test bed also decrease (Table 13). MDP values show high variability for lifts 1 to 4 (COV $> 38\%$), while they were less variable for lifts 5 to 7 (COV $< 30\%$) (Table 13).

Similar analysis for E_{LWD} measurements indicate that for lifts 2 and 3, E_{LWD} of the immediate underlying layer is statistically significant. The statistical significance of lift 2 on lift 3 is lower compared to lift 1 on lift 2 E_{LWD} values, which is evidenced by the t -values (Table 13). For lifts 4, 5, 6, and 7, the effect of E_{LWD} of the underlying layer is not statistically significant. Similar to MDP measurements, as the t -value decrease, the variability (COV) of E_{LWD} measurements along the test bed also decrease (Table 13). E_{LWD} measurements on lifts 1 and 2 showed high variability (COV $> 35\%$) along the test bed, while they were less variable on and above lift 3 (COV $< 13\%$).

A basic premise of this analysis is that MDP and E_{LWD} measurements on a compaction layer reflect the underlying layer soil properties if relatively unstable and highly variable soil conditions exist (i.e., greater COV). If the underlying layer is relatively stable with relatively uniform conditions, the effect of underlying layer on MDP and E_{LWD} measurements is not statistically detectable. Practically, this means that when interpreting correlations between roller-integrated MDP and in-situ spot test measurements that solely represent the properties of the surface layer (e.g NG test, CBR from DCP), the effect of non-uniform underlying layers, if any, must be taken into account.

These insights on the influence of support conditions on roller-integrated and in-situ spot test measurements are important to understand as it aids in better interpretation of relationships during field calibration process and effective implementation of the technology in earthwork practice.

Summary and Key Conclusions

In summary, three controlled TBs were constructed as part of this phase of the research. The TBs were constructed by excavating a 4 feet trench below the existing grade. TB 1 consisted of a concrete pad, TB 2 consisted of a wet and dry subgrade, and TB 3 consisted of a concrete and wet subgrade at the base of the excavation. Seven lifts of CA6-G material were placed and compacted in each test bed. CS563 and CS683 smooth drum machines were used for TB 1, CS 563 smooth drum machine was used for TB 2, and CP563 padfoot machine was used for TB 3. EPCs were installed in TBs 1 and 2 to measure in-ground triaxial stresses developed during roller compaction. In-situ spot test measurements (E_{LWD} and DCP) were conducted after the final pass of compaction on each lift. After completing compaction on the final lift, post-construction QA measurements were conducted on top of each lift in an excavation performed in each test bed to check for differences in the stiffness of each underlying layer. Significant research conclusions from these test bed studies are as follows:

- Peak stresses developed in the ground under the roller drum increase with increasing vibration amplitude.
- Assuming the measurement influence depth of the roller equals the depth at which the applied vertical stresses equal to about 10% of the contact stresses at the surface, a measurement influence depth of about 0.6 to 0.7 m is estimated under the roller for both low and high amplitude settings.
- The interpretation of measurement influence depth as noted above is purely a function of interpreted contact stresses at the surface. Further insights in to quantifying measurement influence depth can be developed by performing a detailed laboratory investigation of the stress-strain characteristics of the soil combined with numerical studies on the response of multi-layered soils.
- MDP and in-situ spot test measurements (E_{LWD} and CBR) are influenced by the stiffness and heterogeneity of the supporting layer conditions. If the underlying layer is relatively stable and homogenous (i.e., $COV < 30\%$ for MDP, and $COV < 15\%$ for E_{LWD-Z3} and CBR), the effect of underlying layer on the compaction layer measurements is not statistically detectable.
- Although the compaction layer properties (as measured by in-situ test measurements) are relatively uniform, the MDP measurements tend to capture the variability of the underlying layers. Differences between MDP and in-situ test measurement influence are important for interpretation of results during field calibration.
- Post-construction tests performed after careful excavation of compaction layers indicate significant (1.5 to 13 times) increases in stiffness of the granular layers. The reason is attributed to possible densification (as evidenced by difference in elevation measurements) of underlying layers during compaction of the layers above and to the effect of increased lateral stresses due to compaction. The later aspect is well documented in the literature (e.g., Lambe and Whitman 1969), but the aspect of post-construction densification of granular materials is not well documented in the literature.

Table 13. Effect of underlying layer measurements on surface layer measurements

Surface layer (depth, m)	MDP (kJ/s)		MDP Ratio*	E _{LWD} (MPa)		E _{LWD} Ratio [§]	Effect of underlying layer(s)	MDP		E _{LWD}	
	μ	COV		μ	COV			t-value	p-value	t-value	p-value
Lift 1 (0.29)	20.6	51	2.3	29.0	63	3.7	Concrete base/soft subgrade	—	—	—	—
Lift 2 (0.59)	8.1	37	1.6	35.4	35	1.9	Lift 1	11.11	< 0.001	6.61	0.0027
Lift 3 (0.80)	5.5	38	1.5	38.6	13	1.2	Lift 2	4.39	< 0.001	3.00	0.004
							Lift 1	Not significant		Not significant	
Lift 4 (1.06)	6.0	43	1.1	37.7	5	1.0	Lift 3	2.78	0.007	Not significant	
							Lifts 2 and 1	Not significant			
Lift 5 (1.26)	7.0	30	1.0	37.7	9	0.9	Lift 4	2.58	0.012	Not significant	
							Lifts 3, 2, and 1	Not significant			
Lift 6 (1.49)	7.0	22	0.9	34.1	13	0.9	Lifts 5, 4, 3, 2 and 1	Not significant		Not significant	
Lift 7 (1.72)	5.9	28	0.9	33.8	7	1.0	Lifts 6, 5, 4, 3, 2, and 1	Not significant		Not significant	

*Ratio of the average MDP in the area underlain by soft/wet subgrade to area underlain by concrete/base for each lift.

[§]Ratio of the average E_{LWD} in the area underlain by concrete base and area underlain by soft/wet subgrade for each lift.

RESEARCH CONCLUSIONS

Repeatability and Reproducibility Study

The precision of roller measurement values CMV, RMV, and MDP from three different machines is quantified in a repeatability and reproducibility context in this study. Repeatability variation refers to the variation observed in repeat measurements made on a test strip under identical conditions. Reproducibility variation refers to the variation observed in repeat measurements on a test strip under changing operating conditions (i.e., change in speed, amplitude, and direction of travel). Some key conclusions from the results and analysis are as follows:

- Data collected from CS 563 roller showed that the CMV data starts to gradually decrease when RMV increases above about 4 (i.e., when roller is double jumping). This is a distinctive feature of CMV and is previously identified in numerical simulations by Adam and Kopf (2004). Increasing RMV (i.e. double jumping) occurs when ground stiffness increases beyond a certain point.
- The relative change in CMV with increasing RMV is important to document when evaluating roller measurement values in any earthwork construction project as it can affect the correlations and target values significantly.
- Double jumping was not noticed when the 563 and 683 rollers were operated at low amplitude.
- CS-563 machine used on the TH 64 project (White et al. 2008) used RMV of 17 for controlling the amplitude in a variable feedback control mode. RMV of 17 appears to be a significantly higher number as double jumping effects are noticed when RMV increases above 4. Further studies are warranted to check the efficiency of variable feedback control system by reducing the controlling RMV-value to 4.
- Maximum CMV on the CS 563 machine used on this project is about 40.
- On average, CMV measured by the CS683 machine at $a = 0.85$ mm and $v = 3.2$ km/h is about 1.4 times lower than CMV measured by the CS563 machine at similar operating conditions.
- The CMV and RMV measurement values are repeatable between each pass under identical operating conditions. The measurement error associated with CS 563 roller measured CMV is found to vary between 1.7 and 2.8. It is also found that the measurement error when the drum is double jumping is also within these limits (~1.9), while it is lower when data from double jump mode is ignored (~1.7). The measurement error associated with CS 683 roller measured CMV is about 3.0.

- The CMV and RMV measurement errors at high amplitude are lower compared to low amplitude for the two speeds tested using the CS 563 roller, when data from double jump area is ignored.
- CMV on CP 563 padfoot roller is not repeatable, while MDP data appears to be repeatable between passes made under identical operation parameters. The CMV measurements were unusual and not typical of CMV measurements from similar CAT machines.
- The MDP measurement error is found to vary between 0.6 and 1.07, and the error appears to increase when the machine is operated at higher speeds. Careful calibration procedures should help minimize the reproducibility variations associated with increasing speed.
- The MDP values are not reproducible with change in amplitude from 0.31 mm to 1.90 mm.
- Reproducibility variations in CMV and RMV for CS 563 roller are not significant with change in speed from 3.2 km/h to 4.8 km/h at low amplitude setting ($a = 0.85$ mm). Results are also reproducible at high amplitude setting ($a = 1.70$ mm) where there is no double jumping.
- Effect of change in amplitude is significant for CMV and RMV measurement values for the CS 563 roller.
- Effect of change in roller direction is significant for CMV but it is not significant for RMV.

Test Bed Studies

In summary, three controlled TBs were constructed as part of this phase of the research. The TBs were constructed by excavating a 4 feet trench below the existing grade. TB 1 consisted of a concrete pad, TB 2 consisted of a wet and dry subgrade, and TB 3 consisted of a concrete and wet subgrade at the base of the excavation. Seven lifts of CA6-G material were placed and compacted in each test bed. CS563 and CS683 smooth drum machines were used for TB 1, CS 563 smooth drum machine was used for TB 2, and CP563 padfoot machine was used for TB 3. EPCs were installed in TBs 1 and 2 to measure in-ground triaxial stresses developed during roller compaction. In-situ spot test measurements (E_{LWD} and DCP) were conducted after the final pass of compaction on each lift. After completing compaction on the final lift, post-construction QA measurements were conducted on top of each lift in an excavation performed in each test bed to check for differences in the stiffness of each underlying layer. Significant research conclusions from these test bed studies are as follows:

- Peak stresses developed in the ground under the roller drum increase with increasing vibration amplitude.

- Assuming the measurement influence depth of the roller equals the depth at which the applied vertical stresses equal to about 10% of the contact stresses at the surface, a measurement influence depth of about 0.6 to 0.7 m is estimated under the roller for both low and high amplitude settings.
- The interpretation of measurement influence depth as noted above is purely a function of interpreted contact stresses at the surface. Further insights in to quantifying measurement influence depth can be developed by performing a detailed laboratory investigation of the stress-strain characteristics of the soil combined with numerical studies on the response of multi-layered soils.
- MDP and in-situ spot test measurements (E_{LWD} and CBR) are influenced by the stiffness and heterogeneity of the supporting layer conditions. If the underlying layer is relatively stable and homogenous (i.e., $COV < 30\%$ for MDP, and $COV < 15\%$ for E_{LWD-Z3} and CBR), the effect of underlying layer on the compaction layer measurements is not statistically detectable.
- Although the compaction layer properties (as measured by in-situ test measurements) are relatively uniform, the MDP measurements tend to capture the variability of the underlying layers. Differences between MDP and in-situ test measurement influence are important for interpretation of results during field calibration.
- Post-construction tests performed after careful excavation of compaction layers indicate significant (1.5 to 13 times) increases in stiffness of the granular layers. The reason is attributed to possible densification (as evidenced by difference in elevation measurements) of underlying layers during compaction of the layers above and to the effect of increased lateral stresses due to compaction. The later aspect is well documented in the literature (e.g., Lambe and Whitman 1969), but the aspect of post-construction densification of granular materials is not well documented in the literature.

REFERENCES

- Adam, D. 1997. Continuous compaction control (CCC) with vibratory rollers. In *GeoEnvironment 97: Proceedings of 1st Australia-New Zealand Conference on Environmental Geotechnics*. Rotterdam, Netherlands: A.A. Balkema, 245–250.
- Adam, D., and Kopf, F. (2004). “Operational devices for compaction optimization and quality control (Continuous Compaction Control & Light Falling Weight Device).” *Proc., of the Intl. Seminar on Geotechnics in Pavement and Railway Design and Construction*, December, Athens, Greece (Invited paper), 97-106.
- Forssblad, L. (1980). “Compaction meter on vibrating rollers for improved compaction control”, *Proc., Intl. Conf. on Compaction*, Vol. II, 541-546, Paris.
- Geodynamik ALFA-030. *Compactometer, Compaction Meter for Vibratory Rollers*, ALFA-030-051E/0203, Geodynamik AB, Stockholm, Sweden.
- Labuz, J.F. and Theroux, B. (2005). “Laboratory Calibration of Earth Pressure Cells”, *Geotechnical Testing Journal*, Vol. 28, No. 2.
- Lambe, W. T., Whitman, R. V. (1969). *Soil mechanics*. John Wiley and Sons, New York.
- Newman, K., and White, D. (2008). “Rapid assessment of cement/fiber stabilized soil using roller-integrated compaction monitoring.” *Transportation Research Record: Journal of the Transportation Research Board*, National Academy Press (accepted).
- Sandström, Å. (1994). *Numerical simulation of a vibratory roller on cohesionless soil*, Internal Report, Geodynamik, Stockholm, Sweden.
- Sandström A.J., and Pettersson, C.B. (2004). "Intelligent systems for QA/QC in soil compaction", *Proc., 83rd Annual Transportation Research Board Meeting*, January 11-14. Washington, D.C.
- Taylor, B. N., Kuyatt, C. E. 1994. *Guidelines for Evaluating and Expressing the Uncertainty of NIST Measurement Results*. NIST Technical Note 1297, National Institute of Standards and Technology, Gaithersburg, MD.
- Thurner, H. and Sandström, Å. (1980). “A new device for instant compaction control.” *Proc., Intl. Conf. on Compaction*, Vol. II, 611-614, Paris.
- Vennapusa, P., White, D. “Comparison of light weight deflectometer measurements for pavement foundation materials”, *Geotech. Test. J.*, ASTM (submitted for review February 2008).
- Weiler, W.A., Kulhawy, F.H. (1982). “Factors affecting stress cell measurements in soil.” *Journal of Geotechnical Engineering Division*, Vol. 108, No. GT 12, 1529.1548.

- White, D.J, Thompson, M., Jovaag, K., Morris, M., Jaselskis, E., Schaefer, V. and Cackler, E. (2006). *Field evaluation of compaction monitoring technology: Phase II*. Final Report, Iowa DOT Project TR-495, Iowa State University, Ames, Ia.
- White, D.J, Jaselskis, E., Schaefer, V., Cackler, T., Drew, I., and Li, L. (2004). *Field Evaluation of Compaction Monitoring Technology: Phase I*, Final Report, Iowa DOT Project TR-495, Iowa State University, Ames, Ia.
- White, D.J, Thompson, M., Vennapusa, P. (2007). *Field study of compaction monitoring systems: self-propelled non-vibratory 825G and vibratory smooth drum CS-533 E rollers*, Final Report, Center of Transportation Research and Education, Iowa State University, Ames, Ia.
- White, D., Thopmson, M., Vennapusa, P., and Siekmeier, J. (2008). "Implementing intelligent compaction specifications on Minnesota TH 64: Synopsis of measurement values, data management, and geostatistical analysis." *Transportation Research Record: Journal of the Transportation Research Board*, National Academy Press (accepted).